# Organic matter composition and dynamic in polygonal tundra soils

I n a u g u r a l - D i s s e r t a t i o n

zur

Erlangung des Doktorgrades
der Mathematisch-Naturwissenschaftlichen Fakultät
der Universität zu Köln

vorgelegt von

Silke Tamara Höfle
aus Bruchsal

Köln, 2015

Berichterstatter: Prof. Dr. Janet Rethemeyer
(Gutachter) Prof. Dr. Lars Kutzbach

Tag der mündlichen Prüfung: 08.04.2015

## Abstract

Arctic permafrost regions are postulated to be most strongly affected by the on-going global warming resulting in longer summer seasons and higher temperatures. This may cause the degradation of permafrost and increase the thickness of the annual superficial thawing layer (active layer) of permafrost soils. Thereby permafrost soils may turn from carbon sinks into carbon sources for the atmosphere as large, previously frozen carbon pools become available for microbial degradation, a key factor in the soil organic matter (OM) degradation.

The aim of this thesis was to investigate soil organic matter of permafrost soil to identify stabilization mechanisms, soil bacterial communities and carbon pools preferably metabolised by soil bacteria using bulk, molecular lipid-biomarker, physical fractionation and radiocarbon analysis. In temperate soils stabilization mechanism of OM, mainly organo-mineral associations and soil aggregations, are well studied by separating the OM into functional pools with different turnover rates, which are determined by their chemical properties and bioavailability. However, little is known about the quality of the soil OM, its stability and its accessibility for the microbial community in permafrost soils. The most important location for microbial metabolic activity in permafrost soils is the active layer. Therefore, this thesis concentrated on investigating different soil horizons of the active layer and the still frozen permafrost top layer of the polygonal tundra in the Siberian Lena Delta, Russia. Soil samples were predominantly taken from Samoylov Island and for the characterisation of soil bacterial communities additional samples from Kurungnakh Island were also analysed.

The results show that the OM of both different cryogenic structures (polygon rim and centre) on Samoylov Island is dominated by little-decomposed, higher plant-derived material as indicated by the dominance of long-chain lipid biomarkers (*n*-alkanes and *n*-fatty acids) and high C/N ratios (16-51). The bulk soil OM of the active layer of the water saturated polygon centre is very young (0 to 43 cm depth: modern to 300 yrs BP) indicating that plant roots introduce modern carbon into deeper soil horizons. In contrast, the $^{14}C$ age of the bulk OM of the polygon rim increases strongly with depth in the active layer (0 to 32 cm depth: modern to 1950 yrs BP) and even further in the permafrost top layer (32-37 cm depth: 3050 yrs BP) suggesting a slow microbial OM degradation in this cold environment. Soil organic carbon in the polygon rim is mainly stored in the clay and fine silt sized fractions (< 6.3 µm). These fractions are surprisingly 'young' with $^{14}C$ contents similar to the bulk soil values suggesting that organo-mineral associations are of little importance in the OM stabilization. Particular OM occluded in soil aggregates has increased carbon contents with depth and higher $^{14}C$ ages (55-3080 yrs BP) than free light particular OM (modern-1240 yrs BP). This indicates that soil aggregation seems to be of a stabilization mechanism occurring only at greater soil depth.

The living microbial soil biomass is dominated by Gram-positive and Gram-negative bacteria as indicated by the dominance of their phospholipid fatty acid biomarkers (PLFAs, membrane lipids of living microbial cells). Another bacterial biomarker are

bacteriohopanepolyols (BHPs), which are almost exclusively produced by bacteria. In different soil horizons on Samoylov and Kurungnakh Island the soil horizons differed in the abundances of methanotrophs, cyanobacteria, soil-marker BHP-producing bacteria and unknown BHP-producing bacteria. The greatest structural diversity and highest BHP concentrations probably indicating a great bacterial diversity and biomass were observed in the uppermost organic soil horizons (Oi) of the polygon rim and centre. It seems that several soil properties as high organic carbon content and relatively low soil pH have a positive influence on the diversity of the BHP-producing bacterial community.

Microorganisms seem to predominantly metabolise the youngest, presumably labile OM pools available, as the $^{14}C$ ages of individual PLFA biomarkers were always lower than the $^{14}C$ ages of the bulk OM from which the biomarkers were isolated. It can be further suggested that the microbial utilized labile OM pools are plant-derived as the microbial PLFA biomarkers have similar $^{14}C$ ages the as long-chain (plant-derived) lipid biomarkers and the free particular organic matter (fPOM). The increasing $^{14}C$ age of microbial PLFAs with soil depths suggested that microorganisms metabolise older carbon sources in greater soil depth. However, these sources are most likely still the most labile and plant-derived OM pools available as fPOM has similar $^{14}C$ ages as the PLFAs. Therefore, it is possible either that ‘old’, presumably more stable carbon pools are not in favour to microbial decomposition or are not bioavailable or are degraded by microorganism other than (aerobic) soil bacteria.

# Zusammenfassung (Summary in German)

Die Permafrostregionen der Arktis werden durch die gegenwärtige globale Erwärmung vermutlich am stärksten beeinflusst, wodurch es zu längeren Sommerperioden und höheren Temperaturen kommen wird. Dies könnte zu einer Degradierung des Permafrostes führen und die jährliche oberflächliche Auftauschicht (active layer) der Permafrostböden an Mächtigkeit gewinnen lassen. Dadurch würden sich die Permafrostböden von Kohlenstoffsenken zu Kohlenstoffquellen für die Atmosphäre wandeln, weil große, früher eingefrorene Kohlenstoffreservoirs für den mikrobiellen Abbau, ein Schlüsselfaktor der Zersetzung von organischer Bodensubstanz, zur Verfügung stünden.

Das Ziel dieser Arbeit war die Untersuchung organischer Bodensubstanz in Permafrostböden zur Identifikation von Stabilisierungsmechanismen, Bodenbakteriengesellschaften und Kohlenstoffpools, die vorranging von Bodenbakterien verstoffwechselt werden. Dies wurde mit Hilfe von bodenkundlichen Summenparametern, molekularen Lipid-Biomarkern, physikalischer Bodenfraktionierung und Radiokohlenstoffanalysen untersucht. In Böden der gemäßigten Zone sind die Stabilisierungsmechanismen der organischen Bodensubstanz (hauptsächlich organo-mineralische Verbindungen und Bodenaggregate) gut untersucht. Dafür wurde die organische Bodensubstanz dieser Böden in verschiedene funktionelle Pools mit unterschiedlichen Umsetzungsraten, die durch die chemischen Eigenschaften und der Bioverfügbarkeit der Pools bestimmt werden, aufgetrennt. Allerdings ist wenig über die Qualität, die Stabilität und die Bioverfügbarkeit für mikrobielle Gemeinschaften von organischer Bodensubstanz in Permafrostböden bekannt. Der Hauptort für mikrobielle Stoffwechselprozesse in Permafrostböden ist die jährliche Auftauschicht (active layer). Deshalb konzentrierte sich diese Arbeit auf die verschiedenen Bodenhorizonte der Auftauschicht und auf den obersten, noch gefrorenen Permafrostbereich in der polygonalen Tundra des sibirischen Lenadeltas, Russland. Die Bodenproben stammten hauptsächlich von der dortigen Insel Samoylov. Für die Charakterisierung der bakteriellen Bodengemeinschaften wurden zusätzlich Proben von der Insel Kurungnakh untersucht.

Die Ergebnisse zeigen, dass die organische Bodensubstanz der beiden kryogenen Strukturen (Polygonwall und Polygonzentrum) auf der Insel Samoylov von wenig zersetztem Material pflanzlichen Ursprungs dominiert wird, da langkettige Lipid-Biomarker (*n*-Alkane und *n*-Fettsäuren) überwiegen und die C/N-Verhältnisse (16-51) hoch sind. Das organische Bodenmaterial der Auftauschicht des wassergesättigten Polygonzentrums ist sehr jung (0 bis 43 cm Tiefe: modern bis 300 Jahre BP). Dies lässt vermuten, dass Pflanzenwurzeln modernen Kohlenstoff in tiefere Bodenhorizonte transportieren und dort abgeben. Im Gegensatz hierzu steigt das $^{14}$C-Alter des organischen Materials im Polygonwall mit zunehmender Tiefe der Auftauschicht stark an (0 bis 32 cm Tiefe: modern bis 1950 Jahre BP) und steigt in der obersten Permafrostschicht sogar noch weiter (32-37 cm Tiefe: 3050 Jahre BP), was eine geringe mikrobielle Umsetzung des organischen Materials in dieser kalten Umwelt vermuten lässt. Organischer Bodenkohlenstoff ist im Polygonwall hauptsächlich in den Ton- und Feinschluff-Fraktionen (< 6.3 µm) gespeichert.

Allerdings sind diese Fraktionen mit $^{14}$C-Gehalten ähnlich des Gesamtbodens überraschend jung, was darauf schließen lässt, dass organo-mineralische Verbindungen bei der Stabilisierung des organischen Materials nur eine untergeordnete Bedeutung spielen. Partikuläres und in Bodenaggregaten gebundenes organisches Material (oPOM) hat mit der Tiefe höhere Kohlenstoffgehalte. Zudem ist das $^{14}$C-Alter der oPOM-Fraktion (55-3080 yrs BP) größer als die des freien partikulären organischen Materials (fPOM: modern-1240 yrs BP), was darauf hindeutet, dass Bodenaggregate nur in größerer Bodentiefe ein Stabilisierungsmechanismus sind.

Die lebende mikrobielle Biomasse wird von Gram-positiven und Gram-negativen Bakterien dominiert, was durch die Dominanz ihrer Phospholipid-Fettsäuren (PLFAs, Membranlipide der lebenden mikrobiellen Zellen) angezeigt wird. Bei der Analyse von Bakteriohopanpolyolen (BHPs), die fast ausschließlich von Bakterien produziert werden, zeigte sich für die verschiedenen Bodenhorizonten der Inseln Samoylov und Kurungnakh eine unterschiedliche Zusammensetzung von Methanotrophen, Cyanobakterien, bodenspezifischen BHP-produzierenden Bakterien und unbekannten BHP-produzierenden Bakterien. Eine große bakterielle Vielfalt und Biomasse scheint in den obersten, organikreichen Oi-Horizonten der Polygonwälle und -zentren vorzuliegen, da dort die höchste strukturelle Diversität und die höchsten Konzentrationen an BHPs gemessen wurden. Es scheint, dass die Bodeneigenschaften wie ein hoher Gehalt an organischem Kohlenstoff und relativ geringe pH-Werte einen positiven Einfluss auf die Diversität der BHP-produzierenden bakteriellen Gemeinschaft haben.

Mikroorganismen scheinen die jüngsten, vermutlich labilsten zur Verfügung stehenden Kohlenstoffpools zu verstoffwechseln, da das $^{14}$C-Alter einzelner PLFA-Biomarker immer geringer war als das $^{14}$C-Alter der Bodenhorizonte aus denen sie isoliert wurden. Es kann zudem vermutet werden, dass diese mikrobiell genutzte organische Bodensubstanz pflanzlichen Ursprungs ist, da die mikrobiellen PLFA-Biomarker ein ähnliches $^{14}$C-Alter wie die langkettigen Lipid-Biomarker (*n*-Alkane und *n*-Fettsäuren) und das freie partikuläre organische Material (fPOM) haben. Das ansteigende $^{14}$C-Alter der mikrobiellen PLFAs mit der Bodentiefe deutet darauf hin, dass Mikroorganismen mit der Tiefe ältere Kohlenstoffquellen nutzen. Diese Quellen scheinen aber immer noch das labilste verfügbare organische Material pflanzlichen Ursprungs zu sein, da die fPOM-Fraktion ein ähnliches $^{14}$C-Alter wie die PLFAs aufweist. Daher ist es möglich, dass entweder ‚alte', vermutlich stabilere Kohlenstoffpools nicht von den Mikroorganismen favorisiert werden oder diese nicht bioverfügbar sind oder diese von anderen als den hier untersuchten (aeroben) Bodenbakterien umgesetzt werden.

# Table of content

# 1. Introduction and objectives

## 1.1 Importance of permafrost

Permafrost is defined as perennially frozen ground which remains for at least two consecutive years at or below 0°C (Jones et al., 2010). The northern permafrost region covers about 16% of the global soil area (Fig, 1A; Tarnocai et al., 2009) and contains large amounts of organic carbon (1300-1370 Pg with an uncertainty range of 630-1690 Pg), twice the amount of carbon currently in the atmosphere (Ciais et al., 2013). Most of the carbon is found in permafrost soils (0-3 m: 1035±150 Pg) while much less is found in the deeper sediments (>3 m: 272±106 Pg; Hugelius et al., 2014). The top meter of the soil holds about 472±27 Pg of organic carbon (Fig. 1B; Hugelius et al., 2013; Hugelius et al., 2014) which is about 50% of the global soil organic carbon storage (Jones et al., 2010). These large soil carbon stocks in high latitudes were formed in unglaciated regions prior to the last glacial maximum (Dutta et al., 2006; Zimov et al., 2006) and also in areas that have been deglaciated since then (Harden et al., 1992).

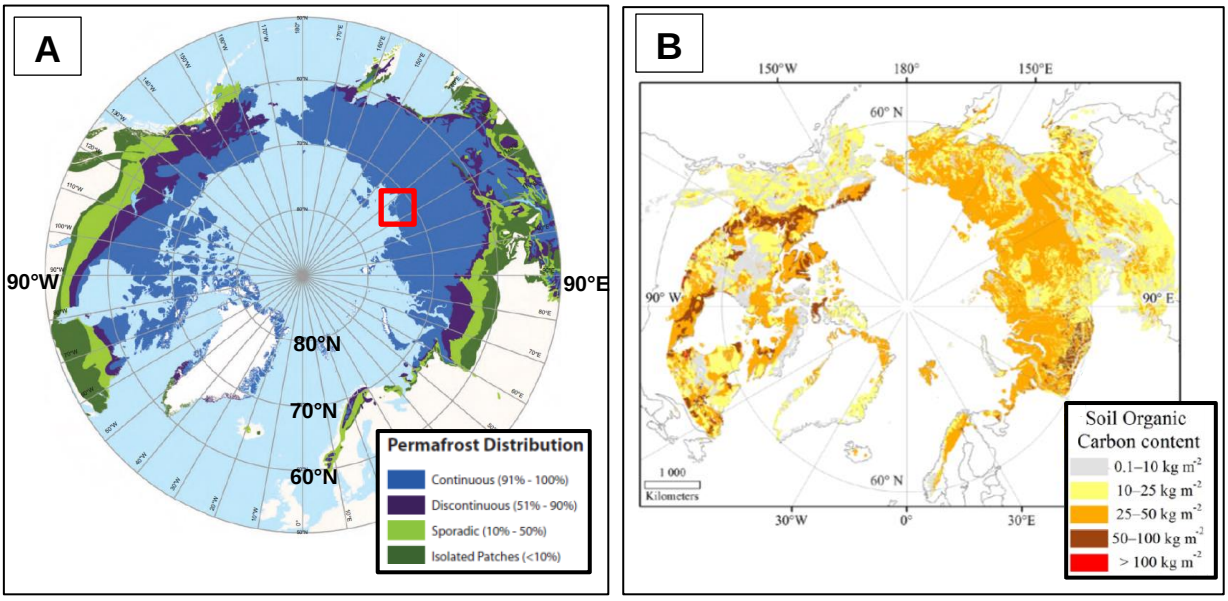


Fig.1: A) Circumpolar permafrost distribution (Jones et al., 2010) and B) soil organic carbon content within the first 1 m of the Arctic permafrost (Hugelius et al., 2013). The red square in Fig. 1 A localises the Siberian Lena-Delta, Russia.

Global warming is predicted to affect the high northern latitudes most strongly. Different models agree that the warming in the Arctic will be greater than the average global warming (Collins et al., 2013). Under the highest warming scenario (RCP 8.5) a temperature increase of 7-11°C is estimated by the end of the 21st century compared to the average air temperatures of 1986-2005 (Collins et al., 2013). Observed air temperatures have already increased in the Arctic by +1.0°C (Overland et al., 2008) accompanied by deep permafrost warming (Vaughan et al., 2013) and loss of sea ice cover (Kwok and Rothrock, 2009). Model simulations have calculated that about 29-60%

of the permafrost area present today will degrade into seasonally frozen ground by 2200 (Saito et al., 2007; Schaefer et al., 2011). Furthermore, the Arctic warming will increase the thickness of the active layer, the permafrost top soil layer thawing annually during summer, which has been already observed in the North-West of Russian and in northern East Siberia during the last 15 years (Romanovsky et al., 2013). Thus, old carbon pools, previously frozen looked for the last hundreds or thousands of years, may get incorporated again into the active carbon cycle and turn this large carbon reservoir into a source of carbon emissions for the atmosphere (Khvorostyanov et al., 2008; Schuur et al., 2009; Schädel et al., 2014).

Recent studies have shown that with deeper thawing of the Arctic permafrost an increased plant and old soil carbon respiration occur, which are initially compensated by an increased net primary productivity, due to longer vegetation growing seasons (Euskirchen et al., 2006; Hartley et al., 2012; Hicks Pries et al., 2013). During a long-term in-situ warming experiment over 20 years in Alaska an increase of carbon in the deep mineral soil has been observed probably due to increasing root exudates and leachates (Sistla et al., 2013). However, due to the large carbon stocks in the soil these processes do not seem able to compensate the carbon release from thawing permafrost on a long term basis. Even a shift from a tundra ecosystem into a boreal forest could only compensate for about 10% of the carbon loss from the thawed permafrost soils (Schuur et al., 2008; Hicks Pries et al., 2013). Therefore, permafrost thawing is likely to have a positive feedback on climate warming, even though the topic is still under debate (Davidson and Janssens, 2006; Ciais et al., 2013) and includes uncertainties about the size and bioavailability of the carbon that is released from the thawing permafrost (e.g., Shaver et al., 2006; Schuur et al., 2008; Nowinski et al., 2010; Harden et al., 2012; Schuur et al., 2013). A recent published synthesis study by Schädel et al. (2014) of long-term (>1 year) incubations of soil effected by permafrost across the Arctic showed that using a three-pool decomposition model less than 5% of all carbon was labile at 5°C and decomposed rapidly within one year. The slow carbon pool contained between 10-90% of total carbon with a turnover time of 5-15 years. The soil organic carbon loss was projected to be between 20% and 90% within 50 incubation years (Schädel et al., 2014). Data of another incubation study of Siberian organic and mineral soils suggest that with higher temperatures recalcitrant compounds are preferentially respired by soil microbes (Biasi et al., 2005). However, incubation studies exclude the in-situ environmental conditions. In-situ studies at various permafrost sites have shown greater amounts of old carbon emissions with increased thawing of the permafrost. An in-situ snow addition experiment with snow fences in Alaska found older carbon emissions with increased thickness of the active layer 13 years after the fence installation (Nowinski et al. 2010). Schuur et al. (2009) compared sites whereby some have experienced permafrost thawing over 15 years and determined greater amounts of old carbon emissions with increased thawing suggesting that old, previously frozen carbon was metabolised. In Abisko, northern Sweden, a study with an in-situ temperature manipulation experiment with open top chambers over 8 years found increased ecosystem respiration rates which mainly (69%) originated from deeper stored carbon (25-50 cm depth) of the active layer (Dorrepaal et

al., 2009). All these studies suggest that the organic carbon in today's still frozen permafrost soils is highly bioavailable for degradation but the actual (today's) occurring degradation and/or stabilization processes in the active layer covering permafrost soils are not understood well.

Microbial metabolic activity is a key factor in the mineralization of soil organic matter (OM) and the active layer is the main place for soil OM decomposition within the permafrost. All three domains of microorganism (bacteria, archaea, and fungi) are present in the harsh permafrost environment (e.g., Jansson and Tas, 2014) dominated by its low temperatures and great annual temperature fluctuations (Fig. 2). Generally, bacteria seem to dominate in diversity and abundances the microbial communities in active layers (Steven et al., 2008; Yergeau et al., 2010) and have adapted to these extreme conditions through metabolic regulation (Jansson and Tas, 2014 and references there in). However, so far it is not well known which carbon pools are preferable metabolised by microorganisms.

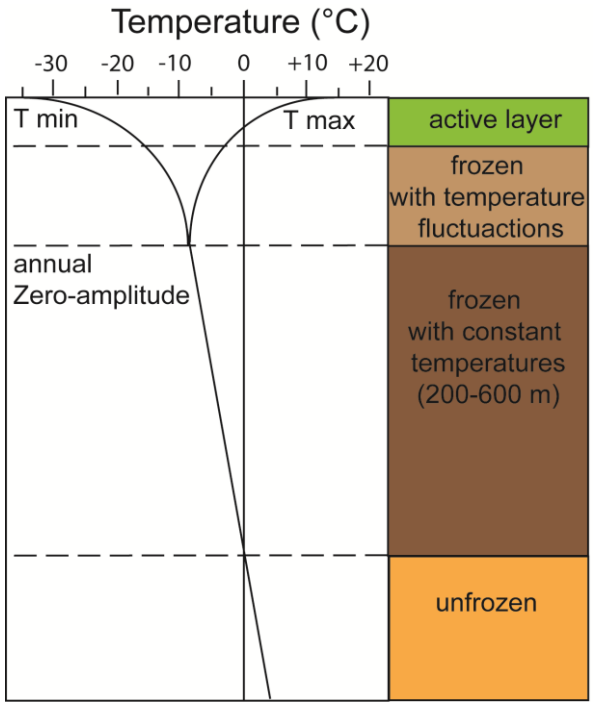


Fig. 2: Permafrost temperature profile with maximum (T max) and minimum temperature (T min) over the year and over depth modified after Washburn (1973) and Boike et al. (2013)

Stabilization of OM in temperate surface soils is well studied (Sollins et al., 1996; von Lützow et al., 2007; Kögel-Knabner et al., 2008). Physical protection mechanisms as the formation of soil aggregation or organo-mineral associations were found to be more important than the chemical recalcitrance of the organic compounds (Marschner et al., 2008). So far it is not well known if these mechanisms may preserve OM in permafrost soils which differ significantly from temperate soils mainly due to the repetitive freezing and thawing circles which affect these soils (Fig. 2).

## 1.2 Objectives

This study concentrates on obtaining basic knowledge about the soil OM composition and dynamic of the polygonal tundra of the Siberian Lena Delta in Russia (Fig. 1 and 3). The polygonal tundra covers only 3% of the Arctic landmass (Minke et al., 2007). However, sustainable amounts of the greenhouse gas $CH_4$ are already being emitted here due to the large areas of wetlands (McGuire et al., 2009) and the deeper old carbon stocks are predicted to turn into additional carbon sources for the atmosphere with permafrost degradation and a thickening active layer due to global warming (e.g., Schuur et al., 2009; Nowinski et al., 2010). Therefore, a basic understanding of today's soil OM composition and dynamic within the active layer is required to project reactions between this system and global warming. Microbial degradation is a key factor in the soil OM dynamic and the main place for microbial activity in permafrost soils is the active layer. Thus, this thesis concentrates on the active layer soil horizons and the still frozen permafrost top layer. So far very little is known about the quality of the soil OM, possible mechanisms for the stabilization of the soil OM and its availability for the living microorganisms in the active layer of permafrost soils in the polygonal tundra.

The main objectives of this thesis were to:

- Determine different exogenous carbon contaminations (process blank) during compound-specific radiocarbon analysis (Manuscript I)
- Characterise the soil organic matter (OM) composition and its distribution in the polygonal tundra soils of the Lena Delta (manuscript II + manuscript IV)
- Identify stabilization mechanisms of the soil OM in polygonal tundra soils of the Lena Delta (manuscript II)
- Investigate the microbial communities in the polygonal tundra soils of the Lena Delta (manuscript III + IV)
- Determine which carbon pools ('young'/labile or 'old'/stable) are metabolised mainly by the microbial community in polygonal tundra soils of the Lena Delta (manuscript IV)

## 1.3 Organisation of the thesis – Overview of the manuscripts

A general introduction into the Siberian study area (Lena Delta) and the methods used in this thesis are given in chapter 2. Chapters 3 to 5 are independent manuscripts (I – III) which have been published or were under review in peer-reviewed international journals during the time this thesis was submitted (February 2015). Chapter 6 includes further results written in the form of a paper manuscript (IV) in preparation for submission. In chapter 7 a synthesis and an overall discussion arising from the studies follow. The thesis ends with a summary and conclusions section (chapter 8). In the following two paragraphs, an overview of the four studies (manuscripts I – IV) is given highlighting the connecting links between the studies.

In chapter 3 (manuscript I) the pre-treatment methods for the radiocarbon measurement of the new CologneAMS dating centre are described in detail. One main subject was the evaluation of process contaminations during the pre-treatment (preparative gas-chromatography) of single organic compounds for $^{14}C$ analysis. The process contaminations are relatively small which allows the $^{14}C$ analysis of individual bacterial and high plant wax lipids, known as compound-specific radiocarbon analysis, to evaluate the degradation of organic material in the active layer of permafrost soils (see manuscript IV/chapter 6).

In chapter 4 (manuscript II) the soil OM of an active layer in the Lena Delta polygonal tundra is characterized and stabilization mechanisms of the OM are investigated. The OM is mainly composed of undecomposed, plant derived material. By analysing physical soil fractions with lipid biomarker and $^{14}C$ analysis, it was suggested that the main stabilization mechanisms of OM in temperate soils (formation of soil aggregates and organo-mineral associations) seem to have little effect on this active layer soil (manuscript II). This suggests that soil OM is available for microbial degradation. In chapter 5 and 6 this statment is further investigated. The microbial community is identified (chapter 5 and 6) using two microbial membrane lipid biomarkers, bacteriohopanepolyols (BHPs; manuscript III) and phospholipid fatty acids (PLFAs; manuscript IV). In chapter 6 (manuscript IV) compound-specific radiocarbon analyses of single or pooled microbial PLFA lipids were performed to identify ‘young’, presumably labile and/or ‘old’, presumably stable carbon pools which are metabolised by microorganisms. In combination with $^{14}C$ analysis of isolated single plant wax lipids (*n*-alkanes and *n*-fatty acids) and further physical soil fractions, information on the origin of the microbial metabolised carbon pools was gained.

# 2. Material and methods

This chapter gives a short overview of the study area and the methods used in this thesis. Further details are described in the individual manuscripts.

## 2.1 Study area – the Siberian Lena Delta

The study sites (Fig. 3) are located in the Lena Delta in Siberia (Russia). Covering 32,000 km$^2$, the Lena Delta is the largest delta in the Arctic (Are and Reimnitz, 2000) and is located in the zone of continuous permafrost with a thickness between 400-600 m in this region (Romanovskii and Hubberten, 2001). The climate is arctic continental with a low annual mean precipitation (125 mm) and low annual mean air temperatures (-12.5°C), but with great seasonal temperature differences between summer (July 10.1°C) and winter (February -33.1°C; Boike et al., 2013).

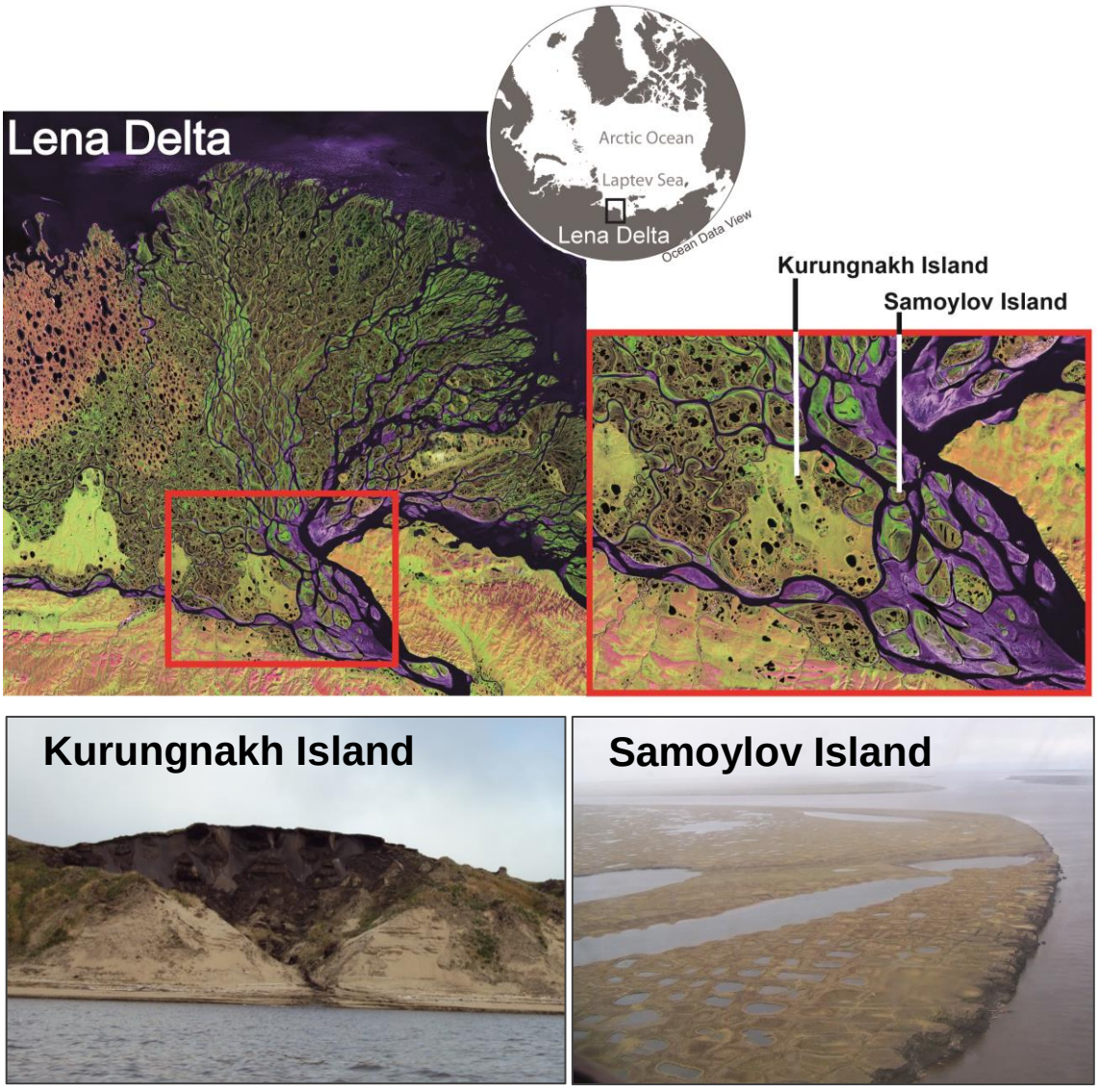


Fig. 3: The Siberian Lena River Delta, Russia and the Islands Samoylov and Kurungnakh in the delta (Landsat 7 image modified from www.earthobservatory.nasa.gov/IOTD/view.php?id=2704)

The Lena River Delta consists of three different geomorphic terraces (Grigoriev, 1993). The first terrace covers the recently active and mainly eastern part of the delta and is made up of Holocene fluvial sediment. It is characterised by an ice-wedge polygonal tundra, large thermokarst lakes and active flood plains. Ice wedges form through seasonal frost-cracking repeatedly pushing material upwards to form elevated rims (Fig. 4; e.g., Fiedler et al., 2004). The second terrace comprises mainly the north-western part of the delta and consists of a several tens of meters thick sediment layer predominated by fluvial sand which was deposited between the Late Pleistocene and early Holocene. Its landscape is dominated by sandy sediments with low ice content and many large thermokarst lakes (Schirrmeister et al., 2011). Erosional remains of a Late Pleistocene accumulation plain in the foreland of the Chekanovsky ridge, south of the delta, form the third terrace. It consists of three units: a lower 15-20 m thick sand unit of fluvial deposits of the Paleo-Lena River, covered by an approx. 15 m thick ice complex (Russian: Yedoma) unit which is made of large ice-wedges and paleosols of clastic material from the Chekanovsky Ridge. On top of the Yedoma is a 2-3 m thick Holocene unit of mostly aeolian silty sand with small ice wedges (3-5 m wide). The landscape of the third terrace is characterised by polygonal tundra and thermokarst features (Schwamborn et al., 2002; Schirrmeister et al., 2003; Morgenstern et al., 2011; Schirrmeister et al., 2011; Zubrzycki, 2013).

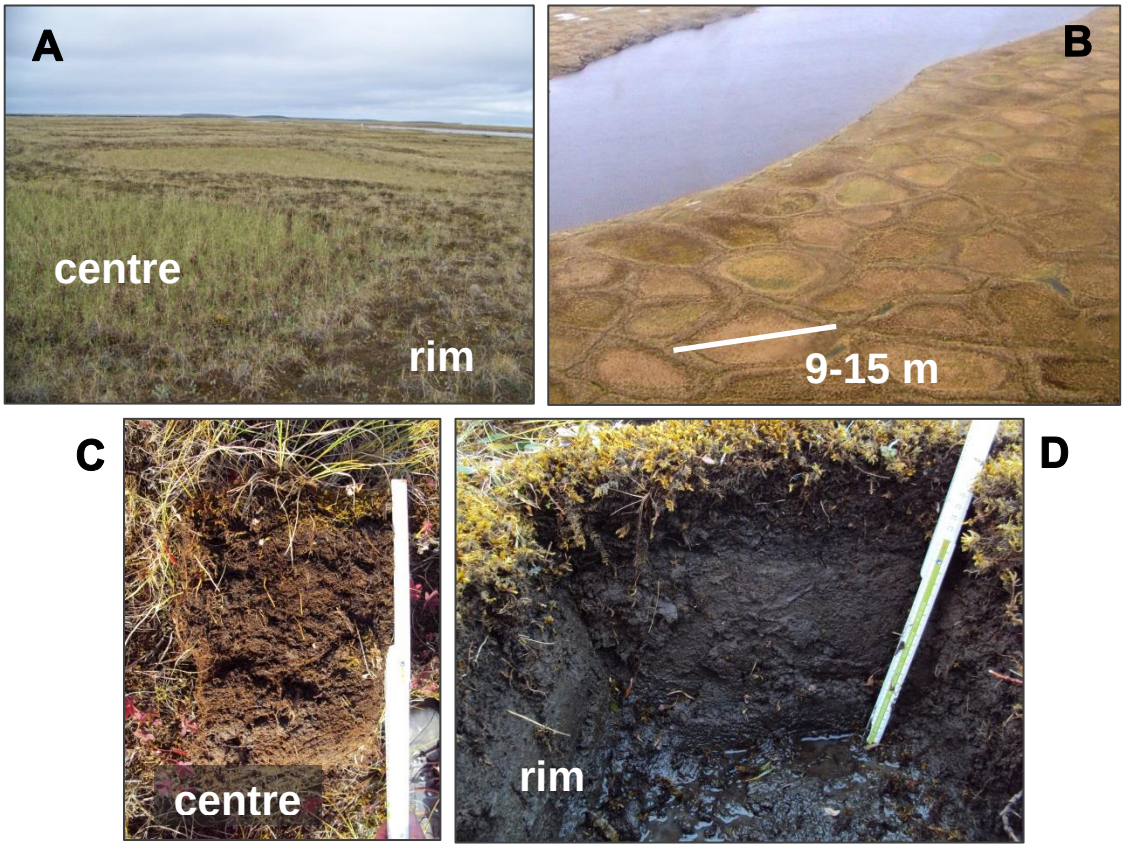


Fig. 4: A and B) Polygonal tundra landscape structures (polygon rim and centre) and active layer soils of a polygon centre (C) and a polygon rim (D)

The vegetation of the Lena Delta is dominated by mosses and grasses. Wet polygon centres also contain some sedges and dry polygon rims lichens, some herbs and willow shrubs (Mueller, 1997; Boike et al., 2013). The tree line is pushed north by the Lena River to the very south of the Delta where small larch (*Larix* spp.) are growing. According to the US Soil Taxonomy, the soils in the Delta belong to the soil type Gelisols represented by various great groups (Soil Survey Staff, 2010). The first and third terraces are dominated by Glacic Aquiturbels on polygon rims and Typic or Ruptic Historthel in depressed polygon centres. Typic Psammoturbel dominate on the second terrace (Zubrzycki et al., 2012). In northern latitudes the soil type Gelisols covers an area of about 27% (Jones et al., 2010).

Within the Lena-Delta the study sites were located on Samoylov Island (72.37° N, 126.48° E) and on Kurungnakh Island (72.32° N, 126.24° E; Fig. 3). Samoylov belongs to the first, recent active delta-terrace and Kurungnakh is part of the third terrace (Yedoma). On both sites only the top Holocene unit was sampled.

## 2.2 Methods

Samples were taken from a soil pit (1x1 m) in August 2009 and 2010 when the active layer thickness is greatest. The soil samples were immediately frozen after sampling and stayed frozen during transport to Germany. Prior to all analyses the soil material was freeze-dried (Fig. 5).

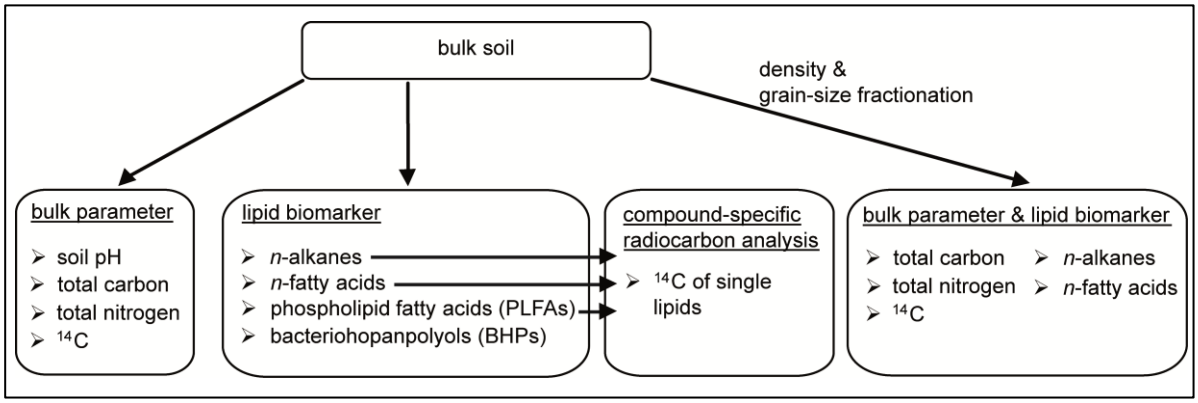


Fig. 5: Overview of methods used in this thesis

### 2.2.1 Bulk parameter methods

A short description of the methods used to measure the bulk parameters in this thesis is given here. Details are provided in the respective manuscripts.

- Total carbon and total nitrogen: with an Analyzer vario MICRO cube (Elementar, Germany; 5 mg soil with 20 mg oxidant; manuscript II, III, and IV)
- soil pH: measured in $H_20$ (ratio 1:2.5) one hour after water addition (IUSS Working Group WRB, 2006; manuscript II, III, and IV)
- soil fractionation: by density fractionation ($1.8g*cm^{-3}$) and grain-size fractionation of the heavy mineral fraction (manuscript II)

- $^{14}C$ of bulk soil and $^{14}C$ of single soil fractions: pre-treatment with 1% HCl and measured as graphite in an accelerated mass spectrometer (AMS; at the ETH Zurich and the CologneAMS; manuscript II and IV)

### 2.2.2 Organic geochemical methods

Several different lipids were analysed in this thesis (Fig. 6). In order to gain the lipids from the samples various analytical steps were necessary (Fig. 7). The total lipid fraction was extracted from the soil with organic solvent (e.g., dichlormethane or methanol) using three different ways:

- with the automatic solvent extraction system (ASE; Dionex, USA; manuscript II, IV)
- placing the mixture of soil and organic solvent in an ultrasonic bath (manuscript II, III)
- shaking the mixture of soil and organic solvent for several hours (manuscript III, IV).

Further wet chemical methods have been used in this thesis to purify the lipid biomarkers:

- Saponification: to free bounded fatty acids by cleavage of ester bounds
- Silica gel chromatography: to separate the neutral lipid fraction into fractions of different polarity: aliphatic hydrocarbons (*n*-alkanes), aromatics (ketones), and hetero-compounds (including alcohols, sterols)
- Methylation: esterification of the COOH-group of the *n*-fatty acids so that the compounds can be measured on the gas chromatograph (GC)

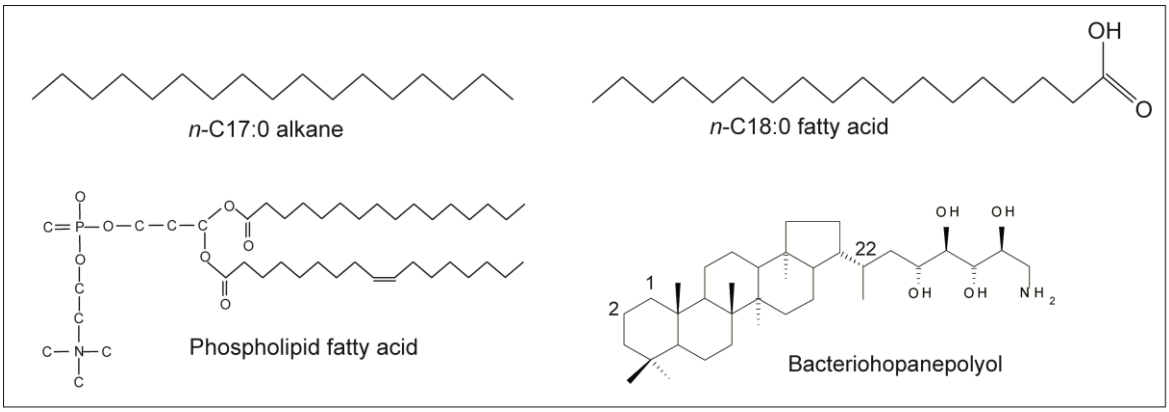


Fig. 6: Examples of biomarkers used in this thesis

Measurements of the different lipid biomarkers were taken using various instruments:

- Gas chromatography with a flame-ionizer detector (GC-FID; 5890 series II plus, HP, Germany): *n*-alkanes and *n*-fatty acids (manuscript II, IV)
- High pressure liquid chromatography – multistage mass spectrometry (HLPC-$MS^n$; ThermoFinnigan, UK) equipped with an atmospheric pressure chemical ionization (APCI) ion source): BHPs (manuscript III)

- Gas chromatography – mass spectrometry (GC-MS; DeltaPLUS XP, Thermo Scientific, USA): PLFAs (manuscript IV)

### 2.2.3 Compound-specific radiocarbon analysis

For the compound-specific radiocarbon analysis (CSRA) larger amounts of soil samples (mostly > 180g) need to be extracted to gain enough material for a single compound (>30-100 µgC) for the $^{14}C$ AMS measurement. Therefore, the lipid extraction with organic solvents was done using the Soxhlet apparatus instead of using an ASE or an ultrasonic method (manuscript IV). After further purification steps described in 2.2.2, single lipids were isolated from the lipid compound class (Fig. 7) by using a preparative gas-chromatograph (prepGC; Fig. 8; Eglinton et al., 1996).

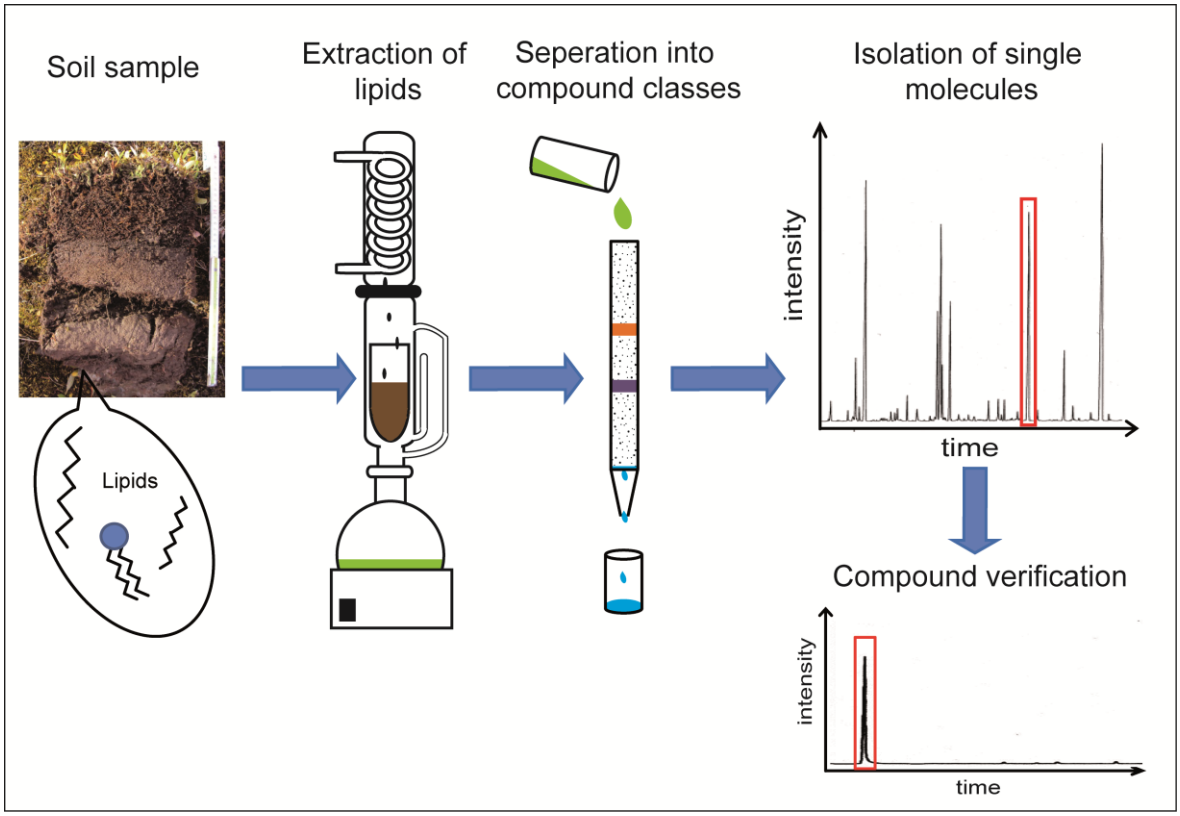


Fig. 7: Schematic diagram of lipid extraction and isolation of single compounds

After the isolation, single lipids were tested for contaminations on a GC-FID. Pure compounds were then transferred using an organic solvent into pre-combusted quartz tubes. The tubes were evacuated, flame sealed and combusted converting the organic carbon into carbon dioxide. The gas was purified and quantified under vacuum and then flame-sealed into small pre-combusted glass tubes. These small glass tubes were then sent to ETH Zurich, Switzerland and were directly connected to the ion gas source of the MICADAS (manuscript IV).

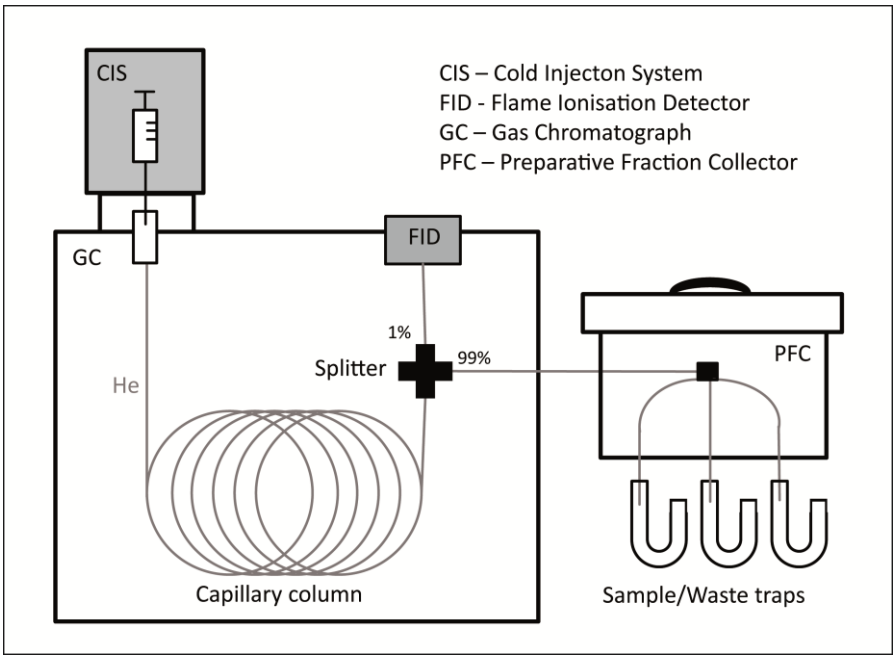


Fig. 8: Schematic diagram of a preparative gas-chromatographic system (prepGC) with a preparative fraction collector (PFC) for the isolation of single molecules

A contamination validation (manuscript I) of the purification prepGC system was completed by analysing *n*-alkane and *n*-fatty acid standards (of each modern and $^{14}C$ free) untreated and treated the same way as the target lipids. After the $^{14}C$ measurements of the target compounds, their $^{14}C$ contents were corrected for the exogenous carbon introduced during the chromatographic isolation and subsequent sample handling (process blank) using an isotopic mass balance calculation (manuscript IV).

# 3. Manuscript I: Quantifying the exogenous carbon contamination for compound-specific radiocarbon analysis – *Status report on sample preparation facilities for $^{14}C$ analysis at the new CologneAMS center*

by

Rethemeyer J., Fülöp R.-H., **Höfle S.**, Wacker L., Heinze S., Hajdas I., Patt U., König S., Stapper B., Dewald A. (2013)

*Nuclear Instruments and Methods in Physics Research B* **294**, 168–172.

Nuclear Instruments and Methods in Physics Research B 294 (2013) 168–172

Contents lists available at SciVerse ScienceDirect

Nuclear Instruments and Methods in Physics Research B

journal homepage: www.elsevier.com/locate/nimb

# Status report on sample preparation facilities for $^{14}C$ analysis at the new CologneAMS center

J. Rethemeyer [a,*], R.-H. Fülöp [a], S. Höfle [a], L. Wacker [b], S. Heinze [c], I. Hajdas [b], U. Patt [a], S. König [a], B. Stapper [a], A. Dewald [c]

[a] Institute of Geology and Mineralogy, University of Cologne, 50674 Cologne, Germany
[b] Ion Beam Physics, ETH Zürich, 8093 Zürich, Switzerland
[c] Institute of Nuclear Physics, University of Cologne, 50674 Cologne, Germany

ARTICLE INFO

*Article history:*
Received 31 May 2011
Received in revised form 7 February 2012
Available online 18 February 2012

*Keywords:*
New AMS facility
Radiocarbon sample preparation
Process blank
Small samples
Compound specific radiocarbon

ABSTRACT

The new AMS facility at the University of Cologne (CologneAMS), Germany, was established in 2010 with the delivery of the HVE 6 MV Tandetron AMS, which will be used for $^{14}C$, $^{26}Al$, $^{36}Cl$, $^{41}Ca$, $^{129}I$, $^{239}U$ and $^{244}Pu$ analyses. Parallel to the AMS installation the radiocarbon group has started to set up and test sample preparation methods and instruments for different materials. We present first results of reference and standard materials that have been processed and graphitized in our lab and measured at the ETH and CologneAMS facilities. The graphitization blank and its influence on small samples sizes processed with an automated graphitization system have been determined. Work on isolation of individual organic compounds with a preparative gas chromatography system has been started. The focus of our future work will be on reducing process blank levels and sample sizes as well as on the application of compound-specific radiocarbon analyses in (paleo-) environmental research.



## 1. Introduction

The new AMS facility at the University of Cologne, Germany (CologneAMS) is based on a 6 MV Tandetron system from High Voltage Engineering Europe (HVE; the Netherlands) that will be used for the analysis of $^{10}Be$, $^{14}C$, $^{26}Al$, $^{36}Cl$, $^{41}Ca$, $^{129}I$, $^{239}U$ and $^{244}Pu$. The AMS was funded by the German Research Foundation (DFG) in 2007 and the installation of the system in the Institute of Nuclear Physics at the University of Cologne was started in May 2010 after completion of extensive reconstructions of an existing building. The CologneAMS facility is run collaboratively by the Institute of Geology and Mineralogy and the Institute of Nuclear Physics with two working groups being responsible for sample preparation.

Parallel to the AMS installation the radiocarbon group, which replaces the former conventional radiocarbon dating laboratory at the Institute of Prehistoric Archaeology, has started to establish and test sample preparation methods for different materials and to set up instruments for sample conversion into AMS graphite targets. The preparation of radiocarbon samples is integrated in the existing organic geochemistry laboratories at the Institute of Geology and Mineralogy. This provides additional possibilities including the gas chromatographic isolation of individual organic molecules for compound-specific radiocarbon analysis.

Here, we present a brief overview of the methods and instruments we currently use for the pretreatment of organic materials, carbonate samples, and bones for AMS radiocarbon dating. First results of tests with reference and standard materials are shown as well as the process blank of the automated graphitization equipment (AGE) [1] and sample size limits that can be processed reliably. We also present first tests performed to determine extraneous carbon added during the isolation of individual organic compounds with preparative gas chromatography. AMS $^{14}C$ measurements were performed with the MICADAS AMS at ETH Zurich (Switzerland) [2,3], and after installation, with our new 6 MV HVE Tandetron AMS [4].

## 2. Sample preparation methods

The amount and type of samples that should be radiocarbon dated define the type and intensity of the necessary pretreatment. The different pretreatment approaches described below are currently used in our laboratory for organic samples, carbonates, and bones.

### 2.1. Pretreatment of organic material

Organic samples are first inspected under a microscope for visible contaminants that can be removed mechanically. Most organic materials including marine and lake sediments, charcoal, wood, and plant remains are chemically extracted by standard acid–alka-

* Corresponding author.
*E-mail address:* janet.rethemeyer@uni-koeln.de (J. Rethemeyer).

0168-583X/$ - see front matter © 2012 Elsevier B.V. All rights reserved.
doi:10.1016/j.nimb.2012.02.012

li–acid extraction (AAA) to remove inorganic carbon and humic substances, which may have been transported from other depth intervals in the soil or sediment layers that should be dated [5].

The AAA procedure starts with an acid extraction of the sample (1% HCl, ca. 10 h, room temp.; carbonate-rich samples are heated ca. 1 h, 60 °C) followed by washing of the residue repeatedly with Milli-Q water (Millipore, USA). For very small samples the extraction time is reduced (1 h, room temp.) and no alkali extraction is applied. The alkali extraction with 1% NaOH (4 h, 60 °C) yields an alkali-soluble fraction and a non-soluble residue (humin). Humic acids are precipitated from the soluble fraction by acidification with 37% HCl to pH < 1 followed by rinsing the precipitate with Milli-Q water to a pH of about 2. The acid and alkali insoluble residue, the humin fraction, is also washed repeatedly with Milli-Q water and treated again with 1% HCl (ca. 10 h, room temp.) to remove atmospheric $CO_2$ which might have been introduced during the alkali extraction, and finally rinsed with Milli-Q water to pH > 4.

### 2.2. Bone pretreatment

A discussion of the various problems associated with bone pretreatment can be found in [6,7]. We have tested the following approach for cleaning of bones and extraction of the collagen fraction: a 3–5 g bone subsample is cut from the original sample. The surface of the subsample is abraded with a diamond drill and cleaned twice with Milli-Q water in an ultrasonic bath (15 min). After drying, the sample is inspected under a microscope for any contamination that might have been introduced during handling and then crushed into small pieces. If necessary, organic contaminants including conservation products are removed with a sequence of organic solvents of increasing polarity starting with hexane, followed by dichloromethane, and methanol (12 h each; modified after [8]). Large samples are extracted in glass fiber thimble in a Soxhlet extractor and small samples in an Accelerated Solvent Extraction system at 120 °C and 75 bar (ASE 200; Dionex, USA) using the same sequence of organic solvents as above and an extraction time of 30 min for each solvent.

The dried samples are decalcified with 1 M HCl (at least 3 h, room temp.). The samples are further cleaned from insoluble contaminants and humic substances by adding Milli-Q water and thereby increasing the pH to about 3 while the sample is placed in the agitating water bath (24 h, 60 °C). After cleaning the samples are converted into gelatin, [9,10] which is subjected to hot filtration (60 °C) through glass fiber filters. If necessary the volume of the filtrate is reduced under a $N_2$ stream while heated at 40 °C, and finally the gelatin is freeze-dried and converted to graphite as described below (Section 2.5).

### 2.3. Carbonate pretreatment and hydrolysis

We use a newly developed hydrolysis system described in detail by Wacker et al. [11] in which carbonates are converted into $CO_2$ with $H_3PO_4$ in septum sealed vials under a He atmosphere. This system eliminates the usage of liquid nitrogen and self-made high vacuum systems for gas purification after carbonate hydrolysis in evacuated glass tubes as it is often done. A further advantage is that the hydrolysis procedure can be automated by using an auto-sampler, which can be coupled with the AGE system.

Briefly, visible contaminations on the carbonate surface are mechanical removed, followed by washing with Milli-Q water in an ultrasonic bath to remove soil remains and recrystallized shell material [12]. The surface of the shell is then leached with 1 M $H_2SO_4$, which is neutralized with Milli-Q water. After drying, the sample is pulverized and transferred to cleaned (dichloromethane rinsed, combustion at 450 °C) 12 ml Labco® vials (Labco Limited, UK), which are closed with septum caps. After air is removed from the vial with a He flow through a double-walled needle (Thermo, Germany) at a rate of 100 ml/min for 12 min, 99% $H_3PO_4$ is added and left to react for 6 h at 75 °C. The evolved $CO_2$ is transferred with a He flow to the AGE system while water is retained on a water trap (phosphorus pentoxide).

### 2.4. Isolation of individual organic compounds

Compound-specific radiocarbon analysis involves the extraction of the desired fraction (often lipids) from the sample material, followed by different purification procedures like chromatographic separation of compound classes of different polarities and often the isolation of individual molecules with preparative gas or liquid chromatography [13,14]. Each step of the complex procedure may introduce contaminants.

We performed first tests with dated GC standards to quantify the amount and origin of extraneous carbon introduced during the gas chromatographic isolation of individual organic compounds. The preparative gas chromatograph (PC-GC) consists of a GC (7680 Agilent, USA) equipped with a CIS 4 injection system (Gerstel, Germany) and a 'megabore' ultra-low bleed capillary column (30 m, 0.53 mm I.D.; Restek, USA), which is coupled with a fraction collector (PFC; Gerstel, Germany). Two *n*-alkanes and two *n*-carboxylic acids GC standards with modern and (close to) fossil $^{14}C$ concentration were chosen in order to monitor possible modern or fossil carbon contributions (Table 1). The standards were dissolved in dichloromethane or hexane and repeatedly injected (50–100×) in the PC-GC system. The column temperature for *n*-alkanes and for *n*-fatty acids was increased from 70 to 150 °C at 20 °C $min^{-1}$ and then to 320 °C at 10 °C $min^{-1}$ and maintained for 9 min. The PFC transfer line was heated constantly at 320 °C. Long-chain compounds (>$C_{24}$) were first trapped at 60 °C but compound recoveries could be increased by leaving the traps of the fraction collector at room temperature for short and long chain compounds. The isolated compounds were recovered from the glass traps of the PFC with 1000 µl dichloromethane and measured on a GC with flame ionization detector (FID) to check purity and recovery of the isolated compound. After solvent evaporation under $N_2$ stream, some compounds were converted to graphite with the AGE system as described below (Section 2.5). Because of the stronger influence of the EA-AGE blank (Section 3.1) on small samples sizes typically isolated with PC-GC, most isolated compounds (30–140 µg C) were combusted in quartz tubes

**Table 1**
First results of recovery and contamination tests of the PC-GC system with dated GC standards (*n*-carboxylic acids, *n*-alkanes). Carboxylic acids were isolated as methyl esters and $^{14}C$ results were corrected for the methyl carbon from methanol (0 pmC). Samples were converted to graphite with the AGE system or by sealed tube combustion to $CO_2$ and measured directly with the MICADAS gas ion source [15,16]. $^{14}C$ values are corrected for combustion and graphitization blank.

| GC standard | Treatment | *n* | Recovery[f] (%) | $^{14}C$ (pmC) |
|---|---|---|---|---|
| Octadecanoic acid[a] | Untreated | 1 | | 106.38 ± 0.15 |
| | PC-GC[e] | 3 | 99 | 101.95 ± 1.62 |
| Triacontanoic acid[b] | Untreated | 1 | | 0.25 ± 0.07 |
| | PC-GC[e] | 4 | 86 | 3.63 ± 1.41 |
| Octadecane[c] | Untreated | 1 | | <0.08 |
| | PC-GC | 4 | 91 | 3.95 ± 0.74 |
| Hexamethyl tetracosane[d] | Untreated | 1 | | 101.87 ± 0.33 |
| | PC-GC | 3 | 72 | 100.42 ± 2.47 |

[a] Fluka, Prod. No. 85679-500MG (Lot. BCBB2165).
[b] Sigma, Prod. No. T3527-100MG (Lot. 018K3760).
[c] Fluka, Prod. No. 74691-5G (Lot. 0001448903).
[d] Fluka, Prod. No. 85629-50ML (Lot. 0001418796).
[e] Includes one compound measured as graphite.
[f] Compound recovery was quantified with GC-FID.

(900 °C, 4 h) with copper oxide (ca. 60 mg), both pre-combusted, and the purified $CO_2$ was measured directly with the MICADAS gas ion source [15,16].

### 2.5. Sample combustion, hydrolysis and graphitization

We use an advanced version of the AGE system [1] coupled with an elemental analyzer (EA; VarioMicroCube, Elementar, Germany) for the combustion and graphitization of organic samples. The EA is equipped with a combustion tube filled with $PbCrO_4$ and copper oxide and a reduction tube with copper and silver wool. Depending on sample size, pretreated organic samples are weighed into tin boats ($H \times W \times D$: 4 × 4 × 11 mm, IVA, Germany) and combusted in the EA. Water evolved during sample combustion is retained on a water trap (phosphorus pentoxide) in the EA and the pure $CO_2$ is transferred to the zeolite trap of the AGE. The $CO_2$ is thermally desorbed from the zeolite trap and released into a reactor of the AGE where it is converted to graphite with hydrogen over iron as catalyst (Alfa-Aesar, iron powder, spherical, <10 micron). We tested the removal of contamination from the tin containers by cleaning them twice with dichloromethane, which reduced blank levels for smaller samples sizes. We thus included this step in our sample processing protocol.

For carbonate hydrolysis, the $CO_2$ transfer line of the EA is disconnected from the AGE and replaced by a transfer line to the hydrolysis device described above (Section 2.3) and in detail by Wacker et al. [this issue]. To prevent contamination all graphitized samples are stored in argon filled glass tubes before pressing into AMS target holders with a pneumatic sample press (ETH Zurich).

## 3. Results and discussion

### 3.1. Process blank

The assessment and minimization of the process blank is essential as it limits the measurement of small samples sizes and old material. Carbon contamination is introduced during chemical processing and transformation into graphite. A major source of contamination is the combustion of organic materials either in quartz ampoules or in EA tin containers [15,17,18]. We evaluated the blank of the AGE and tested to reduce the contamination originating from the tin containers by cleaning them with dichloromethane (GC grade quality). No significant blank reduction (tested with anthracite, RAG Anthrazit Ibbenbueren GmbH, Germany) was discernible for normal sized (1 mg) samples. To improve the blank values obtained, a new coal (Pocahontas #3, Argonne National Laboratory, USA) has been used to test the size dependency of graphitization blanks. The coal was prepared in solvent cleaned tin boats. For small sample sizes ranging from 150 to 350 μg C (Fig. 1a) still reasonable blank value of 0.52 pmC (pmC related to 1950) equivalent to 43,400 ± 600 years BP were obtained. Samples smaller than 120 μg C are strongly influenced by contaminants probably of other origin. The blank calculated according to the model of constant contamination [15,19] assuming a contamination with 75 pmC was fitted to the experimental data (Fig. 1a) yielding about 1.7 μg C (anthracite) and 0.7 μg C (Pocahontas coal). Normal sized (1 mg) samples measured at CologneAMS yield an average blank value of 0.12 pmC for cleaned tin boats (Fig. 1b). The contribution of old contaminants including solvent remains was checked by the analyses of modern standards including OX-II (Fig. 2) and some VIRI samples (Table 2), which were not $^{14}C$ depleted. The scatter in the blank results (Fig. 1a and b) reflects that the contamination introduced is variable in size and $^{14}C$ concentration. More detailed tests need to be performed to evaluate possible sources of contamination besides the tin containers.

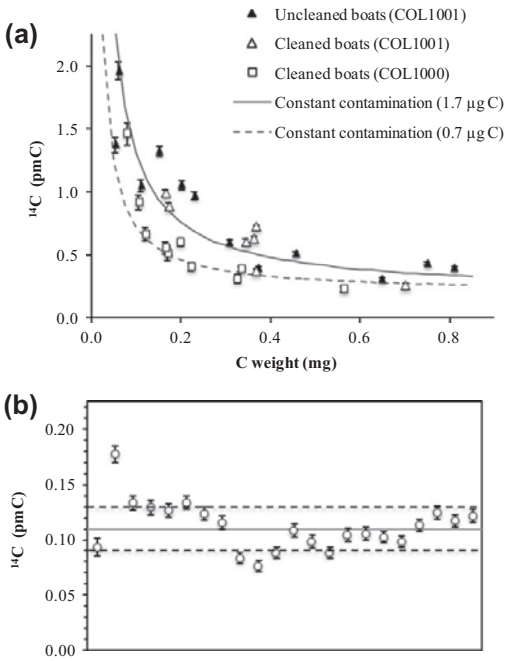


**Fig. 1.** (a) $^{14}C$ concentration of blank material (coal, anthracite) vs. sample size measured at ETH Zurich. The curves are calculated with the model of constant contamination: 1.7 μg C (uncleaned) and 0.7 μg C (cleaned tin containers) of 75 pmC with an offset of 0.2 pmC. (b) Results for normal sized coal (1 mg C) measured at Cologne with 2-σ uncertainties (dashed lines).

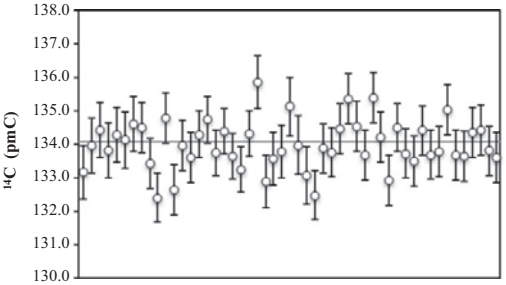


**Fig. 2.** $^{14}C$ result of OX-II (1 mg C) measured in Cologne (line represents reference values).

First results of blank tests of the new carbonate hydrolysis approach in septum sealed vials under a He atmosphere are presented in Wacker et al. [this issue]. The method yields very low blank values even for small sample sizes (e.g. 300 μg C, >48,500 ± 800 years BP). A constant contamination similar to the one of the combustion in the EA is not observed suggesting that the carbon contamination observed for organic samples is introduced during sample combustion in the EA.

### 3.2. PC-GC blank

Compound-specific $^{14}C$ analysis is challenged by the small sample size and the many steps necessary for the extraction and purification of individual organic compounds, which may introduce

**Table 2**
Results for reference materials (ca. 1 mg C) graphitized with the AGE.

| Sample | Material | Measured value | Reference value | *n* | AMS measurement |
|---|---|---|---|---|---|
| IAEA C5[a] | Wood | 23.30 ± 0.12 pmC | 23.05 ± 0.02 pmC | 2 | ETH |
| IAEA C6 | Sucrose | 150.41 ± 0.28 pmC | 150.60 ± 0.10 pmC | 5 | ETH |
| IAEA C8 | Oxalic acid | 15.06 ± 0.09 pmC | 15.03 ± 0.17 pmC | 2 | ETH |
| VIRI M[b] | Wood | 73.61 ± 0.41 pmC | 73.90 ± 0.03 pmC | 4 | COL |
| VIRI O | Cellulose | 98.41 ± 0.55 pmC | 98.46 ± 0.04 pmC | 4 | COL |
| VIRI S | Barley mash | 108.85 ± 0.61 pmC | 109.96 ± 0.04 pmC | 3 | COL |
| VIRI T | Humic acid | 65.75 ± 0.37 pmC | 65.82 ± 0.03 pmC | 3 | COL |
| VIRI U | Humic acid | 22.98 ± 0.15 pmC | 23.08 ± 0.02 pmC | 3 | COL |
| VIRI H | Whale bone | 9618 ± 48 years BP | 9528 ± 7 years BP | 4 | COL |
| VIRI I | Whale bone | 8373 ± 47 years BP | 8331 ± 6 years BP | 4 | COL |
| Ox M[c] | Mammoth bone | 52,290 ± 1583 years BP | >147k years BP | 4 | COL |

[a] IAEA Reference Products, Vienna, Austria.
[b] VIRI: fifth radiocarbon intercomparison [22,23].
[c] Oxford mammoth bone [24].

contamination that is difficult to quantify [14,20,21]. Initial tests with GC standards of modern and fossil origin show compound recoveries for the *n*-alkanes and *n*-carboxylic acids of intermediate ($C_{18}$) and long chain length ($C_{30}$) between 72% and 99% (traps at room temp.; Table 1). Lower recoveries were obtained for long chain compounds initially trapped at 60 °C to avoid compound crystallization in the intersection of the PFC capillaries into the glass traps which apparently caused material losses. Contaminants introduced during the gas chromatographic isolation were determined by GC-FID analysis and were less than 0.6%. The $^{14}C$ depletion of the isolated modern and the $^{14}C$ enrichment of the old/fossil GC standards relative to the untreated material reflect the contribution of exogenous carbon from both, modern and fossil sources as also observed in previous studies [18,21]. The difference in $^{14}C$ concentration between the untreated standard material and the isolated compounds was 3.4 and 4.0 pmC for old/fossil material and for modern material 4.4 and 1.5 pmC (*n*-carboxylic acids and *n*-alkanes, respectively; Table 1). The $^{14}C$ concentration of the exogenous carbon ($^{14}C_{blank}$) and its amount ($C_{blank}$) cannot be determined directly. Thus, dated standard materials processed in a similar way like the target compounds and isotopic mass balance calculation are often used to determine both parameters. Using our results for the isolated standards ($^{14}C_{measured}$ and $C_{measured}$) and for untreated material ($^{14}C_{sample}$ and $C_{sample}$) we estimated $C_{blank}$ by mass balance calculation (Eq. (1)) assuming that $^{14}C_{blank}$ is either modern (106 pmC) or fossil (0 pmC).

$$^{14}C_{measured} \cdot C_{measured} = {}^{14}C_{sample} \cdot C_{sample} + {}^{14}C_{blank} \cdot C_{blank} \quad (1)$$

with $C_{measured} = C_{sample} + C_{blank}$.

The mass of exogenous carbon ($^{14}C_{blank}$: 0 pmC) introduced during GC isolation and subsequent sample preparation for the AMS measurement was about 3.9 ± 1.6 μg C (octadecanoic acid) and 1.1 ± 2.4 μg C (squalane) for modern standard material. For the old standards $C_{blank}$ ($^{14}C_{blank}$: 106 pmC) was in a similar range with 2.1 ± 1.4 μg C (triacontanoic acid) and 3.8 ± 0.7 μg C (octadecane). Possible source of contamination are column and septa bleed, incomplete solvent removal and all steps of sample handling including compound removal from the glass traps and transfer into quartz ampoules, solvent evaporation and sealed tube combustion. We could not remove contamination derived from column bleed by eluting the isolated compound over a silica gel column as suggested by Ohkouchi et al. [22]. Since GC analysis of the isolated compounds shows very little contamination, we suppose that further processing of the isolated compounds and sealed tube combustion are major sources of contamination. Further analyses are necessary to differentiate contaminants introduced during the different processing steps including GC isolation, further sample handling and combustion as well as to explain the relatively large scatter of the $^{14}C$ results for the replicate isolations ($n = 3–4$) of the different standards.

### 3.3. Standards and VIRI samples

To assure the quality of the sample handling and graphitization procedure we measured a selection of organic and bone standard materials from the Fifth Radiocarbon Intercomparison exercise (VIRI; [23,24]), IAEA and the Oxford Radiocarbon Laboratory [25] shown in Table 2. The results are in good agreement with the consensus values. This also applies to the VIRI bone material and the Oxford mammoth bone. The radiocarbon free mammoth bone (>147k years) yields a very good blank value (52k years) without ultrafiltration of the gelatinized collagen.

## 4. Summary

We presented first results for reference and standard materials that have been processed and graphitized in the Radiocarbon laboratory of the new CologneAMS facility, including organic materials and bones, which agree well with consensus values. The process blank for organic samples combusted in an elemental analyzer and graphitized with the AGE for normal sized samples (ca. 1 mg C, measured in Cologne) was 0.12 pmC. A constant contamination of about 0.7 μg C with 75 pmC was determined, which derives mainly from the combustion of organic samples in the elemental analyzer including the tin containers. For small sample sizes of about 150–350 μg C reasonable blank values (40,500 ± 500 years BP for 150–160 μg C) were still obtained, while smaller sample sizes (<150 μg C) were strongly influenced by the contamination introduced preventing the preparation of individual organic compounds isolated with preparative GC with the AGE. $^{14}C$ results of dated GC standards (*n*-alkanes and *n*-carboxylic acids) isolated with preparative GC revealed the contribution of both, fossil and modern contaminants during the GC isolation plus sample handling and combustion procedure. Future work will thus focus on the identification, quantification and reduction of contaminants introduced during all steps of this procedure as well as on the reduction of the AGE process blank for organic materials.

## Acknowledgments

We thank Benedict Behr-Heyder for his assistance in sample preparation. Thanks are also due to Marian Scott (University of Glasgow) for providing VIRI samples and to two anonymous reviewers for their constructive comments.

## References


[1] L. Wacker, M. Němec, J. Bourquin, A revolutionary graphitisation system: fully automated, compact and simple, Nucl. Instr. Meth. B 268 (2010) 931–934.
[2] L. Wacker et al., MICADAS: routine and high-precision radiocarbon dating, Radiocarbon 52 (2010) 252–262.
[3] L. Wacker, M. Christl, H.-A. Synal, Bats: a new tool for AMS data reduction, Nucl. Instr. Meth. Phys. Res. B 268 (2010) 976–979.
[4] A. Dewald et al., A dedicated Center for Accelerator Mass Spectrometry in Germany, this issue.
[5] J. Rethemeyer et al., Age heterogeneity of soil organic matter, Nucl. Instr. Meth. Phys. Res. B 223–224 (2004) 521–552.
[6] R.E.M. Hedges, G.J. van Klinken, A review of current approaches in the pretreatment of bone for radiocarbon dating by AMS, Radiocarbon 34 (1992) 279–291.
[7] C. Bronk Ramsey et al., Improvements to the pretreatment of bone at Oxford, Radiocarbon 46 (2004) 155–163.
[8] I. Hajdas et al., A report on sample preparation at the ETH/PSI AMS facility in Zürich, Nucl. Instr. Meth. B 223–224 (2004) 267–271.
[9] R. Longin, New method of collagen extraction for radiocarbon dating, Nature 230 (1971) 241–242.
[10] F. Brock, C. Bronk Ramsey, T.F.G. Higham, Quality assurance of ultrafiltered bone dating, Radiocarbon 49 (2007) 187–192.
[11] L. Wacker et al., A novel approach to process carbonate samples for radiocarbon measurements, this issue.
[12] I. Hajdas et al., C-14 ages of ostracodes from pleistocene lake sediments of the western Great Basin, USA-results of progressive acid leaching, Radiocarbon 46 (2004) 189–200.
[13] T.I. Eglinton, L.I. Aluwihare, Gas chromatographic isolation of individual compounds from complex matrices for radiocarbon dating, Anal. Chem. 68 (1996) 904–912.
[14] G. Mollenhauer, J. Rethemeyer, Compound-specific radiocarbon analysis – Analytical challenges and applications, Earth Environ. Sci. 5 (2009) 1–9.
[15] M. Ruff et al., On-line radiocarbon measurements of small samples using elemental analyzer and MICADAS gas ion source, Radiocarbon 52 (2010) 1645–1656.
[16] M. Ruff et al., A gas ion source for radiocarbon measurements at 200 kV, Radiocarbon 49 (2007) 307–314.
[17] A. Pearson et al., Microscale AMS $^{14}C$ measurements at NOSMAS, Radiocarbon 40 (1998) 61–75.
[18] G.M. Santos et al., Blank assessment for ultra-small radiocarbon samples: chemical extraction and separation versus AMS, Radiocarbon 52 (2010) 1322–1335.
[19] M. Yoneda et al., AMS $^{14}C$ measurement and preparative techniques at NIES-TERRA, Nucl. Instr. Meth. B 223–224 (2004) 116–123.
[20] S.R. Shah, A. Pearson, Ultra-microscale (5–25 μg C) analysis of individual lipids by $^{14}C$ AMS: assessment and correction for sample processing blanks, Radiocarbon 49 (2007) 69–82.
[21] L.A. Ziolkowski, E.R. Druffel, Quantification of extraneous carbon during compound specific radiocarbon analysis of black carbon, Anal. Chem. 81 (2009) 10156–10161.
[22] N. Ohkouchi, T.I. Eglinton, J.M. Hayes, Radiocarbon dating of individual fatty acids as a tool for refining Antarctic margin sediment chronologies, Radiocarbon 45 (2003) 17–24.
[23] E.M. Scott et al., A report on phase 1 of the 5th international radiocarbon intercomparison (VIRI), Radiocarbon 49 (2007) 409–426.
[24] E.M. Scott, G.T. Cook, P. Naysmith, A report on phase 2 of the fifth international radiocarbon intercomparison (VIRI), Radiocarbon 52 (2010) 846–858.
[25] S.G. Lewis et al., Pleistocene fluvial sediments, palaeontology and archaeology of the upper River Thames at Latton, Wiltshire, Engl. J. Quat. Sci. 21 (2006) 181–205.

# 4. Manuscript II: Stabilization mechanisms of organic matter – *Organic matter composition and stabilization in a polygonal tundra soil of the Lena Delta*

by

**Höfle S.**, Rethemeyer J., Mueller C. W. and John S. (2013)

*Biogeosciences* **10**, 3145-3158.

Biogeosciences, 10, 3145–3158, 2013
www.biogeosciences.net/10/3145/2013/
doi:10.5194/bg-10-3145-2013


Biogeosciences Open Access

# Organic matter composition and stabilization in a polygonal tundra soil of the Lena Delta

**S. Höfle[1], J. Rethemeyer[1], C. W. Mueller[2], and S. John[1]**

[1]Institute of Geology and Mineralogy, University of Cologne, Cologne, Germany
[2]Lehrstuhl für Bodenkunde, Technische Universität München, Freising, Germany

*Correspondence to:* S. Höfle (silke.hoefle@uni-koeln.de)

Received: 22 August 2012 – Published in Biogeosciences Discuss.: 12 September 2012
Revised: 21 February 2013 – Accepted: 26 February 2013 – Published: 8 May 2013

**Abstract.** This study investigated soil organic matter (OM) composition of differently stabilized soil OM fractions in the active layer of a polygonal tundra soil in the Lena Delta, Russia, by applying density and particle size fractionation combined with qualitative OM analysis using solid state $^{13}C$ nuclear magnetic resonance spectroscopy, and lipid analysis combined with $^{14}C$ analysis. Bulk soil OM was mainly composed of plant-derived, little-decomposed material with surprisingly high and strongly increasing apparent $^{14}C$ ages with active layer depth suggesting slow microbial OM transformation in cold climate. Most soil organic carbon was stored in clay and fine-silt fractions (< 6.3 µm), which were composed of little-decomposed plant material, indicated by the dominance of long *n*-alkane and *n*-fatty acid compounds and low alkyl/O-alkyl C ratios. Organo-mineral associations, which are suggested to be a key mechanism of OM stabilization in temperate soils, seem to be less important in the active layer as the mainly plant-derived clay- and fine-silt-sized OM was surprisingly "young", with $^{14}C$ contents similar to the bulk soil values. Furthermore, these fractions contained less organic carbon compared to density fractionated OM occluded in soil aggregates – a further important OM stabilization mechanism in temperate soils restricting accessibility of microorganisms. This process seems to be important at greater active layer depth where particulate OM, occluded in soil aggregates, was "older" than free particulate OM.

## 1 Introduction

The Lena Delta–Laptev Sea region is a key area for studies on the Arctic carbon cycle. The area hosts one of the largest Arctic rivers, the Lena River, with a length of 4337 km, (Lobbes et al., 2000) and its drainage basin is located almost entirely within the zone of permanent permafrost. About 18 % of the total dissolved organic carbon (DOC) and 12–14 % of particulate organic carbon (POC) discharged into the Arctic Ocean are transported by the Lena River (Dittmar and Kattner, 2003) with the major component being terrestrial organic matter (OM) (Lara et al., 1998; Fahl and Stein, 2007).

Previous studies suggest that much of the terrestrial OM in the Lena River and Laptev Sea shelf derives from permafrost soils and riverbank erosion (Charkin et al., 2011; Gustafsson et al., 2011), including an increasing portion of old, strongly transformed DOC and POC most probably exported from thawing permafrost soils (Guo et al., 2007; van Dongen et al., 2008; Gustafsson et al., 2011). However, most of these studies are identifying terrestrial OM from analyses of river and marine sediments as well as of suspended material from both systems (e.g. Schubert and Stein, 1997; Dittmar and Kattner, 2003; Karlsson et al., 2011; Semiletov et al., 2011), but detailed information on the original source, plant material and soil OM in the hinterland of the Laptev Sea area are missing. Few investigations have been conducted so far of the active layer in permafrost soils, which thaws during summer, as a potential source of terrestrial OM to Arctic rivers and the ocean. Due to the expected increase in active layer thickness, which was already proven in some studies (Hinkel and Nelson, 2003; Nelson et al., 2008; Akerman and Johansson, 2008), and which is predicted to accelerate due to global warming (Anisimov and Reneva, 2006; Schaefer et al., 2011), previously frozen OM will become increasingly available for microbial decomposition and export by water (Zimov et al., 2006; Frey and McClelland, 2009). A recent study on polygonal tundra soils in the Lena Delta showed the

**Published by Copernicus Publications on behalf of the European Geosciences Union.**

importance of the active layer for soil organic carbon storage with on average 7.6 kg m$^{-2}$ organic carbon in the active layer (Zubrzycki et al., 2012). However, so far little is known about OM distribution and composition in the active layer and therefore the susceptibility of different OM components to degradation and export into rivers and the Arctic Ocean. Although still discussed controversially, several results from incubation experiments of Arctic soils indicate that microbial activity is temperature sensitive (Guicharnaud et al., 2010) and that after decomposition of labile OM, recalcitrant components will be decomposed at higher soil temperatures due to microbial community changes (Biasi et al., 2005; Knoblauch et al., 2008). However, OM bound to soil minerals may survive biodegradation as suggested by Vonk et al. (2010), who measured high $^{14}$C ages of vascular plant-derived lipids in sediments in front of Arctic river mouths (Vonk, 2010; Gustafsson et al., 2011). Physical and chemical stabilization processes, which are considered to play an important role for OM stabilization in soils and sediments (Arnarson and Keil, 2007; Kögel-Knabner et al., 2008; Marschner et al., 2008), have not been investigated in the active layer of permafrost soils.

OM stabilization has been investigated quite intensively in temperate surface soils (Sollins et al., 1996; von Lützow et al., 2007; Kögel-Knabner et al., 2008). There, physical protection mechanisms were found to be more important for soil OM stabilisation than (intrinsic) chemical recalcitrance of organic compounds (Marschner et al., 2008). However, the active layer soils of permafrost regions differ strongly from temperate soils, e.g. it often contains less mineral substrate, has high root penetration, and is affected by freezing and thawing processes, which may influence aggregation processes.

Various fractionation methods have been used to separate differently stabilized OM and thereby gain information on stabilization processes (von Lützow et al., 2007), which produce quite heterogeneous OM fractions not representative for distinct functional pools (von Lützow et al., 2007; Trumbore, 2009). Therefore, a combination of $^{14}$C and qualitative analysis of soil physical fractions was proposed, which identifies carbon turnover and the chemical properties of OM on a molecular level (Quideau et al., 2000; Schöning and Kögel-Knabner, 2006; Trumbore, 2009). This integrative approach has been applied in marine and terrestrial environments giving useful insights into carbon sources and dynamics. For example, terrestrial carbon input and turnover has been studied in marine sediments of rivers continental margins (Dickens et al., 2006; Wakeham et al., 2009), while in soils different OM sources, their stabilization and decomposition have been identified (Baldock et al., 1992; von Lützow et al., 2008; Mueller et al., 2009).

Solid-state $^{13}$C nuclear magnetic resonance spectroscopy (NMR), recording the relative abundance of different functional groups, can be used to get a non-destructive overview of the chemical OM composition and its decomposition stage (Baldock et al., 1992). However, the precise structure of soil OM or specific organic compounds cannot be determined by this method (Kögel-Knabner, 2000). More detailed information is obtained from macromolecular compounds and diagnostic lipids in soil OM (Simpson and Simpson, 2012). The dynamics of organic carbon in physically defined OM fractions are revealed by $^{14}$C analysis.

In this study we investigated the composition of differently stabilized soil OM compartments in the shallow active layer (ca. 25 cm) and the uppermost still-frozen permafrost in a polygonal rim on Samoylov Island (Lena Delta, Siberia). Soil OM from different depth intervals was separated by particle size and density fractionation. The composition of $^{14}$C dated OM in silt and clay fractions as well as in free and occluded particulate OM was characterized by $^{13}$C cross-polarization magic angle spinning nuclear magnetic resonance spectroscopy analysis ($^{13}$C-CPMAS NMR) and lipid analysis.

## 2 Material and methods

### 2.1 Site description and sampling

Polygonal tundra covers a global area of 250 000 km$^2$, which is about 3 % of the Arctic land mass (Minke et al., 2007). The polygonal tundra investigated in this study is located on Samoylov Island (72.37° N, 126.48° E), which is part of the active eastern section of the Lena Delta, Siberia. The Lena Delta is the largest (32 000 km$^2$) of the Arctic (Are and Reimnitz, 2000) and is located in the zone of continuous permafrost, which has a thickness of 400–600 m in the delta (Romanovskii and Hubberten, 2001). The climate is Arctic continental with low mean annual air temperatures of −14.7 °C, great temperature differences between winter (September–May: −30 °C) and summer (June–August: 7 °C), and low mean annual precipitation of 190 mm yr$^{-1}$. The island is composed mainly of middle Holocene fluvial deposits (Hubberten et al., 2006). Polygonal patterns, dominating the landscape, have formed due to freezing–thawing cycles of ice wedges (Mueller, 1997). The polygon rims cover about 55 % of the area and the several centimetres lower polygon centres ca. 45 % (Kutzbach et al., 2004). The permafrost affected alluvial soils on Samoylov Island are Gelisols (according to US Soil Taxonomy; FAO, 2007) with suborders Glacic Aquiturbels dominant in the polygon rims and Typic Historthels in the polygon centers (Pfeiffer et al., 2002). Gelisols cover an area of about 27 % in northern latitudes (Jones et al., 2010). Soil texture of the Glacic Aquiturbels is silty sand (Ajj), loamy sand (Bjj) and sandy, loamy silt (Bjj2, Bjjf).

Vegetation is mainly formed by mosses and grasses, and additionally on the polygon rims by lichens, some herbs and small shrubs like *Salix* spp. or *Betula* spp. and in the polygon centres by some sedges (Mueller, 1997; Boike et al., 2012).

Soil sampling was done during the LENA-2009 and LENA-2010 expeditions of the Alfred Wegener Institute, Bremerhaven (Germany; Boike et al., 2009). Samples were taken from a soil pit of about 1 m × 1 m size from different soil layers of the active layer (0–25 cm) and of the uppermost still-frozen permafrost (25–$30_p$ cm) of a polygon rim (Table 1) with little visible cryoturbation at the end of the summer season in mid-August to the beginning of September, when the active layer has reached its maximal depth. Because of the complex analyses performed, only one soil profile with four soil horizons has been sampled and no replicates were analysed. However, large amounts of soil per horizon were sampled and mixed to obtain a representative sample at least for the soil pits (ca. 1 m × 1 m). Thus, spatial heterogeneity of organic matter in the active layer soils (e.g. Jones et al., 2010) is not represented by this sample set.

Sample material was stored and transported frozen in precombusted glass jars at −20 °C and freeze-dried prior to analysis.

### 2.2 Physical fractionation

A combined density and particle size fractionation was applied (Mueller et al., 2009). Briefly, 20 g of soil material were suspended in sodium polytungstate solution (1.8 g $cm^{-3}$) and allowed to settle over night. The floating free particulate organic matter (fPOM) was extracted by sucking via a water jet pump. Sodium polytungstate was removed from the fPOM fraction by washing several times with deionized water on a sieve of 20 µm mesh size. The remaining slurry was dispersed ultrasonically (200 J $mL^{-1}$; Bandelin, Sonopuls HD 2200) in order to break down soil aggregates. The energy input had been tested before to avoid disruption of coarse POM. After sonication the occluded POM (oPOM) was separated from the mineral residue by centrifugation. The fraction < 20 µm ($oPOM_{<20}$) was obtained by washing the $oPOM_{>20}$ over a sieve of 20 µm mesh size via pressure filtration until the electric conductivity dropped below 5 µS $cm^{-1}$. Sand (63–2000 µm) and coarse silt (20–63 µm) were separated by wet sieving and medium silt (6.3–20 µm), fine silt (2–6.3 µm) and clay (< 2 µm) by sedimentation. All fractions were freeze-dried and weighed before further analysis. Mass recovery of the SOM fractionation was between 97 % and 99 %.

### 2.3 Bulk analysis

Bulk soil samples and soil fractions were manually ground in a porcelain bowl with liquid nitrogen to gain a fine homogeneous material. Total C and N contents were determined with an elemental analyser (Analyzer vario MICRO cube, Elementar, Germany). The samples were carbonate-free, therefore total C contents were set equal to total organic carbon content (TOC). Soil pH values were measured in $H_20$ (soil water ratio 1 : 2.5) one hour after water addition.

### 2.4 NMR analysis

For $^{13}C$ cross-polarization magic angle spinning nuclear magnetic resonance spectroscopy analysis ($^{13}C$-CPMAS NMR) accomplished with a Bruker DSX 200 spectrometer (Bruker BioSpin GmbH, Karlsruhe, Germany), samples were filled into zirconium dioxide rotors and spun in a magic angle spinning probe at a rotation speed of 6.8 kHz to minimize chemical anisotropy. A ramped $^1H$ pulse was used during a contact time of 1 ms to prevent Hartmann–Hahn mismatches. The delay times ranged from 400 ms for mineral fractions to 1000 ms for POM fractions. Chemical shifts were referenced to tetramethylsilane (TMS = 0 ppm). For integration, chemical shift regions were used as given: alkyl C (10–45 ppm), O-alkyl C (45–110 ppm), aryl/olefine C (110–160 ppm), and carbonyl/carboxyl/amide C (160–220 ppm). Measurements were done on clay and $oPOM_{<20}$ fractions for all soil horizons, except for the second horizon (6–11 cm), where only the clay fraction was measured due to the lack of $oPOM_{<20}$ material.

### 2.5 Extraction of lipids

Lipids were extracted from bulk soil samples by accelerated solvent extraction (Dionex ASE 200, USA) and from soil fractions by sonication. Five (5) g of bulk soil material was extracted by ASE with dichloromethane:methanol (9 : 1, 75 bar, 120 °C, 20 min). Depending on TOC content, 100–3000 mg of each soil fraction was extracted in an ultrasonic bath (room temperature) with a sequence of solvents starting with methanol, dichloromethane : methanol (1 : 1), and finally dichloromethane (25 mL, 5 min each solvent). The three extracts were combined and solvents were rotary evaporated. After saponification of the total lipid extracts with methanolic KOH (0.5 M), neutral lipids were recovered by liquid–liquid phase separation and *n*-fatty acids after acidification with 10 % HCl. The neutral fraction was further separated into aliphatic, aromatic and heterocompound fractions by column chromatography using deactivated $SiO_2$ (mesh size 60) and elution with hexane, followed by dichloromethane : hexane (2 : 1) and methanol, respectively. The *n*-fatty acid fraction was transesterified with methanolic HCl (95 : 5) to form fatty acid methyl esters (FAMEs) and purified over a $SiO_2$-$Na_2SO_4$ column by eluting with dichloromethane : hexane (2 : 1).

The *n*-alkanes and *n*-fatty acid distributions were measured on a gas chromatography – flame ionization detector (GC-FID, 5890 series II plus, Hewlett Packard, USA equipped with DB-5MS column 50 m, 0.2 mm ID, 0.33 µm df). Identification and quantification of lipids was done using external standard mixtures.

**Table 1.** Bulk soil properties in different depths intervals of a polygonal rim (Glacic Aquiturbels, FAO, 2007) on Samoylov Island, Siberia. Total extractable *n*-alkanes ($C_{19}$–$C_{33}$) and *n*-fatty acids ($C_{14}$–$C_{30}$) and summed long-chain, mainly plant-wax-derived *n*-alkanes ($C_{27}$, $C_{29}$, $C_{31}$) and *n*-fatty acids ($C_{24}$, $C_{26}$, $C_{28}$) are related to soil dry weight (DW).

| Depth [cm] | Horizon | pH | TOC [%] | C/N | $^{14}$C [pMC] | *n*-alkanes [µg g$^{-1}$ DW] | | *n*-fatty acids [µg g$^{-1}$ DW] | |
|---|---|---|---|---|---|---|---|---|---|
| | | | | | | Total | Sum $C_{27,29,31}$ | Total | Sum $C_{24,26,28}$ |
| 0–6 | Ajj | 6.1 | 3.0 | 19.5 | 90 | 17 | 11 | 90 | 24 |
| 6–11 | Bjjg1 | 6.4 | 1.5 | 17.8 | 83 | 14 | 9 | 52 | 15 |
| 11–25 | Bjjg2 | 6.3 | 3.0 | 18.4 | 78 | 20 | 11 | 255 | 120 |
| 25–30$_p$ | Bjjf | 6.7 | 2.5 | 16.4 | 68 | 12 | 6 | 178 | 82 |

### 2.6 Radiocarbon analysis

Bulk soil samples and soil fractions were pretreated with 1 % HCl, which was removed by washing with Milli-Q water. After drying (60 °C) the samples were converted to graphite with $H_2$ over iron as catalyst (Rethemeyer et al., 2013). $^{14}$C contents of soil fraction were measured on a 6 MV Tandetron AMS (HVE, the Netherlands) at the University of Cologne (Germany). Bulk soil samples were measured with the MICADAS AMS at the ETH Zurich (Switzerland). $^{14}$C results are reported as percent modern carbon (pMC, related to 1950) with one-sigma uncertainties.

## 3 Results

### 3.1 Bulk parameters

#### 3.1.1 Bulk soil characteristics

Basic soil parameters of the three depth intervals of the shallow active layer (25 cm) and the uppermost ca. 5 cm still-frozen soil are presented in Table 1. The active layer consists of an upper 6 cm mineral soil layer with high root penetration and a 19 cm thick mineral soil with little root penetration. Soil type changed from loamy and silty sand with depth to loamy and sandy silt. Soil OM in the lower mineral soil contained high amounts of only slightly decomposed roots from grasses and small shrubs. The soil layer at 6–11 cm depth contained sandy material of aeolian or fluvial origin. The pH values in the active layer and in the uppermost permafrost layer were around 6.5. The four depth intervals yielded relatively high and little variable TOC contents (2.5–3.0 %) except for the 6–11 cm interval containing a sandy layer, which had a lower content (1.5 %). Similarly, C/N ratios were at a comparable level in all soils and centred around 18. Bulk soil OM $^{14}$C concentrations decreased strongly in the shallow active layer from 90 to 68 pMC, which is equivalent to an apparent age increase from 866 to 3052 yr BP.

#### 3.1.2 Basic parameters of soil fractions

The upper two depth intervals of the active layer (0–11 cm) and the lowermost intervals (11–30$_p$ cm) showed a similar particle size distribution. In the upper two depth intervals, the sand fraction (63–2000 µm) was the largest fraction with over 62 % of the total soil mass, but decreased successively with depth down to ca. 25 % at 25–30$_p$ cm depth (Table 2). Clay-sized material showed a strong increase of 10 % with depth. TOC values were very low for both sand fractions (63–2000 µm: 0.1 %) and coarse silt (20–63 µm: $< 0.6$ %) from all depth intervals. The medium-silt fraction (6.3–20 µm) had still low and decreasing TOC values with soil depth (0.6–2.0 %). Most organic carbon was located in fine silt (2–6.3 µm) and clay ($< 2$ µm) where TOC values were lower only in these fractions from the still-frozen soil at 25–30$_p$ cm depth. TOC storage in the different size fraction related to the mass of each fraction is shown in Fig. 1a, revealing that the fine-silt and clay fractions contained most organic carbon (7.4–15.3 mg C g$^{-1}$ soil dry weight – DW). C/N ratios of the silt and clay fractions (20 and 15, respectively) were highest in the surface layer and decreased with particle size as well as with depth to minimal values around 10 in the frozen soil layer.

The three POM fractions made up together between 0.9–2.4 % of the total soil mass (Table 2) and stored together 2.6–7.8 mg C g$^{-1}$ DW (Fig. 2a). While the mass of fPOM strongly decreased with depth by about 40 %, the oPOM$_{>20}$ mass distribution was nearly constant except for the sandy 6–11 cm depth interval. The mass percentage of the oPOM$_{<20}$ increased and was twice as high in the lowermost depth interval compared to the surface layer (Table 2). Despite the small masses of the POM fractions they had the highest TOC values (21–42 %) in all depths intervals. TOC values were constant over depth for fPOM, but increased for oPOM$_{>20}$ and oPOM$_{<20}$. However, taking the mass of each fraction into account, values for fPOM decreased from 4.7 mg C g$^{-1}$ DW with depth down to 1.8 mg C g$^{-1}$ DW, whereas oPOM$_{>20}$ had almost constant values, except in the sandy depth interval (Fig. 2a). In contrast the amount of TOC in oPOM$_{<20}$ increased with depth. The highest C/N ratios of 31 and 34 were measured in the fPOM and oPOM$_{>20}$ fraction in the surface

**Table 2.** Fraction mass and elemental composition of density and particle size soil fractions.

| Parameter | Depth [cm] | fPOM | oPOM$_{>20}$ | oPOM$_{<20}$ | Coarse + medium sand (200–2000 µm) | Fine sand (63–200 µm) | Coarse silt (20–63 µm) | Medium silt (6.3–20 µm) | Fine silt (2–6.3 µm) | Clay (<2 µm) |
|---|---|---|---|---|---|---|---|---|---|---|
| mass [%] | 0–6 | 1.3 | 0.5 | 0.6 | 30.2 | 32.4 | 16.6 | 9.6 | 3.3 | 5.6 |
| | 6–11 | 0.4 | 0.1 | 0.3 | 31.5 | 36.2 | 14.9 | 8.3 | 3.1 | 5.2 |
| | 11–25 | 0.7 | 0.4 | 0.7 | 8.4 | 24.3 | 27.6 | 17.1 | 7.8 | 12.9 |
| | 25–30$_p$ | 0.5 | 0.5 | 1.2 | 5.5 | 19.7 | 25.8 | 22.3 | 9.4 | 15.0 |
| TOC* [%] | 0–6 | 36.9 | 32.9 | 21.2 | 0.1 | 0.1 | 0.6 | 2.0 | 10.9 | 9.8 |
| | 6–11 | 38.2 | 37.6 | 12.5 | 0.0 | 0.1 | 0.3 | 1.5 | 8.6 | 9.2 |
| | 11–25 | 37.5 | 40.2 | 31.9 | 0.0 | 0.1 | 0.3 | 1.0 | 8.0 | 7.0 |
| | 25–30$_p$ | 37.1 | 42.4 | 32.1 | 0.0 | 0.1 | 0.2 | 0.6 | 5.0 | 5.0 |
| C/N | 0–6 | 31 | 34 | 15 | n.d. | n.d. | 30 | 18 | 20 | 15 |
| | 6–11 | 25 | 28 | 21 | n.d. | n.d. | 25 | 17 | 17 | 13 |
| | 11–25 | 24 | 29 | 21 | n.d. | n.d. | 14 | 14 | 16 | 12 |
| | 25–30$_p$ | 24 | 24 | 21 | n.d. | n.d. | 9 | 11 | 13 | 11 |
| *n*-alkanes total ($C_{19}$-$C_{33}$) [µg g$^{-1}$ DW] | 0–6 | 29 | 23 | 69 | n.d. | n.d. | 6 | 17 | 39 | 21 |
| | 6–11 | 53 | 68 | 91 | n.d. | n.d. | 8 | 5 | 40 | 44 |
| | 11–25 | 15 | 33 | 98 | n.d. | n.d. | 3 | 9 | 35 | 40 |
| | 25–30$_p$ | 34 | 20 | 57 | n.d. | n.d. | 2 | 4 | 14 | 16 |
| *n*-fatty acids total ($C_{14}$-$C_{30}$) [µg g$^{-1}$ DW] | 0–6 | 394 | 99 | 130 | n.d. | n.d. | 5 | 10 | 80 | 70 |
| | 6–11 | 1120 | 283 | 390 | n.d. | n.d. | 2 | 3 | 58 | 40 |
| | 11–25 | 88 | 386 | 218 | n.d. | n.d. | 2 | 6 | 56 | 57 |
| | 25–30$_p$ | 279 | 620 | 223 | n.d. | n.d. | 3 | 8 | 105 | 158 |

* Total organic carbon.

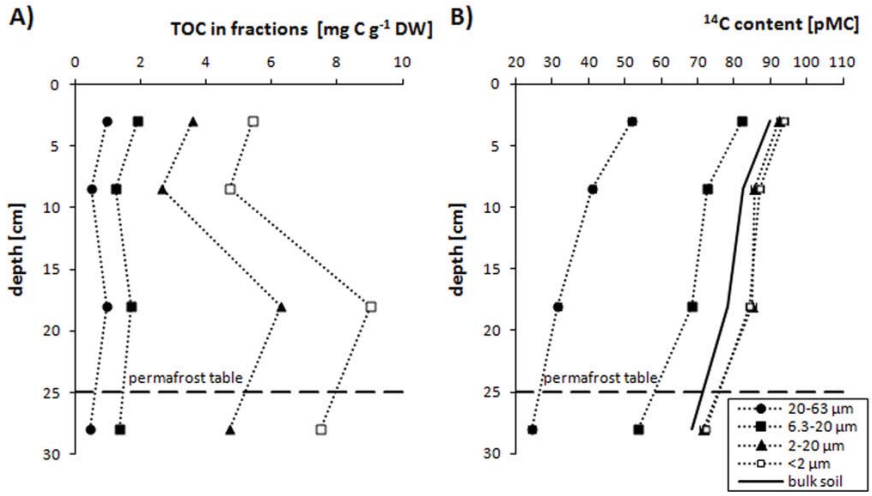


**Fig. 1.** Distribution of **(A)** total organic carbon content (TOC) in particle size fractions related to fraction mass and **(B)** $^{14}$C content (one-sigma measurement uncertainties are indicated by bars on each point) over depth in the coarse silt (20–63 µm), medium silt (6.3–20 µm), fine silt (2–6.3 µm) and clay (< 2 µm) fractions.

soil. The C/N ratios decreased slightly with depth for these two fractions, whereas the oPOM$_{<20}$ fraction had a lower C/N ratio in the uppermost soil (15), which increased in the three subsoil layers to 21. Generally, decreases in C/N ratio with depths were smaller for the POM fractions than for the particle size fractions.

### 3.2 NMR results and lipid concentration

#### 3.2.1 Lipid concentration of bulk soil

The *n*-alkane concentrations of the bulk soil showed a clear odd-over-even predominance with the main compounds being $C_{27}$ and $C_{29}$ (Table 1). Overall, concentrations ($C_{19}$–$C_{33}$)

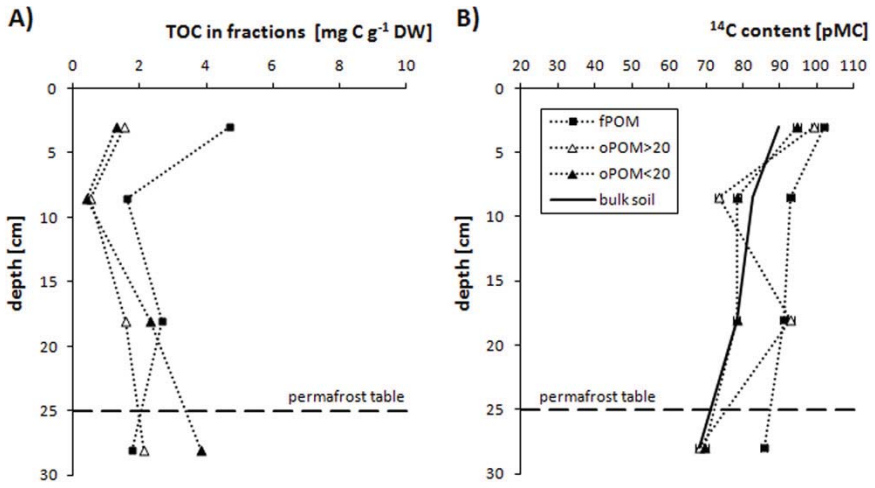


**Fig. 2.** Distribution of **(A)** organic carbon content (TOC) in density fractions related to fraction mass and **(B)** $^{14}C$ content (one-sigma measurement uncertainties are indicated by bars on each point) over depth.

were highest in surface soil and in 11–25 cm (17 and 20 µg g$^{-1}$ DW) and lower in the sandy 6–11 cm layer and in the uppermost still-frozen permafrost layer down to 12 µg g$^{-1}$ DW. *n*-fatty acid concentrations in bulk SOM showed an even-over-odd-predominance with $C_{16}$ and $C_{24}$ as main compounds and overall concentrations ($C_{14}$–$C_{30}$) between 52–255 µg g$^{-1}$ DW (Table 1). The abundance of $C_{16}$ *n*-fatty acid decreased with depth, whereas $C_{24}$ concentrations increased in deeper intervals of the active layer and in the adjacent permafrost.

### 3.2.2 NMR results and lipid concentration of soil fractions

$^{13}C$-CPMAS NMR spectroscopy was applied to clay-sized OM as well as fPOM and oPOM$_{<20}$; fPOM was measured only from the uppermost layer due to the lack of material. oPOM$_{<20}$ and the clay fraction showed intensity differences with depth in their aryl and alkyl regions, while O-alkyl and carboxyl signals were within the same range. The dominant functional group of the oPOM$_{<20}$ and clay fractions from all depth intervals was O-alkyl C (e.g. carbohydrates; (Kögel-Knabner, 2002), which decreased in its abundance with active layer depth (Table 3). Alkyl C (e.g. lipids, suberin, cutin and proteins; Kögel-Knabner, 2002) intensities were slightly higher for the clay fraction (21–28 %) than for the oPOM$_{<20}$ fraction (18–24 %). Larger signals for the aryl C (aromatic carbon; (Baldock et al., 1992) shift region were measured for oPOM$_{<20}$ (16–24 %) compared to the spectra measured in clay (13–19 %). The carboxyl C signals (e.g. fatty acids, fatty ester; (Baldock et al., 1992) remained constant over depth. The fPOM fraction, which was only analysed in the 0–6 cm depth interval, showed a considerably different composition with highest abundances of O-alkyl C and lowest of alkyl and carboxyl C.

Lipid concentrations were analysed in four particle size fractions only, as sand fractions were not considered to be important for soil OM stabilization. Total extractable lipids were highest in fine silt and clay (Table 2). *n*-alkanes showed an odd-over-even predominance with the main compounds being $C_{27}$ and $C_{29}$ (Fig. 3). Overall, concentrations ($C_{19}$–$C_{33}$) were highest in the surface soil and in 11–25 cm (17 and 20 µg g$^{-1}$ DW) and lower in the sandy 6–11 cm layer and in the uppermost still-frozen permafrost layer (12 µg g$^{-1}$ DW). Coarse and medium silt contained extremely low total *n*-alkane concentrations (6–17 µg g$^{-1}$ DW in 0–6 cm), which decreased further with soil depth. While *n*-alkanes in coarse silt showed no characteristic distribution, medium silt was dominated by $C_{27}$ and $C_{29}$ *n*-alkanes (Table 2), which decreased in abundance from about 5 µg g$^{-1}$ DW (0–6 cm) to 1 µg g$^{-1}$ DW (25–30$_p$ cm; data not shown). Fine-silt and clay fractions, which were also dominated by $C_{27}$ and $C_{29}$ compounds, had higher total *n*-alkane concentrations in all depth intervals than the bulk soil. Medium-chain-length *n*-alkanes ($C_{19}$–$C_{24}$) were nearly absent in the coarse and medium-silt-sized fractions (data not shown) and occurred in relatively low abundances in fine silt and clay.

Similar to the *n*-alkanes, total *n*-fatty acid concentrations ($C_{14}$–$C_{30}$) were extremely low (< 10 µg g$^{-1}$ DW) in the coarse- and medium-silt fractions in all depth intervals with no dominant compounds (data not shown), while higher concentrations were determined in fine silt and clay (45–161 µg g$^{-1}$ DW), with $C_{16}$ and $C_{24}$ *n*-fatty acids being the most abundant compounds (Fig. 4). The dominance of the $C_{16}$ *n*-fatty acid in fine silt and clay decreased with depth and

**Table 3.** Relative contents [%] of chemical structures identified by $^{13}$C-CPMAS NMR spectroscopy in the clay fraction (< 2 µm) and in free (fPOM) and occluded particulate organic matter < 20 µm (oPOM$_{<20}$).

| Fraction | Depth [cm] | Alkyl C | O-alkyl C | Aryl C | Carboxyl C | Alkyl C/O-alkyl C | Aryl C/O-alkyl C |
|---|---|---|---|---|---|---|---|
| fPOM | 0–6 | 15 | 56 | 24 | 6 | 0.27 | 0.42 |
| oPOM$_{<20}$ | 0–6 | 21 | 52 | 16 | 12 | 0.40 | 0.30 |
| | 6–11 | n.d. | n.d. | n.d. | n.d. | n.d. | n.d. |
| | 11–25 | 18 | 47 | 24 | 12 | 0.39 | 0.51 |
| | 25–30$_p$ | 24 | 40 | 24 | 12 | 0.59 | 0.60 |
| clay | 0–6 | 23 | 51 | 13 | 14 | 0.45 | 0.25 |
| | 6–11 | 21 | 50 | 19 | 11 | 0.41 | 0.37 |
| | 11–25 | 24 | 49 | 17 | 10 | 0.48 | 0.34 |
| | 25–30$_p$ | 28 | 43 | 15 | 13 | 0.65 | 0.35 |

shifted to $C_{24}$, which is the most abundant compound in the uppermost permafrost still-frozen layer. In these two fractions total *n*-fatty acid concentrations decreased with depth within the active layer (0–25 cm), but increase again to concentrations twice as high in the frozen soil layer (25–30$_p$ cm). This increase mainly resulted from higher abundances of compounds with $>C_{20}$ chain length.

The *n*-alkane concentrations in the fPOM, oPOM$_{>20}$ and oPOM$_{<20}$ fractions were generally higher (15–98 µg g$^{-1}$ DW) than in the bulk soil OM and particle size fractions, and yielded high abundances of medium-chain-length compounds ($C_{19}$–$C_{24}$) representing 33–55 % of the overall concentration. Highest *n*-alkane concentrations were measured in oPOM$_{<20}$ from all depth intervals. Concentration increased with active layer depth in all three fractions, but dropped in the frozen soil layer (25–30$_p$ cm) in fPOM and oPOM$_{<20}$ fractions (Fig. 3). fPOM and oPOM$_{<20}$ were dominated by $C_{23}$ and the long-chain compounds $C_{27}$ and $C_{29}$, while oPOM$_{>20}$ mainly contained *n*-alkanes of medium chain length centring around $C_{23}$.

*n*-fatty acid concentrations of all density fractions (0.1–256.5 µg g$^{-1}$ DW) were one order of magnitude higher compared to *n*-alkanes (0.0–18.4 µg g$^{-1}$ DW), particularly in fPOM for the uppermost two depth intervals, and had a clear even-over-odd predominance (Fig. 4). Overall, concentrations ($C_{14}$–$C_{30}$) varied between 90 and 1129 µg g$^{-1}$ DW and increased with depth in the oPOM$_{>20}$ fraction (from 103 to 625 µg g$^{-1}$ DW). The fPOM and oPOM$_{<20}$ fractions yielded highest *n*-fatty acid concentrations in the sandy depth interval (6–11 cm) with 1129 and 395 µg g$^{-1}$ DW, respectively (Table 2). The dominant compounds in all fractions in the two surface layers were $C_{16}$ and $C_{18}$ *n*-fatty acids. Compound distributions changed with depth to longer chain length, with $C_{24}$ being the major compound in oPOM$_{>20}$ and oPOM$_{<20}$ at 11–30$_p$ cm. In the still-frozen depth interval, highest total *n*-fatty acid concentrations were present in oPOM$_{>20}$, which contained predominantly long-chain compounds ($C_{24}$–$C_{30}$).

### 3.3 Radiocarbon contents of soil fractions

The various soil fractions showed decreasing $^{14}$C contents towards larger fraction size and greater soil depth (Figs. 1b and 2b). Fine silt and clay had similar $^{14}$C contents like bulk OM and also comparable values over all depth intervals (Fig. 1b), which were slightly higher (71–94 pMC) than concentrations of bulk OM (68–90 pMC). The medium-silt fraction had lower $^{14}$C contents (54–82 pMC) than fine-silt and clay fractions and bulk OM. Lowest $^{14}$C contents were measured in the coarse-silt fractions, which decreased most strongly with depth down to 24 pMC in the uppermost permafrost layer (25–30$_p$ cm). This fraction had the lowest contents of all analysed fractions.

The three density fractions also showed decreasing $^{14}$C contents in the order fPOM > oPOM$_{>20}$ > oPOM$_{<20}$ and a decrease with soil depth (Fig. 2b), but concentrations were slightly higher in both surface layers than in bulk soil OM. The highest $^{14}$C contents and the smallest decrease with depth from 102 to 86 pMC was measured for the fPOM fraction. The oPOM fractions decreased more strongly in $^{14}$C content with depth, except for a higher value for oPOM$_{>20}$ from 11–25 cm soil depth, and yielded lowest values in the frozen layer, which are similar to that of the bulk soil.

## 4 Discussion

### 4.1 Distribution and composition of bulk soil organic matter

We found considerable differences of the physical and chemical soil properties in the shallow active layer thawing during summer (0–25 cm) and the uppermost still-frozen permafrost (25–30$_p$ cm) of a polygonal rim on Samoylov Island (Table 2). The distribution of the separated particle size fractions revealed changes in the textural composition from the two near surface intervals (0–6 cm and 6–11 cm) dominated by sand-sized material (60 %) to the two lower horizons (11–25

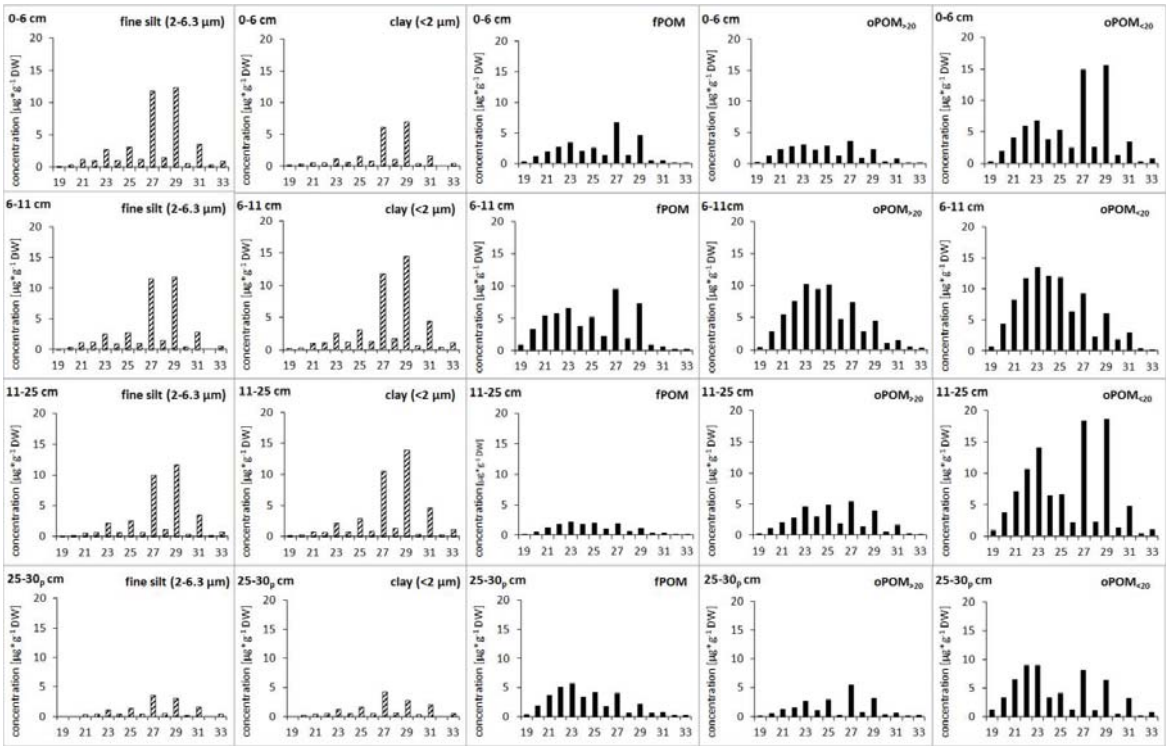


**Fig. 3.** *n*-alkane concentrations in fine silt and clay (striped bars) and in three density fractions (black bars) from different depths intervals. Only odd *n*-alkanes are labelled on the x-axis.

and 25–30$_p$ cm;), which contained more than 65 % silt and clay-sized material. High sand contents are most probably of aeolian origin eroded from the sandbanks of the Lena Delta (Hubberten et al., 2006). Differences in soil texture in the surface soil and near the permafrost table may be explained by soil-developing processes like physical weathering and vertical translocation of fine-grained particles. Intense freezing–thawing cycles as well as the breakup of particles by cryohydration occurring in cold climates may produce fine-grained particles (Jones et al., 2010).

Changes in chemical soil properties in the active layer are reflected by the elemental composition and, in more detail, by the molecular analyses of organic compounds and structures. The TOC contents in the active layer of the polygonal rim (on average 2.5 %; Table 1) are characteristic for OM in tundra soil developed in Holocene fluvial deposits in this area (Zimov et al., 2006; Wagner et al., 2007; Xu et al., 2009). The relatively high C/N ratios around 18 most likely reflect the slow transformation of the OM at cold temperatures and indicate the presence of little-decomposed OM. Likewise, the high and rapidly, nearly linearly, increasing apparent $^{14}$C ages of bulk OM with depth (866–3052 yr BP; Table 1) suggest slow organic carbon turnover and the accumulation of "old" material, respectively, and no significant mixing by cryoturbation. We did not expect such low $^{14}$C values in the shallow active layer since previous results, which were however determined for OM from permafrost cores from Samoylov Island, were around 2300 yr BP in 289 cm and 7900 yr BP in 557 cm (Wagner et al., 2007). Instead, quite similar $^{14}$C results were determined for OM in the active layer of tundra soils in Russia (66° N, 42° E) and on Svalbard (78 – 79° N, 13 – 17° E), Norway, with $^{14}$C concentrations declining from modern values to about 53 pMC equivalent to 5100 yrs BP in the upper 40 cm of soils from various sites (Cherkinsky, 1996) and for OM of three active layers (35–50 cm) from sites in Alaska (64 – 67° N, 147 – 150° W) with $^{14}$C ages between 585 and 3363 yr BP (Waldrop et al., 2010).

The *n*-alkane distribution in bulk OM (Table 1) suggests that a major portion in all depth intervals is plant-derived material indicated by $C_{27}$ and $C_{29}$ *n*-alkanes being the most abundant compounds, which are major compounds of epicuticular waxes (Eglinton and Hamilton, 1967) frequently used as biomarkers for higher plant input to soils and aquatic sediments (e.g. Jambu et al., 1991; Huang et al., 2000). Likewise, the *n*-fatty acid distribution maximizing at $C_{24}$ reflects the terrestrial plant origin of OM in the two surface soil layers

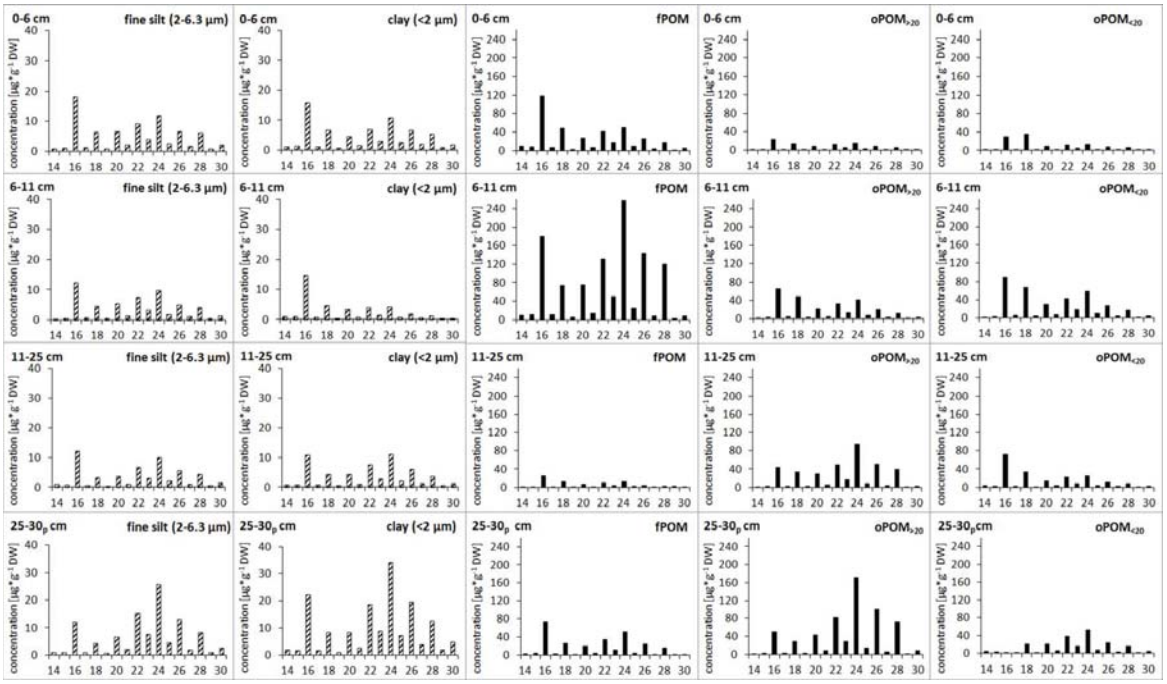


**Fig. 4.** Distribution of *n*-fatty acids in fine silt and clay (striped) and in density fractions (black) from different depths intervals. Only even *n*-fatty acids are labelled on the x-axis; note different scaling of y-axis.

(0–11 cm; data not shown). Since lipid concentrations were found to correlate with TOC contents (Naafs et al., 2004), the strong increase in concentrations of the long-chain *n*-fatty acid compounds in the lowermost active layer interval and in still-frozen soil may result from inputs of other sources than plant material at greater depth or more likely, from in situ secondary production by the transformation of plant wax esters or root-derived polyesters and suberin (Ficken et al., 1998; Bull et al., 2000; Andersson and Meyers, 2012).

In summary, relatively high C/N values and abundances of long-chain *n*-alkanes in the active layer and adjacent upper permafrost layer reflected that soil OM consisted of little-degraded plant material. This result is in contrast to the high and increasing apparent $^{14}C$ ages with active layer depth, which is generally considered to result from the accumulation of strongly transformed, "old" organic matter (Rumpel and Kögel-Knabner, 2011). However, little-degraded, "old" plant material in the depth intervals near the permafrost table may be protected against biodegradation by preservation mechanisms like interaction with clay particles, which increase in abundances in these layers.

### 4.2 Stabilization mechanisms of SOM

Three mechanisms are known to be relevant for OM stability in temperate soils; these are (a) formation of soil aggregates, (b) formation of organo-mineral associations, and (c) the chemical recalcitrance of organic compounds (Sollins et al., 1996; Christensen, 2001; Six et al., 2002; Baldock et al., 2004; Kögel-Knabner et al., 2008). However, so far it is not known if these mechanisms are relevant, and if so, which of them is of primary importance in the active layer of Arctic soils. Since reduced bioaccessibility of OM in soil aggregates and of organo-mineral assemblages was found to be of major importance for OM preservation in various temperate soils (Sollins et al., 2006; Marschner et al., 2008; Sanaullah et al., 2011), we analysed the composition of OM in $^{14}C$ dated particle size and density factions from depth intervals of the active layer and uppermost still-frozen soil of the polygonal rim to get information about OM sources and protection mechanisms.

#### 4.2.1 Organic matter in soil aggregates

The fractions, fPOM, $oPOM_{>20}$ and $oPOM_{<20}$ separated by density fractionation, showed strong differences in their distribution and chemical composition in the active layer (0–25 cm) and the uppermost still-frozen permafrost (25–$30_p$ cm). Similar to previous studies, fPOM material had higher $^{14}C$ contents and thus presumably also a faster turnover than oPOM material (Quideau et al., 2000; Rethemeyer et al., 2005; von Lützow et al., 2007; Trumbore, 2009),

which was attributed to stabilization due to occlusion in aggregates and the recalcitrance of organic components in this fraction (Golchin et al., 1997; Poirier et al., 2005). In general, the POM material from all depth intervals is mainly derived from higher plants as indicated by *n*-alkane distributions dominated by odd numbered plant-derived $C_{23}$ to $C_{29}$ compounds (Eglinton and Hamilton, 1967).

The three fractions, however, showed strong compositional differences between each other and with soil depth. The light fPOM fraction, which is not occluded in aggregated soil structures, representing slightly decomposed root and plant material (Golchin et al., 1994), was the most abundant and carbon-rich fraction in the surface soil (0–6 cm), but decreased rapidly in abundance with active layer depth (Fig. 2a). The composition of fPOM material changed with depth from carbohydrate-rich (O-alkyl C; Table 3) material to more strongly decomposed plant litter as suggested by decreasing C/N ratios (Table 2). However, the absence of the dominant long-chain *n*-alkanes ($C_{27}$ and $C_{29}$) below 11 cm soil depth may also reflect a change in fPOM sources like decreasing proportions of plant leaf wax compounds and higher amounts of still relatively "young" root-derived OM.

Organic matter occluded in soil aggregates, which was released upon sonication, increased in importance in regard to carbon storage near and below the permafrost table (Fig. 2a). Both oPOM fractions, $< 20$ µm and $> 20$ µm, showed a quite similar and stronger $^{14}C$ decrease with depth compared to the small $^{14}C$ decrease in fPOM material, presumably indicative for better preservation of OM occluded in soil aggregates (Golchin et al., 1997). The high value for $oPOM_{>20}$ from 11–25 cm may be biased by the presence of larger plant or root fragments. Despite quite similar $^{14}C$ values, both oPOM fractions showed considerable compositional differences. Surprisingly, the composition of the large $oPOM_{>20}$ fraction obtained after aggregate disruption is quite similar to that of fPOM material, both being little-decomposed, plant-derived OM with high C/N ratios around 30 decreasing slightly with depth. The dominance of medium-chain-length *n*-alkanes and the lack of long-chain compounds in $oPOM_{>20}$ ($C_{27}$ and $C_{29}$), however, suggest either stronger OM transformation or different plant sources contribution to OM in this fraction.

In contrast, OM in the small $oPOM_{<20}$ fraction is apparently derived from other sources since typical leaf wax-derived $C_{27}$ and $C_{29}$ *n*-alkanes were dominant compounds in most depth intervals. Declining abundances of O-alkyl C (carbohydrate-rich material) and higher proportions of aryl C (aromatic compounds) as well as increasing alkyl C/O-alkyl C (Baldock et al., 1992) and aryl C/O-alkyl C ratios (Quideau et al., 2000) with depth suggest a stronger transformation of small OM occluded in aggregates, which was also found in temperate soils (Mueller and Koegel-Knabner, 2009).

The lower $^{14}C$ values and higher TOC content of oPOM compared to fPOM suggest that aggregate formation may play a small but significant role for OM preservation in these Arctic soils, however only at greater active layer depth. The effect seems to be not as prominent as in temperate surface soils under grassland and forest, where oPOM fractions were shown to account for around 5 % of the soil mass, but contained over 30 % of the bulk soil TOC (Mueller and Koegel-Knabner, 2009). In this study the oPOM fractions from the active layer had a cumulative mass of about 1 % containing 0.9–3.9 mg C $g^{-1}$ DW (8–16 % of total soil TOC) (Table 2; Fig. 2a).

#### 4.2.2 Organo-mineral associations

Although the uppermost 11 cm of the active layer were dominated by sand-sized material, most organic carbon was stored in the clay and fine-silt fractions ($< 6.3$ µm) containing up to 15.3 mg C $g^{-1}$ DW (62 % of the total soil TOC) and increasing in importance with depth (Fig. 1a; Table 2). This is quite similar to results for temperate soils where clay and silt fractions also had highest TOC contents of above 65 % (Flessa et al., 2008) and above 50 % (Rumpel et al., 2004). The $^{14}C$ contents of the size fractions showed a surprising trend from highest values for fine silt and clay-sized OM, which were close to that of bulk OM, to extremely low values for coarse silt (20–63 µm). This is in contrast to results of most previous studies of temperate soils, where often clay- to silt-sized OM ($< 63$ µm) both had relatively low $^{14}C$ contents, while sand-sized material (200–2000 µm) often showed highest $^{14}C$ values (Schöning and Kögel-Knabner, 2006; Sollins et al., 2006; von Lützow et al., 2007). Presumably, the very low $^{14}C$ contents of coarse silt may be affected by preserved POM artefacts in micro-aggregate structures.

More intense transformation of OM with decreasing particle size was observed in the uppermost 11 cm of the active layer, where C/N values decreased from sand to clay. However this trend, which was also observed in numerous previous studies of temperate soils and was often attributed to enrichment of microbial reworked products in fine mineral fractions (Sollins et al., 2006; von Lützow et al., 2007; Flessa et al., 2008; Bol et al., 2009; Sollins et al., 2009), is not seen in deeper sampling intervals. Here, closely alike C/N ratios of coarse silt to clay-sized material ($< 63$ µm) suggest a similar transformed OM. The decomposition degree of OM in fine silt and clay slightly increased with depth as shown by decreasing C/N ratios and increasing alkyl C/O-alkyl C ratios in the clay fraction. These results reflect that the labile O-alkyl C structures like carbohydrates are less stabilized, as described already for temperate soils (Rumpel et al., 2004).

Fine silt and clay showed a very similar *n*-alkane and *n*-fatty acid distributions as well as $^{14}C$ values in the different depth intervals. The plant source of soil OM in the fine-silt and clay fraction did not change significantly over depth, as indicated by *n*-alkanes being dominated by leaf wax-derived $C_{27}$ and $C_{29}$. The increase of *n*-fatty acid concentration in the uppermost permafrost layer ($25–30_p$ cm) compared to the concentration in the active layer are most likely the result of

in situ production by the hydrolysis of plant wax esters into its component *n*-alkanols and *n*-fatty acids or contribution of root-derived polyesters and suberin (Ficken et al., 1998).

Despite the lower $^{14}C$ contents of coarse and medium-silt fractions (6.3–63 µm) they are less important for organic carbon storage as both fractions represented very little of the total soil TOC ($< 2$ mg C g$^{-1}$ DW, Fig. 1a). The sand fractions (63–200 µm and 200–2000 µm) were considered to be not important for carbon storage or soil OM stabilization as these fractions contain hardly any carbon ($< 0.3$ mg C g$^{-1}$ DW).

## 5 Conclusions

Organic matter in the active layer of a polygon rim was dominated by only slightly decomposed, mainly higher plant-derived material with relatively high and strongly increasing apparent $^{14}C$ ages. In temperate soils high $^{14}C$ ages have been assumed to reflect the accumulation and stabilization of strongly transformed OM with depth. There, the formation of organo-mineral associations has been thought to be the most important mechanisms for OM stabilization. The results of our model study suggest that this mechanism is less important for OM preservation in the active layer of permafrost soils, indicated by lower organic carbon contents of clay- and fine-silt-sized OM compared to density-fractionated occluded POM (representing organic material occluded in aggregates). A further indicator is the younger apparent $^{14}C$ contents of clay- and fine-silt-sized OM compared to values for the bulk soil. Despite the high TOC contents of occluded POM from all depth intervals, protection of OM in soil aggregates seems to be a mechanism which is important only at greater active layer depth suggested by relatively high $^{14}C$ values in the uppermost 6 cm and low values near the permafrost table compared to the free light POM fraction. These results suggest that other mechanisms like recalcitrance of soil OM compounds defined by its chemical composition and decomposability, which was thought to be of minor importance for OM preservation in temperate soils, may play a more important role in permafrost soil. Therefore, further research is needed to evaluate the importance of the chemical recalcitrance of OM in the active layer as well as the climatic stabilization due to low temperatures.

*Acknowledgements.* The authors thank Stefan Heinze and Lukas Wacker for AMS $^{14}C$ measurements and Benedict Behr-Heyer, Sophia Burghardt and Sven Gelking for their assistance during night shifts. Maria Greiner, Svetlana König, Bianca Stapper and Ulrike Patt are thanked for their assistance with sample preparation and Sebastian Zubrzycki for his help with soil sampling. Gesine Mollenhauer is thanked for providing soil material. We are also grateful for logistical support by the Alfred Wegener Institute, in particular by Waldemar Schneider and Günther Stoof. We also thank two anonymous reviewers for their constructive suggestions.

Edited by: I. Bussmann

## References

Akerman, H. J. and Johansson, M.: Thawing Permafrost and Thicker Active Layers in Sub-arctic Sweden, Permafrost Periglac., 19, 279–292, doi:10.1002/ppp.626, 2008.

Andersson, R. A. and Meyers, P. A.: Effect of climate change on delivery and degradation of lipid biomarkers in a Holocene peat sequence in the Eastern European Russian Arctic, Org. Geochem., 53, 63–72, doi:10.1016/j.orggeochem.2012.05.002, 2012.

Anisimov, O. and Reneva, S.: Permafrost and Changing Climate: The Russian Perspective, AMBIO: A Journal of the Human Environment, 35, 169–175, 2006.

Are, F. and Reimnitz, E.: An Overview of the Lena River Delta Setting: Geology, Tectonics, Geomorphology, and Hydrology, J. Coastal Res., 16, 1083–1093, 2000.

Arnarson, T. S. and Keil, R. G.: Changes in organic matter-mineral interactions for marine sediments with varying oxygen exposure times, Geochim. Cosmochim. Ac., 71, 3545–3556, doi:10.1016/j.gca.2007.04.027, 2007.

Baldock, J. A., Oades, J. M., Waters, A. G., Peng, X., Vassallo, A. M., and Wilson, M. A.: Aspects of the chemical structure of soil organic materials as revealed by solid-state 13C NMR spectroscopy, Biogeochemistry, 16, 1–42, doi:10.1007/bf02402261, 1992.

Baldock, J. A., Masiello, C. A., Gélinas, Y., and Hedges, J. I.: Cycling and composition of organic matter in terrestrial and marine ecosystems, Mar. Chem., 92, 39–64, 2004.

Biasi, C., Rusalimova, O., Meyer, H., Kaiser, C., Wanek, W., Barsukov, P., Junger, H., and Richter, A.: Temperature-dependent shift from labile to recalcitrant carbon sources of arctic heterotrophs, Rapid Commun. Mass Sp., 19, 1401–1408, 2005.

Boike, J., Abramova, K., Bolshiyanov, D. Y., Grigoriev, M. N., Herzschuh, U., Kattner, G., Knoblauch, C., Kutzbach, L., Mollenhauer, G., and Schneider, W.: Russian-German Cooperation SYSTEM LAPTEV SEA: The Expedition Lena 2009, Alfred Wegener Institute for Polar and Marine Research, Bremerhaven, Germany, 34 pp., 2009.

Boike, J., Kattenstroth, B., Abramova, K., Bornemann, N., Chetverova, A., Fedorova, I., Fröb, K., Grigoriev, M., Grüber, M., Kutzbach, L., Langer, M., Minke, M., Muster, S., Piel, K., Pfeiffer, E.-M., Stoof, G., Westermann, S., Wischnewski, K., Wille, C., and Hubberten, H.-W.: Baseline characteristics of climate, permafrost, and land cover from a new permafrost observatory in the Lena River Delta, Siberia (1998–2011), Biogeosciences Discuss., 9, 13627–13684, doi:10.5194/bgd-9-13627-2012, 2012.

Bol, R., Poirier, N., Balesdent, J., and Gleixner, G.: Molecular turnover time of soil organic matter in particle-size fractions of an arable soil, Rapid Commun. Mass Sp., 23, 2551–2558, doi:10.1002/rcm.4124, 2009.

Bull, I. D., van Bergen, P. F., Nott, C. J., Poulton, P. R., and Evershed, R. P.: Organic geochemical studies of soils from the Rothamsted classical experiments – V. The fate of lipids in different long-term experiments, Org. Geochem., 31, 389–408, 2000.

Charkin, A. N., Dudarev, O. V., Semiletov, I. P., Kruhmalev, A. V., Vonk, J. E., Sánchez-García, L., Karlsson, E., and Gustafsson, Ö.: Seasonal and interannual variability of sedimentation

and organic matter distribution in the Buor-Khaya Gulf: the primary recipient of input from Lena River and coastal erosion in the southeast Laptev Sea, Biogeosciences, 8, 2581–2594, doi:10.5194/bg-8-2581-2011, 2011.

Cherkinsky, A. E.: 14C dating and soil organic matter dynamcis in arctic and subarctic ecosystems, Radiocarbon, 38, 241–245, 1996.

Christensen, B. T.: Physical fractionation of soil and structural and functional complexity in organic matter turnover, Eur. J. Soil Sci., 52, 345–353, doi:10.1046/j.1365-2389.2001.00417.x, 2001.

Dickens, A. F., Baldock, J. A., Smernik, R. J., Wakeham, S. G., Arnarson, T. S., Gélinas, Y., and Hedges, J. I.: Solid-state 13C NMR analysis of size and density fractions of marine sediments: Insight into organic carbon sources and preservation mechanisms, Geochim. Cosmochim. Ac., 70, 666–686, 2006.

Dittmar, T. and Kattner, G.: The biogeochemistry of the river and shelf ecosystem of the Arctic Ocean: a review, Mar. Chem., 83, 103–120, doi:10.1016/S0304-4203(03)00105-1, 2003.

Eglinton, G. and Hamilton, R. J.: Leaf epicuticular waxes, Science, 156, 1322–1335, 1967.

Fahl, K. and Stein, R.: Biomarker records, organic carbon accumulation, and river discharge in the Holocene southern Kara Sea (Arctic Ocean), Geo-Mar. Lett., 27, 13–25, doi:10.1007/s00367-006-0049-8, 2007.

FAO – Food and Agriculture Organization: WRB – World reference base for soil resources 2006, 1st update 2007, FAO, Rom, 1–128, 2007.

Ficken, K. J., Barber, K. E., and Eglinton, G.: Lipid biomarker, $\delta$13C and plant macrofossil stratigraphy of a Scottish montane peat bog over the last two millennia, Org. Geochem., 28, 217–237, 1998.

Flessa, H., Amelung, W., Helfrich, M., Wiesenberg, G. L. B., Gleixner, G., Brodowski, S., Rethemeyer, J., Kramer, C., and Grootes, P. M.: Storage and stability of organic matter and fossil carbon in a Luvisol and Phaeozem with continuous maize cropping: A synthesis, J. Plant Nutr. Soil Sc., 171, 36–51, doi:10.1002/jpln.200700050, 2008.

Frey, K. E. and McClelland, J. W.: Impacts of permafrost degradation on arctic river biogeochemistry, Hydrol. Process., 23, 169–182, doi:10.1002/hyp.7196, 2009.

Golchin, A., Oades, J., Skjemstad, J., and Clarke, P.: Study of free and occluded particulate organic matter in soils by solid state $^{13}$C CP/MAS NMR spectroscopy and scanning electron microscopy, Soil Research, 32, 285–309, doi:10.1071/SR9940285, 1994.

Golchin, A., Baldock, J. A., and Oades, J. M.: A model linking organic matter decomposition, chemistry and aggregate dynamics, in: Soil Processes and the Carbon Cycle, edited by: Stewart, B. A. E., CRC Press, Boca Raton, FL, 245–266, 1997.

Guicharnaud, R., Arnalds, O., and Paton, G. I.: Short term changes of microbial processes in Icelandic soils to increasing temperatures, Biogeosciences, 7, 671–682, doi:10.5194/bg-7-671-2010, 2010.

Guo, L., Ping, C.-L., and Macdonald, R. W.: Mobilization pathways of organic carbon from permafrost to arctic rivers in a changing climate, Geophys. Res. Lett., 34, L13603, doi:10.1029/2007gl030689, 2007.

Gustafsson, Ö., van Dongen, B. E., Vonk, J. E., Dudarev, O. V., and Semiletov, I. P.: Widespread release of old carbon across the Siberian Arctic echoed by its large rivers, Biogeosciences, 8, 1737–1743, doi:10.5194/bg-8-1737-2011, 2011.

Hinkel, K. M. and Nelson, F. E.: Spatial and temporal patterns of active layer thickness at Circumpolar Active Layer Monitoring (CALM) sites in northern Alaska, 1995–2000, J. Geophys. Res., 108, 8168–8181, doi:10.1029/2001JD000927, 2003.

Huang, Y. S., Dupont, L., Sarnthein, M., Hayes, J. M., and Eglinton, G.: Mapping of C4 plant input from North West Africa into North East Atlantic sediments, Geochim. Cosmochim. Ac., 64, 3505–3513, 2000.

Hubberten, H.-W., Wagner, D., Pfeiffer, E.-M., Boike, J., and Gukov, A. Y.: The Russian-German research station Samoylov, Lena Delta – A key site for polar research in the Siberian Arctic, Polarfoschung, 73, 111–116, 2006.

Jambu, P., Amblès, A., Dinel, H., and Secouet, B.: Incorporation of natural hydrocarbons from plant residues into an hydromorphic humic podzol following afforestation and fertilization, J. Soil Sci., 42, 629–636, 1991.

Jones, A., Stolbovoy, V., Tarnocai, C., Broll, G., Spaargaren, O., and Montanarella, L.: Soil Atlas of the northern circumpolar region, European Commission, Publications Office of the European Union, Luxembourg, 2010.

Karlsson, E. S., Charkin, A., Dudarev, O., Semiletov, I., Vonk, J. E., Sánchez-García, L., Andersson, A., and Gustafsson, Ö.: Carbon isotopes and lipid biomarker investigation of sources, transport and degradation of terrestrial organic matter in the Buor-Khaya Bay, SE Laptev Sea, Biogeosciences, 8, 1865–1879, doi:10.5194/bg-8-1865-2011, 2011.

Knoblauch, C., Zimmermann, U., Blumenberg, M., Michaelis, W., and Pfeiffer, E.-M.: Methane turnover and temperature response of methane-oxidizing bacteria in permafrost-affected soils of northeast Siberia, Soil Biol. Biochem., 40, 3004–3013, 2008.

Kögel-Knabner, I.: Analytical approaches for characterizing soil organic matter, Org. Geochem., 31, 609–625, 2000.

Kögel-Knabner, I.: The macromolecular organic composition of plant and microbial residues as inputs to soil organic matter, Soil Biol. Biochem., 34, 139–162, 2002.

Kögel-Knabner, I., Guggenberger, G., Kleber, M., Kandeler, E., Kalbitz, K., Scheu, S., Eusterhues, K., and Leinweber, P.: Organo-mineral associations in temperate soils: Integrating biology, mineralogy, and organic matter chemistry, J. Plant Nutr. Soil Sc., 171, 61–82, doi:10.1002/jpln.200700048, 2008.

Kutzbach, L., Wagner, D., and Pfeiffer, E.-M.: Effect of microrelief and vegetation on methane emission from wet polygonal tundra, Lena Delta, Northern Siberia, Biogeochemistry, 69, 341–362, doi:10.1023/B:BIOG.0000031053.81520.db, 2004.

Lara, R. J., Rachold, V., Kattner, G., Hubberten, H. W., Guggenberger, G., Skoog, A., and Thomas, D. N.: Dissolved organic matter and nutrients in the Lena River, Siberian Arctic: Characteristics and distribution, Mar. Chem., 59, 301–309, 1998.

Lobbes, J. M., Fitznar, H. P., and Kattner, G.: Biogeochemical characteristics of dissolved and particulate organic matter in Russian rivers entering the Arctic Ocean, Geochim. Cosmochim. Ac., 64, 2973–2983, 2000.

Marschner, B., Brodowski, S., Dreves, A., Gleixner, G., Gude, A., Grootes, P. M., Hamer, U., Heim, A., Jandl, G., Ji, R., Kaiser, K., Kalbitz, K., Kramer, C., Leinweber, P., Rethemeyer, J., Schäffer, A., Schmidt, M. W. I., Schwark, L., and Wiesenberg, G. L. B.: How relevant is recalcitrance for the stabilization of organic matter in soils?, J. Plant Nutr. Soil Sc., 171, 91–110,

doi:10.1002/jpln.200700049, 2008.

Minke, M., Donner, N., Karpov, N. S., Klerk, P. D., and Joosten, H.: Distribution, diversity, development and dynamics of polygon mires: examples from Northeast Yakutia (Siberia), Peatlands International, 1, 36–40, 2007.

Mueller, C. and Koegel-Knabner, I.: Soil organic carbon stocks, distribution, and composition affected by historic land use changes on adjacent sites, Biol. Fert. Soils, 45, 347–359, doi:10.1007/s00374-008-0336-9, 2009.

Mueller, C., Brüggemann, N., Pritsch, K., Stoelken, G., Gayler, S., Winkler, J., and Kögel-Knabner, I.: Initial differentiation of vertical soil organic matter distribution and composition under juvenile beech (*Fagus sylvatica* L.) trees, Plant Soil, 323, 111–123, doi:10.1007/s11104-009-9932-1, 2009.

Mueller, K.: Oberflächenstrukturen und Eigenschaften von Permafrostböden im nordsibirischen Lena-Delta, Z. Pflanz. Bodenkunde, 160, 497–503, doi:10.1002/jpln.19971600410, 1997 (in German).

Naafs, D. F. W., van Bergen, P. F., Boogert, S. J., and de Leeuw, J. W.: Solvent-extractable lipids in an acid andic forest soil; variations with depth and season, Soil Biol. Biochem., 36, 297–308, doi:10.1016/j.soilbio.2003.10.005, 2004.

Nelson, F. E., Shiklomanov, N. I., Hinkel, K. M., and Brown, J.: Decadal Results from the Circumpolar Active Layer Monitoring (CALM) Program, NICOP: Ninth internationcal conference on permafrost, 29 June–3 July 2008, University of Alaska Fairbanks, 1273–1280, 2008.

Pfeiffer, E.-M., Wagner, D., Kobabe, S., Kufzbach, L., A. Kurchatova, Stoof, G., and Wille, C.: Modern Processes in Permafrost Affected Soils, Reports on Polar and Marine Research, 426, 21–41, 2002.

Poirier, N., Sohi, S. P., Gaunt, J. L., Mahieu, N., Randall, E. W., Powlson, D. S., and Evershed, R. P.: The chemical composition of measurable soil organic matter pools, Org. Geochem., 36, 1174–1189, 2005.

Quideau, S. A., Anderson, M. A., Graham, R. C., Chadwick, O. A., and Trumbore, S. E.: Soil organic matter processes: characterization by 13C NMR and 14C measurements, Forest Ecol. Manag., 138, 19–27, 2000.

Rethemeyer, J., Kramer, C., Gleixner, G., John, B., Yamashita, T., Flessa, H., Andersen, N., Nadeau, M.-J., and Grootes, P. M.: Transformation of organic matter in agricultural soils: radiocarbon concentration versus soil depth, Geoderma, 128, 94–105, 2005.

Rethemeyer, J., Fülöp, R. H., Höfle, S., Wacker, L., Heinze, S., Hajdas, I., Patt, U., König, S., Stapper, B., and Dewald, A.: Status report on sample preparation facilities for 14C analysis at the new CologneAMS center, Nuclear Instruments and Methods in Physics Research Section B: Beam Interactions with Materials and Atoms, 294, 168–172, doi:10.1016/j.nimb.2012.02.012, 2013.

Romanovskii, N. N. and Hubberten, H.-W.: Results of permafrost modelling of the lowlands and shelf of the Laptev Sea Region, Russia, Permafrost Periglac., 12, 191–202, doi:10.1002/ppp.387, 2001.

Rumpel, C. and Kögel-Knabner, I.: Deep soil organic matter – a key but poorly understood component of terrestrial C cycle, Plant Soil, 338, 143–158, doi:10.1007/s11104-010-0391-5, 2011.

Rumpel, C., Eusterhues, K., and Kögel-Knabner, I.: Location and chemical composition of stabilized organic carbon in topsoil and subsoil horizons of two acid forest soils, Soil Biol. Biochem., 36, 177–190, 2004.

Sanaullah, M., Chabbi, A., Leifeld, J., Bardoux, G., Billou, D., and Rumpel, C.: Decomposition and stabilization of root litter in top- and subsoil horizons: what is the difference?, Plant Soil, 338, 127–141, doi:10.1007/s11104-010-0554-4, 2011.

Schaefer, K., Zhang, T., Bruhwiler, L., and Barrett, A. P.: Amount and timing of permafrost carbon release in response to climate warming, Tellus B, 63, 165–180, doi:10.1111/j.1600-0889.2011.00527.x, 2011.

Schöning, I. and Kögel-Knabner, I.: Chemical composition of young and old carbon pools throughout Cambisol and Luvisol profiles under forests, Soil Biol. Biochem., 38, 2411–2424, 2006.

Schubert, C. J. and Stein, R.: Lipid Distribution in surface sediments from the eastern central Arctic Ocean, Mar. Geol., 138, 11–25, 1997.

Semiletov, I. P., Pipko, I. I., Shakhova, N. E., Dudarev, O. V., Pugach, S. P., Charkin, A. N., McRoy, C. P., Kosmach, D., and Gustafsson, Ö.: Carbon transport by the Lena River from its headwaters to the Arctic Ocean, with emphasis on fluvial input of terrestrial particulate organic carbon vs. carbon transport by coastal erosion, Biogeosciences, 8, 2407–2426, doi:10.5194/bg-8-2407-2011, 2011.

Simpson, M. and Simpson, A.: The Chemical Ecology of Soil Organic Matter Molecular Constituents, J. Chem. Ecol., 38, 768–784, doi:10.1007/s10886-012-0122-x, 2012.

Six, J., Conant, R. T., Paul, E. A., and Paustian, K.: Stabilization mechanisms of soil organic matter: Implications for C-saturation of soils, Plant Soil, 241, 155–176, doi:10.1023/a:1016125726789, 2002.

Sollins, P., Homann, P., and Caldwell, B. A.: Stabilization and destabilization of soil organic matter: mechanisms and controls, Geoderma, 74, 65–105, 1996.

Sollins, P., Swanston, C., Kleber, M., Filley, T., Kramer, M., Crow, S., Caldwell, B. A., Lajtha, K., and Bowden, R.: Organic C and N stabilization in a forest soil: Evidence from sequential density fractionation, Soil Biol. Biochem., 38, 3313–3324, doi:10.1016/j.soilbio.2006.04.014, 2006.

Sollins, P., Kramer, M. G., Swanston, C., Lajtha, K., Filley, T., Aufdenkampe, A. K., Wagai, R., and Bowden, R. D.: Sequential density fractionation across soils of contrasting mineralogy: evidence for both microbial- and mineralcontrolled soil organic matter stabilization, Biogeochemistry, 96, 209–231, doi:10.1007/s10533-009-9359-z, 2009.

Trumbore, S.: Radiocarbon and Soil Carbon Dynamics, Annu. Rev. Earth Pl. Sc., 39, 47–66, doi:10.1146/annurev.earth.36.031207.124300, 2009.

van Dongen, B. E., Semiletov, I., Weijers, J. W. H., and Gustafsson, Ö.: Contrasting lipid biomarker composition of terrestrial organic matter exported from across the Eurasian Arctic by the five great Russian Arctic rivers, Global Biogeochem. Cy., 22, GB1011, doi:10.1029/2007gb002974, 2008.

von Lützow, M., Kögel-Knabner, I., Ekschmitt, K., Flessa, H., Guggenberger, G., Matzner, E., and Marschner, B.: SOM fractionation methods: Relevance to functional pools and to stabilization mechanisms, Soil Biol. Biochem., 39, 2183–2207, doi:10.1016/j.soilbio.2007.03.007, 2007.

von Lützow, M., Kögel-Knabner, I., Ludwig, B., Matzner, E., Flessa, H., Ekschmitt, K., Guggenberger, G., Marschner, B., and Kalbitz, K.: Stabilization mechanisms of organic matter in four temperate soils: Development and application of a conceptual model, J. Plant Nutr. Soil Sc., 171, 111–124, doi:10.1002/jpln.200700047, 2008.

Vonk, J. E.: Molecular and isotopic characterization of terrestrial organic carbon released to (sub-)Arctic coastal waters, Ph.D. thesis, Department of Applied Environmental Science, Stockholm University, Stockholm, 51 pp., 2010.

Wagner, D., Gattinger, A., Embacher, A., Pfeiffer, E.-M., Schloter, M., and Lipski, A.: Methanogenic activity and biomass in Holocene permafrost deposits of the Lena Delta, Siberian Arctic and its implication for the global methane budget, Glob. Change Biol., 13, 1089–1099, doi:10.1111/j.1365-2486.2007.01331.x, 2007.

Wakeham, S. G., Canuel, E. A., Lerberg, E. J., Mason, P., Sampere, T. P., and Bianchi, T. S.: Partitioning of organic matter in continental margin sediments among density fractions, Mar. Chem., 115, 211–225, 2009.

Waldrop, M. P., Wickland, K. P., White III, R., Berhe, A. A., Harden, J. W., and Romanovsky, V. E.: Molecular investigations into a globally important carbon pool: permafrost-protected carbon in Alaskan soils, Glob. Change Biol., 16, 2543–2554, doi:10.1111/j.1365-2486.2009.02141.x, 2010.

Xu, C., Guo, L., Ping, C.-L., and White, D. M.: Chemical and isotopic characterization of size-fractionated organic matter from cryoturbated tundra soils, northern Alaska, J. Geophys. Res., 114, G03002, doi:10.1029/2008jg000846, 2009.

Zimov, S. A., Davydov, S. P., Zimova, G. M., Davydova, A. I., Schuur, E. A. G., Dutta, K., and Chapin III, F. S.: Permafrost carbon: Stock and decomposability of a globally significant carbon pool, Geophys. Res. Lett., 33, L20502, doi:10.1029/2006GL027484, 2006.

Zubrzycki, S., Kutzbach, L., Grosse, G., Desyatkin, A., and Pfeiffer, E.-M.: Organic carbon and total nitrogen stocks in soils of the Lena River Delta, Biogeosciences Discuss., 9, 17263–17311, doi:10.5194/bgd-9-17263-2012, 2012.

# 5. Manuscript III: Identification of microbial communities in active layer soils – *Characterization of bacterial populations in Arctic permafrost soils using bacteriohopanepolyols*

by

**Höfle S.**, Kusch S., Talbot H. M., Mollenhauer G., Zubrzycki S., Burghardt S., Rethemeyer J.

under review by *Organic Geochemistry*
(07.01.2015)

# Characterization of bacterial populations in Arctic permafrost soils using bacteriohopanepolyols

Silke Höfle[a], Stephanie Kusch[a], Helen M. Talbot[b], Gesine Mollenhauer[c], Sebastian Zubrzycki[d], Sophia Burghardt[a], Janet Rethemeyer[a]

[a] *Institute of Geology and Mineralogy, University of Cologne, Zuelpicher Str. 49a, 50674 Cologne, Germany*

[b] *School of Civil Engineering and Geosciences, Drummond Building, Newcastle University, Newcastle upon Tyne, NE1 7RU, UK*

[c] *Alfred-Wegener-Institute for Polar and Marine Research, Am Handelshafen 12, 27570 Bremerhaven, Germany*

[d] *Institute of Soil Science, Center for Earth System Research and Sustainability (CEN), Universität Hamburg, Allende-Platz 2, 20146 Hamburg, Germany*

## Abstract

Bacteriohopanepolyols (BHPs) have a great capacity as biomarkers providing taxonomically and environmentally diagnostic information. Because of the recalcitrance of hopanoid hydrocarbons, BHPs may help to unravel bacterial communities residing in recent as well as in ancient permafrost soils and sediments and may give information on associated environmental conditions. However, detailed data on their distribution in the heterogeneous Arctic environment are scarce. Here, the distribution and structural diversity of BHPs were studied in the annually thawing (active) layer of three different sites in the polygonal tundra of the Lena Delta in the Siberian Arctic. Variations between different permafrost structures caused by differences in the physical and chemical soil properties were observed. The greatest structural diversity and highest BHP concentrations probably indicating a great bacterial biomass and diversity were found in the uppermost organic soil horizon (Oi) consisting of non-degraded plant litter. Apparently structural diversity is linked to relatively low pH and high organic matter content, but may also be a function of soil temperature. Taxonomically diagnostic BHPs found in the permafrost soils include amine-functionalized BHPs from methanotrophic bacteria only occurring in the water-saturated, oxygen-depleted polygon centres, cyanobacterial BHPs, which show highest abundances in the organic horizons, and the adenosylhopane-type soil-marker BHPs, which are significantly more abundant in the well aerated polygon rims than in the centres. These results agree well with published 16S rRNA based community structure assessments highlighting the usefulness of BHPs to represent bacterial populations in permafrost soils.

## 1. Introduction

Permafrost soils are a very distinct habitat for life given their sub-zero temperatures and significant temperature fluctuations (Gilichinsky et al., 1995). Nonetheless, microorganisms have adapted to these harsh conditions through metabolic regulation (Jansson and Tas, 2014 and reference therein). Bacterial activity and cell growth have been reported at ambient permafrost temperatures of down to -25°C (Mykytczuk et al., 2013). Generally, bacteria seem to occur in higher diversity and higher abundance when compared to both archaea and fungi (Steven et al., 2008, Yergeau et al., 2010). Amongst the most frequently observed bacterial phyla (based on 16S rRNA sequencing) are Proteobacteria, Firmicutes, Chloroflexi, Acidobacteria, Actinobacteria and Bacteroidetes (Jansson and Tas, 2014).

One means to study bacterial biomass is the analysis of their membrane lipids. Phospholipid fatty acids (PLFAs) are the main constituents of the bacterial bilayer membrane. However, PLFAs are degraded within days to weeks after cell death and, thus, reflect the viable microbial community (Kaur et al., 2005) and do not allow tracing of bacterial biomass through space and time. Bacteriohopanepolyols (BHPs) are pentacyclic triterpenoids, which are produced almost exclusively by bacteria while they are absent in archaea (Ourisson and Albrecht, 1992). In contrast to PLFAs, the degradation products of BHPs can be preserved in sedimentary records (e.g., Brocks et al., 1999). BHPs are believed to help organisms adapt to physiological stress by modulating the fluidity and organization of the bacterial phospholipid membrane (Rohmer et al., 1984; Kannenberg and Poralla, 1999; Rohmer, 2008; Welander et al., 2009). To date a suite of structurally different side chains have been identified of which some are proposed to provide taxonomic and/or physiological information (Rohmer, 1993; Talbot and Farrimond, 2007). For example, some amine-functionalized BHPs such as 35-aminobacteriohopane-31,32,33,34-tetrol (aminotetrol; **Ia**, see Appendix for structures) and 35-aminobacteriohopane-30,31,32,33,34-pentol (aminopentol; **Ib**) are characteristic for aerobic methanotrophic bacteria and are found in many species and environments (Neunlist and Rohmer, 1985b; Cvejic et al., 2000; Talbot and Farrimond, 2007; Zhu et al., 2010; van Winden et al., 2012; Talbot et al., 2014). However, low levels of aminotetrol and in one case trace levels of aminopentol have been found in some species of sulphate-reducing bacteria of the genus *Desulfovibrio* (Blumenberg et al., 2006; Blumenberg et al., 2009; Blumenberg et al., 2012). BHPs methylated at the C-2 position (**II**) have previously been used as markers for cyanobacteria (e.g. Summons et al., 1999; Zhang et al., 2007; Talbot et al., 2008) although this interpretation has been questioned as the *hpnP* gene, required for C2-methylation, has also be identified in Alphaproteobacteria and at least one Acidobacterium (Welander et al., 2010). Furthermore, the occurrence of C-2 methylation in Alphaproteobacteria appears to be particularly common in species involved in plant-microbe interactions (Ricci et al., 2014).

The BHP adenosylhopane (**Ic**) has been reported to be the precursor to all other side chain extended BHPs (Bradley et al., 2010). Adenosylhopane, together with several related structures also containing a cyclised side chain (**Id, Ie**) and their C-2 methylated

homologues (**IIc**, **IId**, **IIe**), are potential environmental rather than taxonomic markers. These compounds have been identified to be abundant in soils while occurring only in minor concentrations in marine and lacustrine sediments (Talbot and Farrimond, 2007; Cooke et al., 2009; Xu et al., 2009; Blumenberg et al., 2010; Rethemeyer et al., 2010; Kim et al., 2011; Sáenz et al., 2011; Taylor and Harvey, 2011; Zhu et al., 2011; Doğrul Selver et al., 2012; Wagner et al., 2014). Adenosylhopane and its related structures (hereafter referred to as soil-marker BHPs) have also been studied in Arctic environment where they have been used as indicators for the export of terrigeneous organic matter into Arctic Rivers and the Arctic Ocean (van Dongen et al., 2008; Cooke et al., 2009; Taylor and Harvey, 2011). In all studies mainly marine and riverine samples were investigated, while information from the alleged terrestrial source – permafrost soils – remains scarce.

To date only Rethemeyer et al. (2010) studied BHPs in Arctic permafrost soils from Svalbard in which a larger and more diverse bacterial community was observed in the organic horizons compared to the underlying mineral soils while no study has been performed so far in the organic-rich and extremely heterogeneous Arctic tundra. We thus investigated BHP distributions in the seasonally thawing surface layer, the active layer, of characteristic polygonal tundra soils in the Siberian Arctic in order to (a) evaluate their spatial variability and (b) to characterize the bacterial communities present and compare these results with other methods including PLFA analyses and DNA/RNA sequencing.

## 2. Study area

The Lena Delta in Siberia, Russia, is the largest Arctic river delta covering approximately 32,000 $km^2$ (Are and Reimnitz, 2000). It is located in the zone of continuous permafrost under an Arctic continental climate characterised by low mean annual precipitation (125 mm), low mean annual air temperatures (-12.5°C), and a large seasonal temperature amplitude between summer (July 10.1°C) and winter (February -33.1°C; Boike et al., 2013).

The Lena Delta consists of over 1,000 islands including Samoylov Island and Kurungnakh Island (Fig. 1). Samoylov Island belongs to the recent active delta region (1-12 m a.s.l.) and is made up of Holocene fluvial sediment. It is characterised by ice wedge polygonal tundra with thermokarst lakes and an active flood plain. Ice wedges form through seasonal frost-cracking repeatedly pushing material upwards to form elevated rims surrounding depressed centres (e.g., Fiedler et al., 2004). Kurungnakh Island (30-60 m a.s.l.) consists of a lower 15-20 m thick Paleo-Lena River sand unit overlain by a ca. 20 m thick late Pleistocene ice-rich, fine-grained permafrost sequence (ice complex; Schirrmeister et al., 2011). The ice complex formation, often synonymously called ‘Yedoma’, is covered by a 2 - 3 m thick unit of Holocene aeolian silty sand in which polygonal tundra developed with small, 3-5 m wide ice wedges (Morgenstern et al., 2011; Schirrmeister et al., 2011; Zubrzycki, 2013).

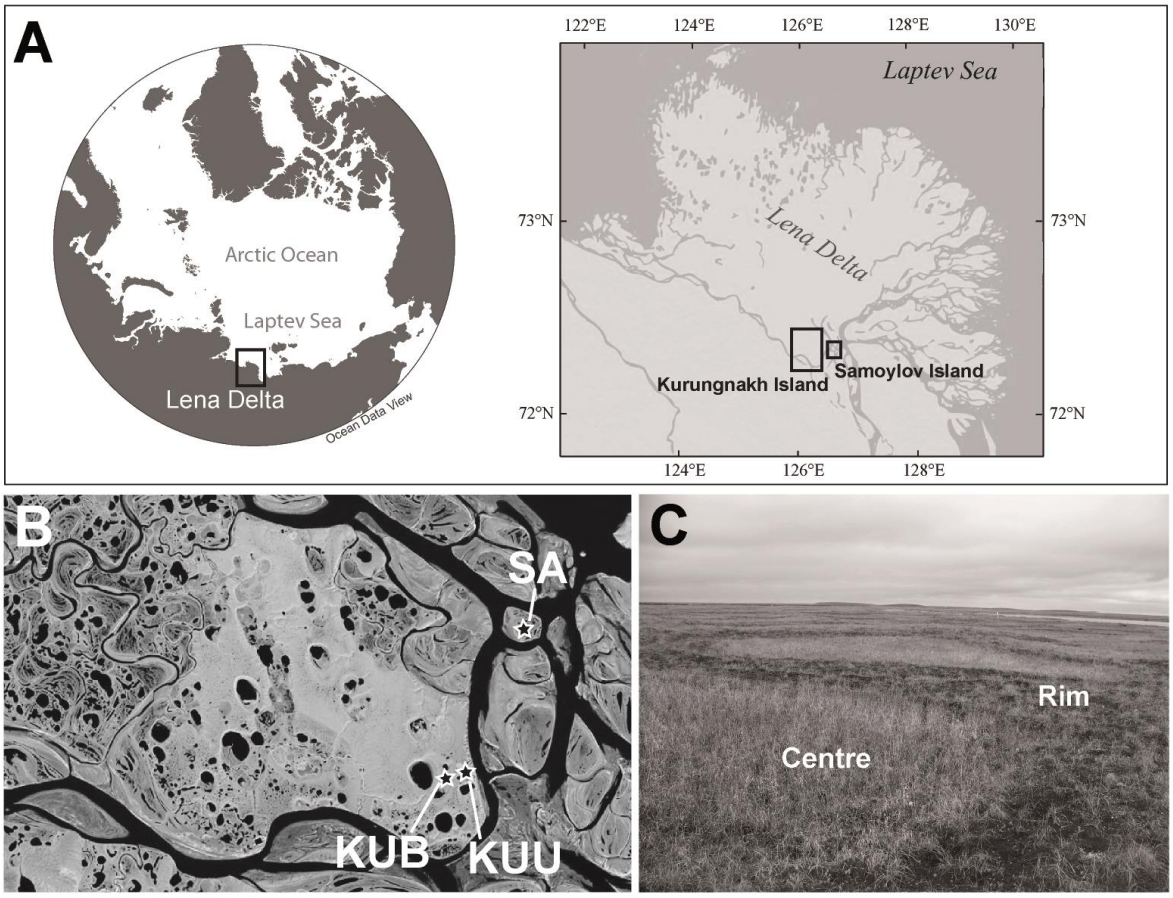


Fig. 1: (A) Study area in the Lena Delta including (B) sampling sites on Samoylov (SA) and Thermokarst basin (KUB) and Upland (KUU) on Kurungnakh Island (Landsat 7 image modified from http:\\www.earthobservatory.nasa.gov/IOTD/view.php?id=2704), and (C) the different landscape structures (polygon centre and rim on SA).

The soils on Samoylov and Kurungnakh Islands belong to the order of Gelisols (Soil Survey Staff, 2010) with polygon rims dominated by Glacic Aquiturbels and depressed polygon centres characterized by Typic or Ruptic Historthels with sandy loam to silt loam soil texture (Table 2; Zubrzycki et al., 2012). Mosses, grasses, sedges, and dwarf willow shrubs dominate the vegetation at both study sites with different distributions on polygon rims and centres (Boike et al., 2013).

## 3. Material and methods

### 3.1 Sampling

In total, three sampling sites were chosen according to their morphological differences (Table 1): a polygon in a relatively recently developed thermokarst basin (KUB) and a polygon on the elevated (55 m a.s.l) upland (KUU) on Kurungnakh Island as well as a polygon developed on typical modern fluvial deposits on Samoylov Island (SA). In comparison to the aeolian origin of the KUU polygon, the KUB polygon developed on

aeolian and lacustrine sediment of a former thermokarst lake, which drained about 5.7 ka BP (Morgenstern et al., 2013).

Table 1: Study sites in the Lena Delta, Siberia (Russia).

| Site | Latitude (N) | Longitude (E) | Elevation [m a.s.l.] |
|---|---|---|---|
| Samoylov Island (SA) | 72° 22' 22'' | 126° 29' 05'' | 12 |
| Kurungnakh Island – Thermokarst basin (KUB) | 72° 19' 24'' | 126° 13' 22'' | 38 |
| Kurungnakh Island – Upland (KUU) | 72° 19' 31'' | 126° 15' 56'' | 55 |

At all sites, the polygons had diameters of ca. 9-13 m. Both the depressed, water saturated polygon centres (C) and the several decimetres elevated and relatively dry polygon rims (R) were sampled at the end of the summer, i.e. at maximal thaw depth of the active layer in August 2009 and 2010. Samples were taken from the characteristic horizons of the active layer (Table 2), which was about 29 to 43 cm thick; shallower in polygon rims and deeper in centres. At site SA, a sample of the uppermost still frozen permafrost was also retrieved from the polygon rim (SA-$R_{Bjjf}$).

Table 2: Basic soil properties.

| Site location | Soil type – Great Group[a] | Horizon | Depth [cm] | Texture[a] | Water saturated | pH | TOC[b] [%] | Total N [%] | C/N |
|---|---|---|---|---|---|---|---|---|---|
| ***Kurungnakh Island*** | | | | | | | | | |
| Thermokarst basin- | Glacic | Oi | 0-12 | litter | no | 5.0 | 22.7 | 0.5 | 47 |
| polygon rim | Aquiturbels | Oe | 12-18 | litter | no | 5.0 | 6.9 | 0.4 | 19 |
| (KUB-R) | | Bjjg | 18-30 | loam | temporary | 4.9 | 4.2 | 0.2 | 19 |
| Thermokarst basin- | Ruptic | Oi | 0-5 | litter | yes | 6.3 | 28.4 | 0.8 | 35 |
| polygon centre | Historthels | Oe | 5-12 | litter | yes | 4.9 | 23.0 | 0.7 | 33 |
| (KUB-C) | | Oe2 | 12-20 | litter | yes | 4.6 | 10.7 | 0.4 | 29 |
| | | A | 20-28 | silt loam | yes | 4.7 | 15.7 | 0.7 | 23 |
| | | Bg | 28-45 | loamy sand | yes | 5.2 | 5.6 | 0.3 | 22 |
| Upland- | Glacic | Oi | 0-10 | litter | no | 4.4 | 19.1 | 0.3 | 69 |
| polygon rim | Aquiturbels | A | 10-14 | sandy loam | no | 5.9 | 8.4 | 0.4 | 19 |
| (KUU-R) | | Bjj | 14-16 | sandy loam | no | 5.3 | 8.4 | 0.5 | 16 |
| | | Bg | 16-29 | sandy loam | temporary | 5.3 | 5.0 | 0.2 | 22 |
| Upland- | Typic | Oi | 0-6 | litter | yes | na | 21.1 | 0.6 | 35 |
| polygon centre | Historthels | Oe | 6-22 | litter | yes | 4.5 | 9.3 | 0.4 | 23 |
| (KUU-C) | | A | 22-33 | silt loam | yes | 4.7 | 11.2 | 0.6 | 18 |
| | | Bg | 33-48 | sandy loam | yes | 4.8 | 3.8 | 0.1 | 31 |
| ***Samoylov Island*** | | | | | | | | | |
| Samoylov- | Glacic | Oi | 0-7 | litter | no | 5.0 | 10.3 | na | na |
| polygon rim | Aquiturbels | Ajj | 7-13 | sandy loam | no | 6.1[c] | 3.0[c] | 0.2 | 19[c] |
| (SA-R) | | Bjjg | 13-18 | loamy sand | no | 6.4[c] | 1.5[c] | 0.1 | 18[c] |
| | | Bjjg2 | 18-32 | silt loam | temporary | 6.3[c] | 3.0[c] | 0.2 | 18[c] |
| | | Bjjf | 32-37 | silt loam | temporary | 6.7[c] | 2.5[c] | 0.2 | 16[c] |
| Samoylov- | Typic | Oi | 0-14 | litter | yes | na | 23.0 | 0.5 | 45 |
| polygon centre | Historthels | Oe | 14-40 | litter | yes | 4.8 | 8.7 | 0.2 | 51 |
| (SA-C) | | B | 40-43 | sandy loam | yes | 5.9 | 4.2 | 0.2 | 35 |

[a] according to US Soil Taxonomy (Soil Survey Staff, 2010)

[b] total organic carbon

[c] Höfle et al. 2013 (depth of Ajj set to zero in the paper)

na – not analysed

All samples were stored in pre-combusted glass jars and kept frozen until analysis. Prior to analysis, samples were freeze-dried and ground.

### 3.3 Bulk soil analysis

Total carbon and nitrogen contents were determined on 5-10 mg soil using a Vario MICRO cube elemental analyser (Elementar, Germany). All samples were carbonate-free, therefore total C contents equal total organic carbon content (TOC). Soil pH values were measured in water (soil:water 1:2.5; w:w) one hour after water addition (IUSS Working Group WRB, 2006).

### 3.4 BHP extraction and analysis

BHPs were extracted using the method described in Cooke et al. (2008). Briefly, samples (2 g) were sonicated three times using chloroform/methanol/water (5:10:4; v:v) followed by liquid-liquid extraction of the organics from the aqueous phase. The total lipid extract was subsequently acetylated using acetic anhydride and pyridine (1:1, v:v; heated at 50°C for one hour, left overnight), dried, and re-dissolved in methanol/propan-2-ol (3:2, v:v) for filtration over 0.45 µm PTFE syringe filters prior to LC/$MS^n$ measurements. Reversed-phase LC-$MS^n$ analysis was performed using a Surveyor LC system (ThermoFinnigan, UK) equipped with an atmospheric pressure chemical ionization (APCI) ion source operated in positive ion mode. Separation of BHPs was achieved following the method and setup described by Talbot et al. (2007b).

BHPs were identified according to their characteristic APCI base peak (m/z; Table 3) and quantified using an internal standard (5α–Pregnane-3β,20β-diol) added prior to the measurements. Additionally, an external standard mixture was run six times (relative SD for the single BHPs: 3-11%) to ensure high quality of measurements. One sample (SA-$C_{Oi}$) was measured thrice to check reproducibility (relative SD for the single BHPs: 5-42%).

Table 3: List of identified BHPs according to BHP group including trivial name, structure, characteristic APCI base peak ion (m/z), and known source organisms.

| BHP group | BHP trivial name and structure number | Base peak (m/z) | Source organisms | Supporting reference |
|---|---|---|---|---|
| Cyanobacteria | 2-Me BHT (**IIf**) | 669 | Cyanobacteria + PNSB[a] | Bisseret et al., 1985; Rashby et al., 2007 |
| | unsaturated BHT pentose (**III** or **IVi**) | 941 | Cyanobacteria | Talbot et al., 2008 |
| | BHT pentose (**Ii**) | 943 | Cyanobacteria | Talbot et al., 2008 |
| | 2-Me BHT pentose (**IIi**) | 957 | Cyanobacteria | Talbot et al., 2008 |
| Methanotrophs | Aminotetrol (**Ia**) | 772 | Methanotrophs + sulfate reducing bacteria | Neunlist and Rohmer, 1985a; Blumenberg et al., 2006 |
| | Aminopentol (**Ib**) | 830 | Methanotrophs type 1 | Neunlist and Rohmer, 1985b |
| Soil-marker | Adenosylhopane (**Ic**) | 746 | PNSB + $N_2$ fixing + *Nitrosomonas europaea* + *Methylocella palustris* | Neunlist and Rohmer, 1985c; Bravo et al., 2001; Seemann et al., 1999; Talbot et al., 2007b; van Winden et al., 2012 |
| | Adenosylhopane-type-2 (**Id**) | 761 | PNSB | Talbot et al., 2007b |
| | 2-Me adenosylhopane-type-2 (**IId**) | 775 | Unknown | Cooke et al., 2008 |
| | Adenosylhopane-type-3 (**Ie**) | 802 | Unknown | Rethemeyer et al., 2010 |
| Various sources | Bacteriohopanetetrol (BHT) (**If**) | 655 | Cyanobacteria + PNSB + $N_2$ fixing + other sources | Bisseret et al., 1985; Neunlist and Rohmer, 1985b; Neunlist et al., 1988; Cvejic et al., 2000; Blumenberg et al., 2006; Talbot et al., 2008 |
| | Amino triol (**Ih**) | 714 | Cyanobacteria + PNSB + $N_2$ fixing + methanotrophs + other sources | Neunlist and Rohmer, 1985b; Flesch and Rohmer, 1988; Neunlist et al., 1988; Seemann et al., 1999; Bravo et al., 2001; Blumenberg et al., 2006; Talbot et al., 2008 |
| | BHT cyclitol ether (BHT-CE) (**Ig**) | 1002 | Cyanobacteria + PNSB + $N_2$ fixing + other sources | Renoux and Rohmer, 1985; Neunlist et al., 1988; Talbot et al., 2003; Joyeux et al., 2004; Talbot et al., 2007b; Talbot et al., 2008 |
| | BHT glucosamine (**Ij**) | 1002 | Cyanobacteria + PNSB + $N_2$ fixing + other sources | Renoux and Rohmer, 1985; Talbot et al., 2007b |
| | BHpentol-CE (**Ik**) | 1060 | Cyanobacteria + $N_2$ fixing + other sources | Talbot et al., 2003; Joyeux et al., 2004; Talbot et al., 2007a |
| Unknown sources | BHhexol-CE (**Im**) | 1118 | Unknown | Talbot and Farrimond, 2007 |
| | Bhhexol-Comp (**In**) | 1132 | Unknown | Cooke, 2011 |

[a] PNSB – purple non-sulfur bacteria

## 4. Results

### 4.1 Bulk soil characteristics

TOC contents range from 2% to 28% between the different sites and soil horizons, generally decreasing with depth at all sites (Table 2). Soils on KU have higher TOC contents (from 4% to 28%) than soils on SA (2% to 23%). Between sites, TOC contents

differ most significantly in the O horizons consisting of mainly non-degraded plant litter, which is reflected by high C/N ratios of up to 69. The KUB polygon has the highest TOC contents (28%) in the uppermost organic soil horizons (Oi) of all sites compared to significantly lower TOC contents in KUU (19-23%) and SA (ca. 10%). These differences may be due to the differences of the vegetation between sites, particularly between polygon rims (dominated by moss, grasses, and shrubs) and polygon centres (dominated by moss and sedges). TOC contents are lower in the Oe horizons characterized by more strongly decomposed plant litter at all three sites with very similar values ranging from 7% to 11% (except in KUB-C with 23%) and C/N ratios of 19 to 51. At all sites the A and B horizons have lower TOC contents (2% to 16%) particularly at site SA-R (2% to 3%) and lower C/N ratios (16 to 35).

Soil pH values vary from pH 4.5 to 6.7 (Table 2). Except for the KUB polygon (KUB-R and KUB-C) where pH values are similar in all horizons. At all other locations pH values increase about 1 to 1.5 pH units with depth. Between sites, it is evident that pH values are slightly lower in the A and B horizons on KU (pH 4.5 to pH 6.3) than on SA (pH 4.8 to pH 6.7), which may be due to the different parent material at both sites.

### 4.2 Distribution of BHPs

Total BHP concentrations range from 84 to 1111 μg $g^{-1}$ TOC showing different trends with increasing soil depth at the three sites (Fig. 2, Table 4). On SA BHP concentrations in the polygon rim and centre decrease with depth paralleling decreasing TOC values (from 523 to 286 μg $g^{-1}$ TOC in the rim, and from 1111 to 84 μg $g^{-1}$ TOC in the centre). On KU a moderate increase of BHP concentrations with soil depth is observed at KUB-C (from 107 to 244 μg $g^{-1}$ TOC). In the other three soil profiles on KU a bimodal pattern of increasing and decreasing BHP concentrations is seen (KUB-R between 129 and 262 μg $g^{-1}$ TOC; KUU-R between 105 and 333 μg $g^{-1}$ TOC; KUU-C between 187 and 439 μg $g^{-1}$ TOC). Differences of BHP concentrations are not associated with specific soil horizons. Only on SA the Oi horizons are characterised by the highest BHP concentrations (rim: 523 μg $g^{-1}$ TOC and centre: 1111 μg $g^{-1}$ TOC) while the Oi horizons on KU have the lowest BHP concentrations in the respective profiles (KUB-R: 129 μg $g^{-1}$ TOC; KUB-C: 107 μg $g^{-1}$ TOC; KUU-R; 105 μg $g^{-1}$ TOC; KUU-C: 187 μg $g^{-1}$ TOC).

In total, 17 different BHPs were identified (Table 4) in agreement with previously published results from the Arctic (Rethemeyer et al., 2010; Cooke et al., 2009). At all three sites the organic horizons (Oi and Oe) have higher structural diversity (10 to 15 BHPs) than the deeper A and B horizons, which consist of humified organic matter (4 to 10 BHPs; Fig. 3). Furthermore, the A and B horizons on KU have a higher structural diversity (4-10 BHPs) than on SA (6-8 BHPs). The most abundant BHPs in all samples are bacteriohopanetetrol (BHT; **If**), adenosylhopane (**Ic**), adenosylhopane-type-2 (**Id**), and BHT cyclitol ether (BHT-CE; **Ig**) accounting for 56-100% of the total BHP abundance similar to previous soil studies from various environmental locations (e.g., Cooke et al., 2008; Rethemeyer et al., 2010; Kim et al., 2011; Zhu et al., 2011). Aminobacteriohopane-32,33,34-triol (aminotriol;

**Ih**) and 2-Me BHT (**IIf**) were also present at lower concentrations at all sites and depths except sample KUU-$R_{Bg}$. At all sites, the less abundant BHPs BHT pentose (**Ii**) and 2β-Me-bacteriohopane-32,33,34,35-tetrol pentose (2-Me BHT pentose; **IIi**), BHT glucosamine (**Ij**), bacteriohopane-31,32,33,34,35-pentol cyclitol ether (BHpentol-CE; **Ik**), bacteriohopane-30,31,32,33,34,35-hexol cyclitol ether (BHhexol-CE; **Im**), and a novel composite hexafunctionalised BHP (BHhexol-Comp; **In**) are almost exclusively found in the O horizons except for BHT glucosamine in samples KUB-$R_{Bjjg}$ and SA-$C_B$ as well as BHpentol-CE and BHhexol-CE in samples KUB-$C_A$ and KUU-$R_{Bjj}$ (Table 4, Fig. 3). Furthermore, aminotetrol (**Ia**) and aminopentol (**Ib**) are only present in the polygon centres, except aminopentol in sample KUU-$R_{Bjj}$, and occur there almost only in the Oe and A horizons (except SA-$C_B$; Table 4, Fig. 3). Besides the frequently occurring adenosylhopane (**Ic**) and adenosylhopane-type-2 (**Id**) two more soil-marker BHPs are observed. The methylated structure 2-Me adenosylhopane-type-2 (**IId**) is only found in the KU samples and at low concentrations. In contrast, adenosylhopane-type-3 (**Ie**), which was first identified in active layer soils on Svalbard (Rethemeyer et al., 2010), occurs more often on SA than on KU, where it is present only in the Oe horizons (and one A horizon; KUU-$R_A$).

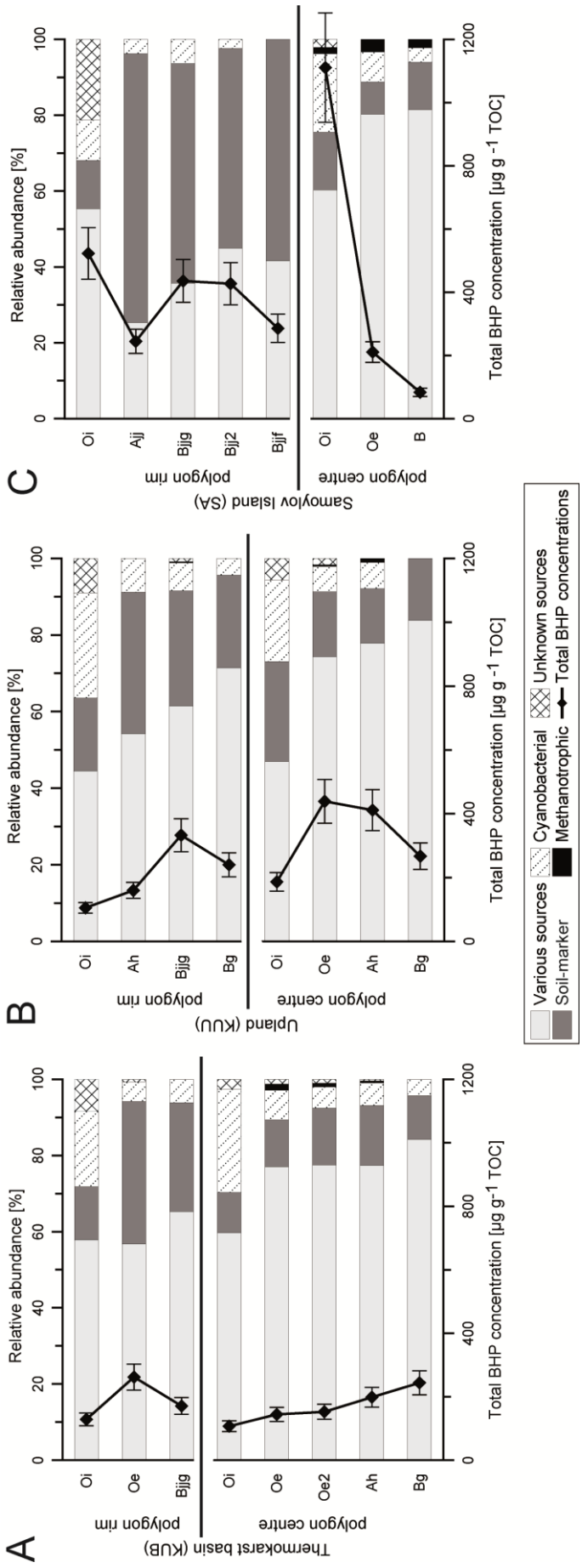


Fig 2: Relative abundance of BHPs [%] grouped according to source organisms and total BHP concentrations [µg $g^{-1}$ TOC]. A) Thermokarst basin (KUB), B) Upland (KUU), C) Samoylov Island (SA). Error bars are the mean error of all BHPs based on the mean SD (15.6%) calculated using relative SD of triplicate injections (5.1% - 42.3%).

Table 4: BHP concentrations [µg $g^{-1}$ TOC] of Kurungnakh Island (KU) and Samoylov Island (SA) soils. The compound structure number is given followed by base peak m/z.

| Site location | Depth [cm] | Horizon | Number of BHPs | Cyanobacteria | | | | Methanotrophs | | Soil markers | | | | Various sources | | | | | Unknown | | Total BHPs |
|---|---|---|---|---|---|---|---|---|---|---|---|---|---|---|---|---|---|---|---|---|---|
| | | | | IIf - 669 | IIIi or IVi - 941 | Ii - 943 | IIi - 957 | Ia - 772 | Ib - 830 | Ic - 746 | Id - 761 | IId - 775 | Ie - 802 | If - 655 | Ih - 714 | Ig - 1002 | Ij - 1002 | Ik - 1060 | Im - 1118 | In - 1132 | |
| ***Kurungnakh Island*** | | | | | | | | | | | | | | | | | | | | | |
| Thermokarst basin- | 0-12 | Oi | 12 | 6 | | 20 | | | | 7 | 9 | 2 | | 41 | 5 | 24 | 2 | 2 | 7 | 4 | 129 |
| polygon rim | 12-18 | Oe | 10 | 13 | | | | | | 43 | 38 | 7 | 11 | 65 | 5 | 74 | | 4 | 2 | | 262 |
| (KUB-R) | 18-30 | Bjjg | 8 | 10 | | | | | | 14 | 29 | 7 | | 56 | 5 | 49 | 2 | | | | 171 |
| Thermokarst basin- | 0-5 | Oi | 11 | 8 | | 12 | 9 | | | 3 | 8 | | | 37 | 1 | 26 | | 1 | 2 | 1 | 107 |
| polygon centre | 5-12 | Oe | 13 | 11 | | | | 1 | 1 | 6 | 11 | 1 | | 42 | 3 | 64 | 1 | 1 | 1 | 1 | 144 |
| (KUB-C) | 12-20 | Oe2 | 12 | 8 | | | | 1 | 1 | 8 | 10 | 2 | 3 | 49 | 6 | 62 | | 1 | 1 | | 152 |
| | 20-28 | A | 10 | 12 | | | | 1 | | 10 | 17 | 4 | | 56 | 4 | 92 | | 1 | 1 | | 198 |
| | 28-45 | Bg | 6 | 10 | | | | | | 11 | 17 | | | 127 | 9 | 69 | | | | | 244 |
| Upland - | 0-10 | Oi | 13 | 6 | 13 | 10 | | | | 8 | 10 | 2 | | 25 | 3 | 16 | 1 | 2 | 2 | 7 | 105 |
| polygon rim | 10-14 | A | 8 | 14 | | | | | | 14 | 36 | 4 | 5 | 60 | 3 | 24 | | | | | 160 |
| (KUU-R) | 14-16 | Bjj | 10 | 24 | | | | | 1 | 28 | 59 | 13 | | 74 | 10 | 117 | | 3 | 3 | | 333 |
| | 16-29 | Bg | 6 | 10 | | | | | | 23 | 35 | | | 108 | 8 | 55 | | | | | 240 |
| Upland - | 0-6 | Oi | 13 | 10 | | 19 | 10 | | | 20 | 27 | 1 | | 46 | 1 | 32 | 1 | 7 | 5 | 5 | 187 |
| polygon centre | 6-22 | Oe | 12 | 29 | | | | | 2 | 22 | 47 | 4 | 2 | 110 | 12 | 201 | | 3 | 4 | 3 | 439 |
| (KUU-C) | 22-33 | A | 9 | 28 | | | | 3 | 2 | 16 | 36 | 6 | | 149 | 16 | 155 | | | | | 411 |
| | 33-48 | Bg | 4 | | | | | | | 17 | 26 | | | 157 | | 67 | | | | | 267 |
| ***Samoylov Island*** | | | | | | | | | | | | | | | | | | | | | |
| Samoylov - | 0-7 | Oi | 10 | 30 | | 26 | | | | 47 | 20 | | | 114 | 20 | 135 | | 20 | 44 | 67 | 523 |
| polygon rim | 7-13 | Ajj | 7 | 9 | | | | | | 52 | 112 | | 9 | 45 | 5 | 12 | | | | | 245 |
| (SA-R) | 13-18 | Bjjg | 7 | 28 | | | | | | 28 | 212 | | 12 | 127 | 8 | 21 | | | | | 436 |
| | 18-32 | Bjjg2 | 7 | 10 | | | | | | 81 | 126 | | 18 | 108 | 19 | 65 | | | | | 427 |
| | 32-37 | Bjjf | 6 | | | | | | | 68 | 83 | | 16 | 81 | 16 | 23 | | | | | 286 |
| Samoylov - | 0-14 | Oi | 15 | 34 | | 108 | 88 | 11 | 8 | 59 | 106 | | 4 | 201 | 45 | 383 | 16 | 25 | 14 | 10 | 1111 |
| polygon centre | 14-40 | Oe | 12 | 3 | | 7 | 7 | 5 | 2 | 11 | 7 | | | 51 | 37 | 76 | 3 | 1 | | | 211 |
| (SA-C) | 40-43 | B | 8 | 3 | | | | 2 | | 4 | 6 | | | 32 | 14 | 20 | 2 | | | | 84 |

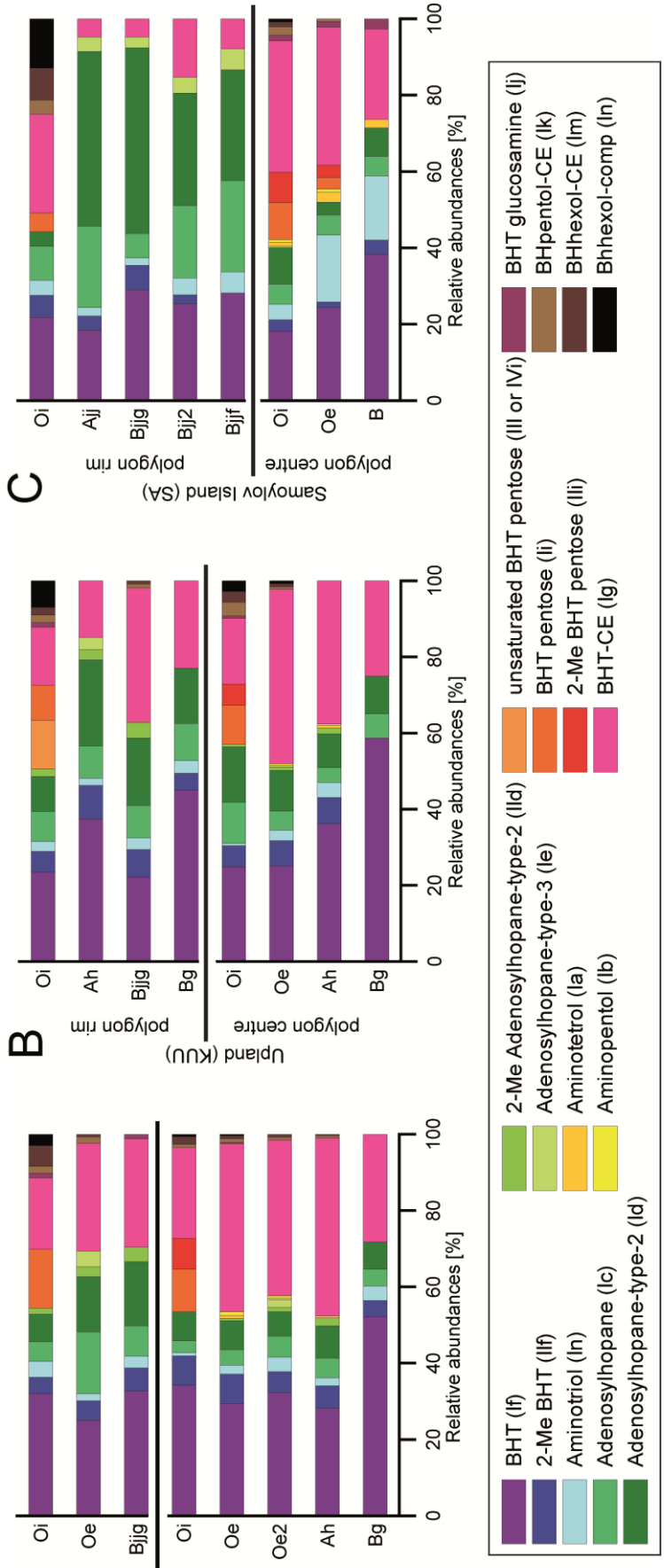


Fig. 3: Relative abundances of BHPs [%] on Kurungnagkh Island in (A) the Thermokarst basin (KUB) and (B) the upland site (KUU), and (C) on Samoylov Island (SA)

## 5. Discussion

### 5.1 Spatial distribution of BHPs

Permafrost soils are often influenced by cryoturbation (Jones et al., 2010), which may result in an up- or downward transport of organic matter within the soil profile. However, at all sites distortion of soil horizons in the active layer was not obvious and from pre-tests we know that $^{14}C$ results of bulk organic matter show a nearly linear increase in age with soil depth (Höfle et al., 2013). We therefore assume that the spatial distribution of BHPs is not altered by cryoturbation but mirrors the in situ signal of the microbial community.
In general, the observed total BHP concentrations in the active layer on KU and SA (84-523 µg $g^{-1}$ TOC; excluding sample SA-$C_{Oi}$, which has the extraordinarily high total BHP concentration of 1111 µg $g^{-1}$ TOC) are in the range of previously reported results for the active layer near Ny-Ålesund, Svalbard (Rethemeyer et al., 2010: 18-661 µg $g^{-1}$ TOC in 0-90 cm depth), but are higher than results for two Alaskan peat samples (40-85 µg $g^{-1}$ TOC; Taylor and Harvey, 2011). Similar to our permafrost soils, Cooke et al. (2009) found BHP concentrations of 236-613 µg $g^{-1}$ TOC in East Siberian shelf sediments including one sample off the Lena River, which had BHP concentrations of 289 µg $g^{-1}$ TOC. The surface sediment collected off the Lena Delta also had a similar structural diversity (12 BHPs; Cooke et al., 2009) to our samples (4 to 15 BHPs).

The observed relative BHP distribution varies spatially between sampling locations, i.e., the fluvial deposits on SA and aeolian deposits on KU, and with depth, i.e., in the different horizons of the active layer. These differences are likely due to a range of physical and chemical soil properties such as soil texture, moisture, temperature, pH, and redox conditions as well as sources and content of organic carbon, which all influence bacterial diversity and activity (Jansson and Tas, 2014; Landesman et al., 2014). The most obvious difference between the BHP distribution on SA and KU is the relative abundance of soil-marker BHPs. Overall, soil-marker BHP concentrations are significantly higher in the A and B horizons of the polygon rim on SA (53-71% of total BHPs) than in the same horizons on KU (11-37% of total BHPs; Fig. 2). Specifically, adenosylhopane-type-2 (**Id**) can be detected in much higher (relative) abundance in the mineral horizons of the polygon rim on SA (SA-R: Ajj, Bjjg, Bjjg2, Bjjf; 29-49% of total BHPs) compared to KU (KUB-R: Bjjg; KUU-R: A, Bjj, Bg; 15-23%). Simultaneously, 2-Me adenosylhopane-type-2 (**IId**) is absent on SA (SA-R, SA-C), while it could be detected in all organic and mineral horizons on KU except KUB-$C_{Oi}$, KUB-$C_{Bg}$, KUU-$R_{Bg}$, and KUU-$C_{Bg}$. Furthermore, in the polygon centres aminotriol is much more abundant on SA (4-18% of total BHPs) than in both KU polygon centres (1-4%). The different soil-marker BHP assemblages coincide with different abundances of non- source specific BHPs, i.e., BHT (**If**), aminotriol (**Ih**), and BHT-CE (**Ig**). BHT and BHT-CE are less abundant in those samples on SA, which are characterized by high adenosylhopane-type-2 (**Id**) concentrations (polygon rim, A and B horizons) than in the mineral A and B horizons on KU. Whilst adenosylhopane (**Ic**) is reported to be the precursor to all other side chain extended BHPs, the function of the other side chain cyclised BHPs (e.g. **Id, Ie**) is currently unknown. Potentially, in this location and in other (cold) environments where accumulation of soil-marker BHPs is

particularly high (e.g. Canada and Svalbard; Xu et al., 2009; Rethemeyer et al., 2010), modification of the C-35 terminal group is favoured over opening of the pentacyclic ring. This may be controlled by a number of factors such as pH and temperature, in turn controlling the indigenous hopanoid-producing population.

We do not observe a clear trend of soil-marker BHPs over depth analogous to Rethemeyer et al. (2010) who found increasing concentrations with soil depth in an active layer on Svalbard, which the authors suggest to result from either better preservation or downward transport by leaching of these BHPs.

### 5.1.1 Influence of soil properties

On SA, total BHP concentrations decrease with depth while they show a small depth-related increase at both sites on KU (Fig. 2). The lower BHP concentrations on SA are concurrent with slightly higher pH values. Similarly, Kim et al. (2011) found higher total BHP concentrations in soils with lower pH values in the Têt watershed, Southern France. However, when the peat samples from this study were excluded (4 out of 29 samples) this relationship was no longer evident. For our data, we observe no linear correlation of total BHP concentrations with pH (Fig. 4A).

However, the soil pH seems to have an influence on the structural diversity, which is higher at lower soil pH (Fig. 4B), a relationship also observed by Kim et al. (2011). The correlation is strongest for the SA soils ($r^2$ = 0.94), where the polygon rim and centre structural diversity differs much more (rim: 6-10 BHP structures, centre: 8-15 BHP structures) than on KU (4-13 BHP structures). This could indicate that organisms capable of BHP production can better adapt to lower soil pH as demonstrated in recent studies of *Rhodopseudomonas palustris* (Welander et al., 2009), an organism which produces a range of BHPs including adenosylhopane. Reduction in pH has also been shown to increase the total hopanoid content of *Alicyclobacillus acidocaldarius* (Poralla et al., 1984). Alternatively, a lower pH could also increase BHP preservation since previous soil studies suggest decreasing microbial activities at lower pH (van Bergen et al., 1998; Nierop et al., 2005).

However, soil temperature is another important parameter affecting the organic and the mineral horizons differently. The mean soil temperatures in the upper 20 cm of the polygon rims can increase to up to 4°C during the summer months (max. in August) while they can be as low as -24°C during winter (min. in February; Boike et al., 2013). This yearly temperature amplitude decreases with depth (Boike et al., 2013). Gibson et al. (2014) observed a higher level of BHP complexity and functionality in silicate sinter samples deposited at higher temperatures in a New Zealand geothermal vent system. Likewise, Rethemeyer et al. (2010) interpreted the absence of two highly functionalised BHPs (BHpentol-CE and BHhexol-CE) in the deeper mineral soil horizons on Svalbard (while abundant in the organic horizons) as the result of inhibited production of more functionalised BHPs at lower temperatures consistent with previous observations from culture studies (e.g. Joyeux et al., 2004). Both parameters, TOC content and soil

temperature, may be prerequisites for yet unknown specialised bacterial species producing the observed highly functionalised BHPs.

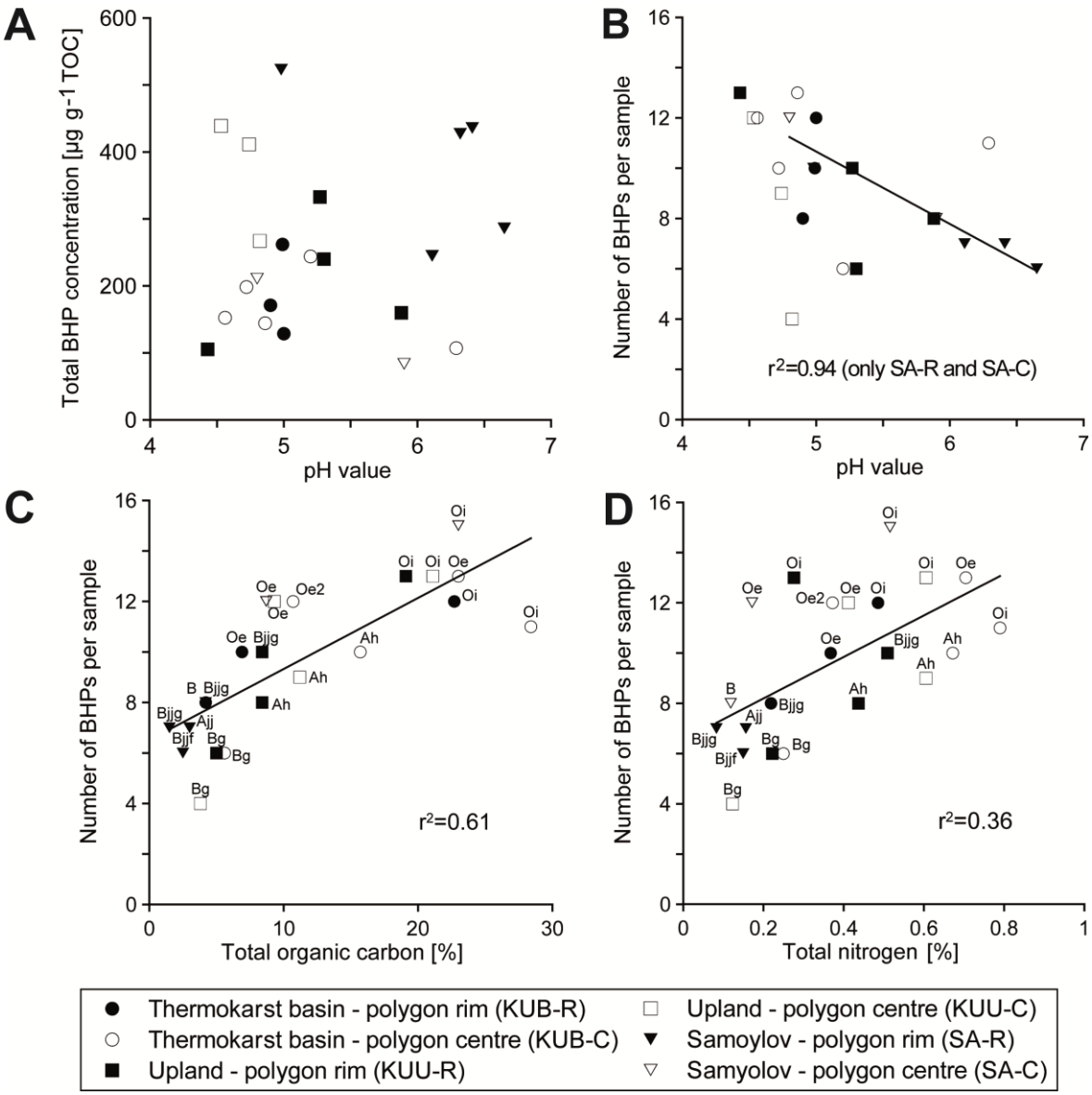


Fig. 4: Correlation of soil pH with (A) total BHP concentrations [µg $g^{-1}$ TOC], (B) structural diversity (as number of BHPs per sample), and correlation of structural diversity with (C) total organic carbon content [%], and with (D) total nitrogen content [%].

Among the less abundant BHPs, the highly functionalised composite BHPs BHT pentose (**Ii**), 2-Me BHT pentose (**IIi**), unsaturated BHT pentose (**IIIi** or **IVi**), BHT-glucosamine (**Ij**), BHpentol-CE (**Ik**), BHhexol-CE (**Im**), and BHhexol-Comp (**In**) are present almost exclusively in the organic horizons (Oi and Oe; Table 4, Fig. 3) and are virtually absent in the A and B horizons. Minor concentrations of BHpentol-CE (**Ik**) and BHhexol-CE (**Im**) were each only detected in some mineral horizons on KU (KUB-$C_A$ and KUU-$R_{Bjj}$) and BHT-glucosamine (**Ij**) was present in the deepest horizon of the polygon centre on SA (SA-$C_B$). This is in line with the study on Svalbard where BHPs were more diverse in the organic horizons compared to the mineral soils (Rethemeyer et al., 2010). The greater

BHP structural diversity in the organic horizons may reflect greater bacterial diversity, which is in agreement with the spatial pattern observed in a 16S rRNA gene sequencing study on SA (Liebner et al., 2008). In this study the authors attributed the higher diversity to the higher availability of oxygen, nutrients, and dissolved organic matter in the near surface soil. Additionally, the supply of bacterial species via aeolian input was considered as a factor contributing to higher diversity, while at greater depth, selection may have favoured certain species over time (Liebner et al., 2008). Since the O horizons are characterized by significantly higher TOC contents and C/N ratios than the corresponding deeper A and B horizons (Table 2), the quantity and quality of organic substrate and nutrients might control the distribution of BHP producing bacteria. BHT pentose (**Ii**), 2-Me BHT pentose (**IIi**), unsaturated BHT pentose (**IIIi** or **IVi**), BHT-glucosamine (**Ij**), BHpentol-CE (**Ik**), BHhexol-CE (**Im**), and BHhexol-Comp (**In**) could therefore potentially represent BHPs produced by bacteria specialised in organic matter degradation since heterotrophic bacteria should thrive under the observed carbon-rich conditions (Fig. 4C). Alternatively, the higher structural diversity in the O horizons could result from N-limitation since many BHP-producing bacteria can fix $N_2$ and could, thus, outcompete other bacteria in low N environments (e.g., Bravo et al., 2001; Rosa-Putra et al., 2001; Ricci et al., 2014). However, there is only a weak correlation between the structural diversity and N content (Fig. 4D).

The depth-related BHP distribution pattern could also simply be a function of BHP preservation. If more highly functionalised BHPs were more readily prone to degradation, this could be indicated by the concurrent decrease of structurally more complex BHPs such as BHT pentose, BHpentol-CE, BHhexol-CE, and BHhexol-Comp and increase in low complexity BHPs such as BHT (**If**) or 2-Me BHT (**IIf**) from O horizons towards the deeper A and B horizons. In such a scenario, low complexity-BHPs (i.e. non-composite structures) could represent degradation products of more complex BHPs. Indeed, BHT has been shown to be a degradation product of BHT glucosamine (**Ij**) during simulated diagenetic conditions (Schaeffer et al., 2010). However, several other BHPs including all observed soil-marker BHPs and BHT glucosamine show increasing absolute concentrations with depth at all sites, thus, the observed pattern may in fact rather reflect different bacterial communities in the different soil horizons. Nonetheless, it should also be considered that as the first intermediate in BHP production via side chain elongation (Bradley et al., 2010), adenosylhopane (and related structures), may accumulate if BHP-producers are essentially dormant at greater depths.

### 5.2 Effect of permafrost structures (Polygon rim vs. polygon centre)

The major physical differences between the Ruptic and Typic Historthels of the water saturated polygon centres and the Glacic Aquiturbels of the relatively dry polygon rims (Table 2) include water content and associated redox conditions as well as vegetation cover. Considering the large difference in redox conditions, C/N ratios and pH values are quite similar between rims and centres at each location (Table 2). The oxygen-depleted centres are characterized by slightly elevated TOC contents (on average 5% higher)

compared to the rims in the thicker O and A horizons, which consist of relatively fresh plant material. Earlier studies on SA observed TOC differences of more than 10% between centres and rims in several neighbouring polygons concurrent with higher methane production in the polygon centres (Wagner et al., 2005; Liebner and Wagner, 2007).

BHP concentrations and assemblages differ between polygon rims and centres at each of our three locations (Table 4). Most obviously, aminotetrol and aminopentol are only present in the polygon centres except for one rim sample (KUU-$R_{Bjj}$), which contains low concentrations of aminopentol (Table 4). Within the polygon centres, aminotetrol and aminopentol occur almost exclusively in the Oe and A horizons (except SA-$C_B$) consistent with high methane oxidation rates in these horizons as observed by Wagner et al. (2005). Both BHPs have so far only been identified in methanotrophic bacteria (Neunlist and Rohmer, 1985a; Neunlist and Rohmer, 1985b; Cvejic et al., 2000; Coolen et al., 2008; Talbot et al., 2008; van Winden et al., 2012) and a few species of the strictly anoxygenic sulphate-reducing genus *Desulfovibrio* (Blumenberg et al., 2006; Blumenberg et al., 2012). Accordingly, we consider the almost exclusive occurrence of aminotetrol and aminopentol in the polygon centres indicative for bacteria adapted to the oxygen-depleted conditions. This differentiation between rims and polygon centres is consistent with 16S rRNA gene sequencing results of Liebner et al. (2008) who found polygon centres on SA were dominated by Thermomicrobia and rims by Bacteriodetes and Actinobacteria. The 16S rRNA data of Wagner et al. (2009) indicate both different bacterial communities and activities between the anaerobic and aerobic parts of a polygon centre on SA. In both studies, the redox conditions were considered the most important factor controlling the bacterial community structure.

### 5.3 Assessment of BHP-producing bacterial communities

In the following section, we provide an assessment of the BHP-producing bacterial community structure found in the active layer of the polygonal tundra aiming to extend the limited taxonomic information carried by BHPs through comparison with published gene sequencing as well as other lipid data from the study area.

#### 5.3.1 Methanotrophic bacteria

As discussed above (section 5.2), the polygon centres and rims are defined by different redox conditions, which is reflected also in higher methane production and oxidation in the centres (Wagner et al., 2005). Given the high methane concentrations and the fact that the polygon centres are not fully anoxic (Zubrzycki, 2013), we exclude *Desulfovibrio sp*. as a source of aminotetrol and aminopentol and consider methanotrophic bacteria the most likely source organisms (Talbot et al., 2014).

Methanotrophs use two different ways to assimilate carbon; type I methanotrophs use the ribulose monophosphate (RuMP) pathway, while type II methanotrophs use the serine

pathway (Hanson and Hanson, 1996). While aminotetrol is produced by both type I and type II methanotrophs, am1inopentol seems to be a marker for most type I methanotrophs (Neunlist and Rohmer, 1985a; Talbot et al., 2001; van Winden et al., 2012). In our samples, aminotetrol and aminopentol were detected in similar quantities (aminotetrol being slightly more abundant; Table 4), therefore, type I methanotrophs must be the dominant source of both amino-BHPs. This is in agreement with previous studies in the Lena Delta. Here, Wagner et al. (2005) used a PLFA-based approach to characterize the microbial community in a similar polygon on SA and only found the type I methanotroph-specific PLFA *cis*-8-hexadecenoic acid (*Methylococcaceae*) in the polygon centre, while a PLFA indicative for type II methanotrophs (*cis*-10-octadecenoic acid; *Methylocystaceae*) was detected in both the polygon centre and rim. Similarly, Knoblauch et al. (2008) found the *cis*-8-hexadecenoic acid to represent the vast majority of biomarkers in yet another polygon centre on SA.

Wagner et al. (2005) and Liebner et al. (2009) also determined higher cell counts of methanotrophic bacteria in the polygon rims on SA than in the corresponding centres. We only detected aminopentol in one polygon rim sample (KUU-$R_{Bjj}$) and no aminotetrol in any rim suggesting that the concentration might be too low to be detected or both BHPs are readily oxidised under the more oxygenic conditions in the rims.

Among the type I methanotrophs Liebner (2007) only identified *Methylobacter psychrophilus* (family Methylococcaceae) in a polygon rim on SA, which has not yet been identified as BHP-producer. However, several genera of the Methylococcaceae (type I methanotrophs) including *Methylococcus, Methylomonas*, and *Methylocaldum*, as well as the *Methylovulum*-like strain M200 produce aminotetrol and/or aminopentol (Neunlist and Rohmer, 1985a; Neunlist and Rohmer, 1985b; Cvejic et al., 2000; van Winden et al., 2012) or possess the squalene-hopene cyclase gene (*sqhC*) required for BHP production (Fischer and Pearson, 2007; Pearson and Rusch, 2009). Accordingly, aminotetrol and aminopentol in the active layers on SA and KU either indicate the presence of any of these type I methanotrophic genera not resolved by 16S rRNA (Liebner, 2007) or *Methylobacter psychrophilus* could be a yet unknown producer of these amino-BHPs. However, the absence of C-3 methylated aminopentol, abundant in various methanotrophic genera like *Methylococcus* and *Methylocaldum* (Cvejic et al., 2000), makes it unlikely that species of these two genera are present in the studied active layers.

### 5.3.2 Soil-marker BHP-producing bacteria

Amongst those four BHPs regarded the most specific soil-markers adenosylhopane (**Ic**) and adenosylhopane-type-2 (**Id**) have previously been identified in the $N_2$-fixing Alphaproteobacteria *Rhodopseudomonas palustris* and *Bradyrhizobium japonicum* (e.g. Bravo et al., 2001; Talbot et al., 2007b) as well as in the $N_2$-fixing purple non-sulphur bacteria (PNSB) *Rhodoblastus acidophilus* and *Rhodomicrobium vannielii* (all Alphaproteobacteria; Neunlist and Rohmer, 1985c; Flesch and Rohmer, 1988; Neunlist et al., 1988; Talbot et al., 2007b). Furthermore, adenosylhopane was found in the

ammonium oxidizing bacterium *Nitrosomonas europaea* (Betaproteobacteria; Seemann et al., 1999) and most recently in very low levels in the type II methanotrophic bacterium *Methylocella palustris* (Alphaproteobacteria; van Winden et al., 2012). In contrast, 2-Me adenosylhopane-type-2 (**IId**) and adenosylhopane-type-3 (**Ie**) have not yet been identified in any cultured organism.

Using 16S rRNA sequencing, Liebner et al. (2008) found that Bacteriodetes, Actinobacteria, and Thermomicrobia dominate the soil bacterial communities in similar polygon soils on SA, none of which have been shown to produce BHPs albeit one Actinobacterial species (the thermophile *Rubrobacter xylanophilus*; Pearson and Rusch, 2009) possesses the *sqhC* gene. Liebner et al. (2008) and Liebner (2007) also identified Alpha- and Betaproteobacteria including the family Bradyrhizobiaceae and the order Nitrosomonadales, respectively, in 6-10 cm soil depth of the investigated polygon. These authors could not identify Bradyrhizobiaceae beyond the family level or Nitrosomonadales beyond the order level, but adenosylhopane (**Ic**) and adenosylhopane-type-2 (**Id**) in our active layer profiles may indicate the presence of *Bradyrhizobium japonicum* and/or *Rhodopseudomonas palustris* (both Bradyrhizobiaceae) and/or *Nitrosomonas europaea* (order Nitrosomonadales). Additionally, adenosylhopane and related compounds could be produced by related species of the Bradyrhizobiaceae and/or Nitrosomonadaceae from which several species of the genera *Bradyrhizobium* and *Nitrobacter* (Bradyrhizobiaceae) as well as *Nitrosospira* and *Nitrosomonas* (Nitrosomonadaceae) have so far been identified to carry the *sqhC* gene (Fischer and Pearson, 2007; Pearson and Rusch, 2009) and are, thus, putative BHP-producers also for the yet unassigned 2-Me adenosylhopane-type 2 (**IId**) adenosylhopane-type-3 (**Ie**).

### 5.3.3 Cyanobacteria

High abundances of C-2 methylated BHPs have been observed in many cyanobacterial cultures, although other cyanobacterial species only produce non-methylated compounds or do not produce BHPs at all (Talbot et al., 2008 and references therein). Cyanobacterial mats from geothermal systems are also frequently found to contain C-2 methylated BHPs (e.g., Jahnke et al., 2004; Zhang et al., 2007). Often, therefore, these compounds have been regarded as indicative for cyanobacteria (Summons et al., 1999). Indeed, various cyanobacterial genera like *Nostoc*, *Phormidium*, *Cyanothece*, *Calothrix*, *Chlorogloeopsis*, *Gloeocapsa*, and *Chroococcidiopsis* have actually been demonstrated to produce 2-Me BHPs (Talbot et al., 2008). A range of other genera including for example *Gloebacter*, *Thermosynechococcus*, and *Acaryochloris* have not been tested yet for BHPs but possess the *sqhC* gene (Fischer and Pearson, 2007; Pearson and Rusch, 2009). However, 2-Me BHPs, or the gene required for methylation at C-2 have also been found in various species of the class Alphaproteobacteria, especially within the family Bradyrhizobiaceae (Vilcheze et al., 1994; Bravo et al., 2001; Rashby et al., 2007; Welander et al., 2009; Blumenberg et al., 2013).

In our samples 2-Me BHT (**IIg**), unsaturated BHT pentose (**IIIi or IVi**), BHT pentose (**Ii**), and 2-Me BHT pentose (**IIi**) are present, which have, except for 2-Me BHT, only been detected in cyanobacteria, specifically in an enrichment culture of *Gloeocapsa* sp. isolated from an Arctic hypolith (Talbot et al., 2008). 2-Me BHT was found in cyanobacteria but also in *Methylobacterium organophilum*, a bacterium producing large amounts of 2β-methyl diplopterol, and acetylated 2-Me BHT was subsequently recovered after recrystallisation of a large sample of acetylated BHT from the mother liquors after reversed-phase HPLC (Renoux and Rohmer, 1985). 2-Me BHT was also identified in a strain of PNSB and $N_2$-fixing species *Rhodopseudomonas palustris* (phylum Proteobacteria; Rashby et al., 2007) although analyses of other strains of this organism identified only non-methylated BHPs including BHT, aminotriol and adenosylhopane (Talbot et al., 2007 and references therein). 16S rRNA gene sequences from SA (Liebner et al. 2008; Liebner 2007) only assigned phototrophic cyanobacteria to the top soil (6-10 cm depth) of the polygon rims. We also found the greatest relative abundances of cyanobacterial BHPs in the uppermost Oi horizons, but also detected C2-methylated BHPs at greater depth. This is consistent with other reports of these composite compounds, particularly the unsaturated component, which were found to be most abundant in the uppermost layers of a *Sphagnum* peat core from Moorhouse (UK; van Winden et al., 2012). This could either indicate that the organic horizon and active layer soils contain larger amounts of cyanobacteria not identifiable with 16S rRNA data or preservation of these BHPs at greater soil depth. Any of the yet identified cyanobacterial BHP-producers (if occurring in soils) and *Rhodopseudomonas palustris* are putative sources on SA and KU, but further interpretations remain speculative.

### 5.3.4 Unknown BHP-producing bacteria

Most information about BHP production comes from culture studies (see Talbot et al., 2008 for review), however, >99% of all bacterial species are not cultivatable (Epstein, 2013). Metagenomics and bioinformatics studies indicate that sequences from BHP-producers in environmental samples agree less than 60% (at the amino acid level) with their relative BHP-producers in pure cultures (Pearson et al., 2007; Pearson and Rusch, 2009). Accordingly, the vast majority of BHP-producing bacterial species remain unidentified.

Unassigned BHPs in our samples include 2-Me adenosylhopane-type-2 (**Id**), adenosylhopane-type-3 (**Id**), BHhexol-CE (**Im**), and BHhexol-Comp (**In**) although a structurally similar BHhexol-manosamine has been reported from a species of *Alicyclobacillus* (Řezanka et al., 2011). As stated above, species of the families Bradyrhizobiaceae and Nitrosomonadaceae could be producers of the 2-Me adenosylhopane-type-2 and of the adenosylhopane-type-3.

Both unassigned composite BHhexols (**Im**, **In)** only occur in the O horizons on SA and KU and amongst these with higher abundance in the well-aerated rims. Liebner (2007) found several bacterial species (*Geobacter propionicus* and *Geobacter bremensis*) and

unaffiliated genera including *Syntrophus*, *Planctomyces*, and *Rubrobacter* in the active layers of a polygon on SA, which have so far not been investigated for BHP synthesis. Within the genus *Geobacter*, *Geobacter sulfurreducens* and *Geobacter metallireducens* are known to produce BHPs (Fischer et al., 2005; Eickhoff et al., 2013). However, Liebner (2007) only detected *Geobacter* in the deeper, more anaerobic soil horizons of the polygon rim and in the anaerobic centres. Furthermore, guanidine-substituted BHT cyclitol, a major BHP product of the two *Geobacter* species (Fischer et al., 2005; Eickhoff et al., 2013), is not detected in any of our samples. Therefore, it is most unlikely that species of the genera *Geobactera* are potential BHP-producers of the composite BHhexols in the active layer profiles investigated. Several species of the bacterial genera found on SA have been recognised to possess the *sqhC* gene including *Syntrophobacter fumaroxidans*, *Planctomyces maris*, and *Rubrobacter xylanophilus* (Fischer and Pearson, 2007; Pearson and Rusch, 2009). However, 16S rRNA data identified the genus *Rubrobacter* mainly in the deeper, less oxygenated soil horizons (Liebner, 2007). Like *Geobacter*, it is therefore unlikely that species of this genus produce the unassigned composite BHhexols exclusively found in the O horizons of this study. Accordingly, species of the genus *Syntrophus* and/or the phylum *Planctomyces*, which were also specifically identified in the uppermost soil horizons by Liebner (2007), may be potential producers of BHhexol-CE and BHhexol-Comp.

## 6. Conclusion

BHP distributions differ between soil horizons and between permafrost structures (polygon rim and centre) of the three investigated active layer profiles in the Siberian Lena Delta. The different soil properties of the permafrost structures investigated, most importantly redox conditions and pH, seem to influence the BHP-producing microbial community. Biomarkers for methanotrophic bacteria are almost exclusively present in polygon centres, which seems indicative of bacteria adapted to water-saturated and oxygen-depleted conditions. Furthermore, the BHP structural diversity shows a strong correlation with pH values on SA, which could indicate that a lower soil pH favours a more diverse BHP-producing bacterial population. The BHP structural diversity also differs in the different soil horizons of the active layer. The uppermost organic horizon (Oi) has the highest structural diversity compared to the deeper organic (Oe) and mineral horizons (A and B). Higher soil temperature, higher TOC contents, and less degraded plant material in the Oi horizons may be conditions for yet unknown specialised bacterial species producing highly functionalised BHPs.

The BHP distribution in the different soil horizons agrees well with previously published bacterial community assessments based on 16S rRNA and PLFA analyses. In some instances, the information obtained from BHPs seems to be even more taxonomically specific than 16S rRNA sequences. Overall, the good agreement of our BHP data with 16S rRNA and PLFA based analyses on SA suggests that BHPs are promising biomarkers to provide taxonomic and environmental information in recent Arctic

permafrost, thus, providing a tool to also study bacterial biomass and communities in ancient permafrost.

**Acknowledgements**

This study was funded by the German Ministry of Education and Research (BMBF) within the German-Russian project 'CarboPerm' (grant 03G0836 to JR). The authors acknowledge the Alfred Wegener Institute for Polar and Marine Research (Unit Potsdam) for the very good logistical support during the expeditions "Lena 2009" and "Lena 2010". We also thank the Natural Environment Research Council (NERC) grant NE/I027967/1 to HMT and Science Research Investment Fund (SRIF) from HEFCE for funding the purchase of the ThermoFinnigan LCQ ion trap mass spectrometer and Frances Sidgwick for technical assistance (Newcastle).

## Appendix

Ring system and side chains of BHPs observed in Lena Delta samples. Side chain structures **d**, **e**, **i**, **m** and **n** are based on LC-MS$^n$ analysis only. All other side chain structures shown have previously been unambiguously identified by NMR. When identified in this study using LC-MS$^n$ only where stereochemistry cannot be confirmed, we have assumed the structure to be the same as that previously characterised but the occurrence of additional/alternative isomers cannot be excluded. Structures **d** and **e** differ in the mass of the terminal group (R) and are distinguished by LC-MS$^n$ based on protonated molecular ions (see Table 3).

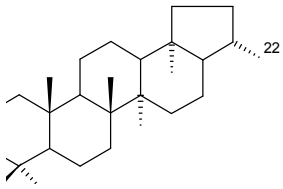


**I**

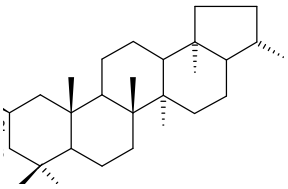

**II**

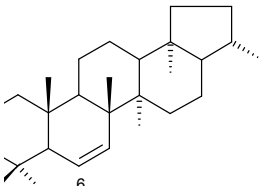

**III**

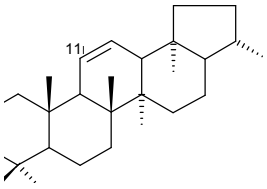


**IV**

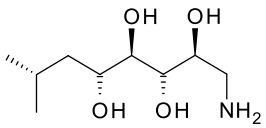


**a**

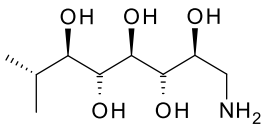


**b**

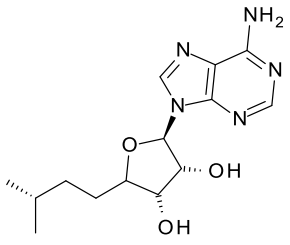


**c**

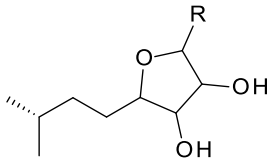

**d** or **e**

(R = unknown)

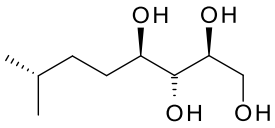

**f**

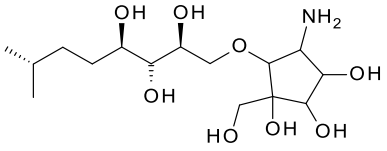

**g**

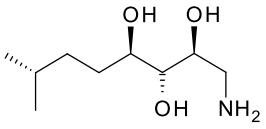

**h**

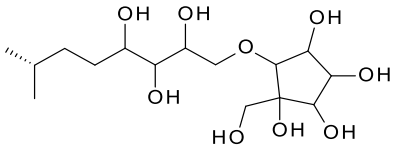

**i**

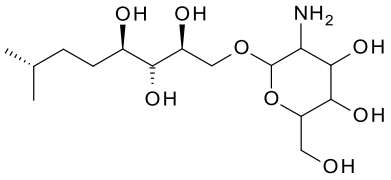

**j**

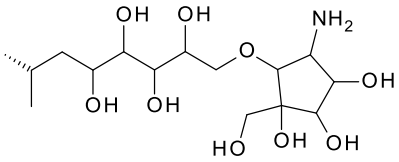

**k**

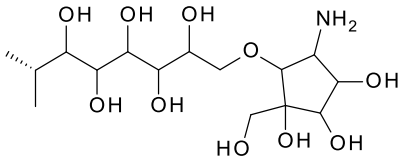

**m**

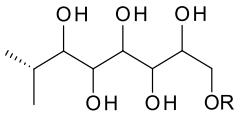

**n** (R= unknown)

**References**

Are F. and Reimnitz E. (2000) An overview of the Lena River Delta setting: Geology, tectonics, geomorphology, and hydrology. *J. of Coastal Research* **16**, 1083-1093.

Bisseret P., Zundel M. and Rohmer M. (1985) Prokaryotic triterpenoids: 2.2P-Methylhopanoids from *Methyfobacterium organophilum* and *Nostoc muscorum*, a new series of prokaryotic triterpenoids. *European J. Biochem.* **150**, 29-34.

Blumenberg M., Krüger M., Nauhaus K., Talbot H. M., Oppermann B. I., Seifert R., Pape T. and Michaelis W. (2006) Biosynthesis of hopanoids by sulfate-reducing bacteria (genus *Desulfovibrio*). *Environ. Microbiol.* **8**, 1220-1227.

Blumenberg M., Oppermann B. I., Guyoneaud R. and Michaelis W. (2009) Hopanoid production by *Desulfovibrio bastinii* isolated from oilfield formation water. *FEMS Microbiol. Letters* **293**, 73-78.

Blumenberg M., Mollenhauer G., Zabel M., Reimer A. and Thiel V. (2010) Decoupling of bio- and geohopanoids in sediments of the Benguela Upwelling System (BUS). *Org. Geochem.* **41**, 1119-1129.

Blumenberg M., Hoppert M., Krüger M., Dreier A. and Thiel V. (2012) Novel findings on hopanoid occurrences among sulfate reducing bacteria: Is there a direct link to nitrogen fixation? *Org. Geochem.* **49**, 1-5.

Blumenberg M., Arp G., Reitner J., Schneider D., Daniel R. and Thiel V. (2013) Bacteriohopanepolyols in a stratified cyanobacterial mat from Kiritimati (Christmas Island, Kiribati). *Org. Geochem.* **55**, 55-62.

Boike J., Kattenstroth B., Abramova K., Bornemann N., Chetverova A., Fedorova I., Fröb K., Grigoriev M., Grüber M., Kutzbach L., Langer M., Minke M., Muster S., Piel K., Pfeiffer E. M., Stoof G., Westermann S., Wischnewski K., Wille C. and Hubberten H. W. (2013) Baseline characteristics of climate, permafrost and land cover from a new permafrost observatory in the Lena River Delta, Siberia (1998-2011). *Biogeosciences* **10**, 2105-2128.

Bradley A. S., Pearson A., Sáenz J. P. and Marx C. J. (2010) Adenosylhopane: The first intermediate in hopanoid side chain biosynthesis. *Org. Geochem.* **41**, 1075-1081.

Bravo J.-M., Perzl M., Härtner T., Kannenberg E. L. and Rohmer M. (2001) Novel methylated triterpenoids of the gammacerane series from the nitrogen-fixing bacterium *Bradyrhizobium japonicum* USDA 110. *European J. Biochem.* **268**, 1323-1331.

Brocks J. J., Logan G. A., Buick R. and Summons R. E. (1999) Archean Molecular Fossils and the Early Rise of Eukaryotes. *Science* **285**, 1033-1036.

Cooke M. P., Talbot H. M. and Farrimond P. (2008) Bacterial populations recorded in bacteriohopanepolyol distributions in soils from Northern England. *Org. Geochem.* **39**, 1347-1358.

Cooke M. P., van Dongen B. E., Talbot H. M., Semiletov I., Shakhova N., Guo L. and Gustafsson Ö. (2009) Bacteriohopanepolyol biomarker composition of organic matter exported to the Arctic Ocean by seven of the major Arctic rivers. *Org. Geochem.* **40**, 1151-1159.

Cooke M. P. (2011) The role of bacteriohopanepolyols as biomarkers for soil bacterial communities and soil derived organic matter. PhD Thesis, Newcastle University, http://hdl.handle.net/10443/1139.

Coolen M. J. L., Talbot H. M., Abbas B. A., Ward C., Schouten S., Volkman J. K. and Damsté J. S. S. (2008) Sources for sedimentary bacteriohopanepolyols as revealed by 16S rDNA stratigraphy. *Environ. Microbiol.* **10**, 1783-1803.

Cvejic J. H., Bodrossy L., Kovács K. L. and Rohmer M. (2000) Bacterial triterpenoids of the hopane series from the methanotrophic bacteria *Methylocaldum spp*.: phylogenetic implications and first evidence for an unsaturated aminobacteriohopanepolyol. *FEMS Microbiol. Letters* **182**, 361-365.

Doğrul Selver A., Talbot H. M., Gustafsson Ö., Boult S. and van Dongen B. E. (2012) Soil organic matter transport along an sub-Arctic river–sea transect. *Org. Geochem.* **51**, 63-72.

Eickhoff M., Birgel D., Talbot H. M., Peckmann J. and Kappler A. (2013) Bacteriohopanoid inventory of *Geobacter sulfurreducens* and *Geobacter metallireducens*. *Org. Geochem.* **58**, 107-114.

Epstein S. S. (2013) The phenomenon of microbial uncultivability. *Current Opinion in Microbiol.* **16**, 636-642.

Fiedler S., Wagner D., Kutzbach L. and Pfeiffer E.-M. (2004) Element redistribution along hydraulic and redox gradients of low-centered polygons, Lena Delta, Northern Siberia. *Soil Sci. Soc. Am. J.* **68**, 1002-1011.

Fischer W. W., Summons R. E. and Pearson A. (2005) Targeted genomic detection of biosynthetic pathways: anaerobic production of hopanoid biomarkers by a common sedimentary microbe. *Geobiology* **3**, 33-40.

Fischer W. W. and Pearson A. (2007) Hypotheses for the origin and early evolution of triterpenoid cyclases. *Geobiology* **5**, 19-34.

Flesch G. and Rohmer M. (1988) Prokaryotic hopanoids: the biosynthesis of the bacteriohopane skeleton. *European J. Biochem.* **175**, 405-411.

Gibson R. A., Sherry A., Kaur G., Pancost R. D. and Talbot H. M. (2014) Bacteriohopanepolyols preserved in silica sinters from Champagne Pool (New Zealand) indicate a declining temperature gradient over the lifetime of the vent. *Org. Geochem.* **69**, 61-69.

Gilichinsky D. A., Wagener S. and Vishnevetskaya T. A. (1995) Permafrost microbiology. *Permafrost and periglacial processes* **6**, 281-291.

Hanson R. S. and Hanson T. E. (1996) Methanotrophic Bacteria. *Microbiol. reviews* **60**, 439-471.

Höfle S., Rethemeyer J., Mueller C. W. and John S. (2013) Organic matter composition and stabilization in a polygonal tundra soil of the Lena Delta. *Biogeosciences* **10**, 3145-3158.

IUSS Working Group WRB (2006) *World Reference Base for Soil Resources 2006. Erstes Update 2007. Deutsche Ausgabe. – Übersetzt von Peter Schad.* Bundesanstalt für Geowissenschaften und Rohstoffe, Hannover.

Jahnke L. L., Embaye T., Hope J., Turk K. A., Van Zuilen M., Des Marais D. J., Farmer J. D. and Summons R. E. (2004) Lipid biomarker and carbon isotopic signatures for stromatolite-forming, microbial mat communities and Phormidium cultures from Yellowstone National Park. *Geobiology* **2**, 31-47.

Jansson J. K. and Tas N. (2014) The microbial ecology of permafrost. *Nat. Rev. Micro.* **12**, 414-425.

Jones A., Stolbovoy V., Tarnocai C., Broll G., Spaargaren O. and Montanarella L. (2010) *Soil Atlas of the northern circumpolar region*. European Commission, Publications Office of the European Union, Luxembourg.

Joyeux C., Fouchard S., Llopiz P. and Neunlist S. (2004) Influence of the temperature and the growth phase on the hopanoids and fatty acids content of *Frateuria aurantia* (DSMZ 6220). *FEMS Microbiol. Ecology* **47**, 371-379.

Kannenberg E. L. and Poralla K. (1999) Hopanoid Biosynthesis and Function in Bacteria. *Naturwissenschaften* **86**, 168-176.

Kaur A., Chaudhary A., Kaur A., Choudhary R. and Kaushik R. (2005) Phospholipid fatty acid – A bioindicator of environment monitoring and assessment in soil ecosystem. *Current Science* **89**, 1103-1112.

Kim J.-H., Talbot H. M., Zarzycka B., Bauersachs T. and Wagner T. (2011) Occurrence and abundance of soil-specific bacterial membrane lipid markers in the Têt watershed (southern France): Soil-specific BHPs and branched GDGTs. *Geochem. Geophys. Geosyst.* **12**, Q02008.

Knoblauch C., Zimmermann U., Blumenberg M., Michaelis W. and Pfeiffer E.-M. (2008) Methane turnover and temperature response of methane-oxidizing bacteria in permafrost-affected soils of northeast Siberia. *Soil Biology and Biochemistry* **40**, 3004-3013.

Landesman W. J., Nelson D. M. and Fitzpatrick M. C. (2014) Soil properties and tree species drive ß-diversity of soil bacterial communities. *Soil Biology and Biochemistry* **76**, 201-209.

Liebner S. (2007) Adaptation, spatial variability, and phylogenetic characterization of methanotrophic communities in permafrost soils of the Lena Delta, Siberia. PhD Thesis, Universität Bremen, www.marmic.mpg.de/marmic/uploads_edit/PhD_Susanne_Liebner.pdf.

Liebner S. and Wagner D. (2007) Abundance, distribution and potential activity of methane oxidizing bacteria in permafrost soils from the Lena Delta, Siberia. *Environ. Microbiol.* **9**, 107-117.

Liebner S., Harder J. and Wagner D. (2008) Bacterial diversity and community structure in polygonal tundra soils from Samoylov Island, Lena Delta, Siberia. *International Microbiol.* **11**, 195-202.

Liebner S., Rublack K., Stuehrmann T. and Wagner D. (2009) Diversity of aerobic methanotrophic bacteria in a permafrost active layer soil of the Lena Delta, Siberia. *Microb. Ecol.* **57**, 25–35.

Morgenstern A., Grosse G., Günther F., Fedorova I. and Schirrmeister L. (2011) Spatial analyses of thermokarst lakes and basins in Yedoma landscapes of the Lena Delta. *The Cryosphere* **5**, 849-867.

Morgenstern A., Ulrich M., Günther F., Roessler S., Fedorova I. V., Rudaya N. A., Wetterich S., Boike J. and Schirrmeister L. (2013) Evolution of thermokarst in East Siberian ice-rich permafrost: A case study. *Geomorphology* **201**, 363-379.

Mykytczuk N. C. S., Foote S. J., Omelon C. R., Southam G., Greer C. W. and Whyte L. G. (2013) Bacterial growth at -15°C; molecular insights from the permafrost bacterium *Planococcus halocryophilus Or1*. *ISME J* **7**, 1211-1226.

Neunlist S. and Rohmer M. (1985a) The Hopanoids of '*Methylosinus trichosporium*': aminobacteriohopanetriol and aminobacteriohopanetetrol. *J. Gen. Microbiol.* **131**, 1363-1367.

Neunlist S. and Rohmer M. (1985b) Novel hopanoids from the methylotrophic bacteria *Methylococcus capsulatus* and *Methylomonas methanica*. (22S)-35-aminobacteriohopane-30,31,32,33,34-pentol and (22S)-35-amino-3 beta-methylbacteriohopane-30,31,32,33,34-pentol. *Biochemical J.* **231**, 635-639.

Neunlist S. and Rohmer M. (1985c) A novel hopanoid, 30-(5'-adenosyl)hopane, from the purple non-sulphur bacterium *Rhodopseudomonas acidophila*, with possible DNA interactions. *Biochemical J.* **228**, 769-771.

Neunlist S., Bisseret P. and Rohmer M. (1988) The hopanoids of the purple non-sulfur bacteria *Rhodopseudomonas palustris* and *Rhodopseudomonas acidophila* and the absolute configuration of bacteriohopanetetrol. *European J. Biochem.* **171**, 245-252.

Nierop K. G. J., Naafs D. F. W. and van Bergen P. F. (2005) Origin, occurrence and fate of extractable lipids in Dutch coastal dune soils along a pH gradient. *Org. Geochem.* **36**, 555-566.

Ourisson G. and Albrecht P. (1992) Hopanoids. 1. Geohopanoids: The most abundant natural products on earth? *Acc. Chem. Res.* **25**, 398-402.

Pearson A., Flood Page S. R., Jorgenson T. L., Fischer W. W. and Higgins M. B. (2007) Novel hopanoid cyclases from the environment. *Environ. Microbiol.* **9**, 2175-2188.

Pearson A. and Rusch D. B. (2009) Distribution of microbial terpenoid lipid cyclases in the global ocean metagenome. *ISME J.* **3**, 352-363.

Poralla K., Härtner T. and Kannenberg E. (1984) Effect of temperature and pH on the hopanoid content of *Bacillus acidocaldarius*. *FEMS Microbiol. Letters* **23**, 253-256.

Rashby S. E., Sessions A. L., Summons R. E. and Newman D. K. (2007) Biosynthesis of 2-methylbacteriohopanepolyols by an anoxygenic phototroph. *Proc. Natl. Acad. Sci.* USA **104**, 15099-15104.

Renoux J.-M. and Rohmer M. (1985) Prokaryotic triterpenoids: New bacteriohopanetetrol cyclitol ethers from the methylotrophic bacterium *Methylobacterium organophilum*. *European J. Biochem.* **151**, 405-410.

Rethemeyer J., Schubotz F., Talbot H. M., Cooke M. P., Hinrichs K.-U. and Mollenhauer G. (2010) Distribution of polar membrane lipids in permafrost soils and sediments of a small high Arctic catchment. *Org. Geochem.* **41**, 1130-1145.

Řezanka T., Siristova L., Melzoch K. and Sigler K. (2011) N-Acylated Bacteriohopanehexol-mannosamides from the thermophilic bacterium *Alicyclobacillus acidoterrestris. Lipids* **46**, 249-261.

Ricci J. N., Coleman M. L., Welander P. V., Sessions A. L., Summons R. E., Spear J. R. and Newman D. K. (2014) Diverse capacity for 2-methylhopanoid production correlates with a specific ecological niche. *ISME J.* **8**, 675-684.

Rohmer M., Bouvier-Nave P. and Ourisson G. (1984) Distribution of Hopanoid Triterpenes in Prokaryotes. *J. Gen. Microbiol.* **130**, 1137-1150.

Rohmer M. (1993) The biosynthesis of triterpenoids of the hopane series in the Eubacteria: A mine of new enzyme reactions. *Pure & Applied Chemistry* **85**, 1293-1298.

Rohmer M. (2008) From Molecular Fossils of Bacterial Hopanoids to the Formation of Isoprene Units: Discovery and Elucidation of the Methylerythritol Phosphate Pathway. *Lipids* **43**, 1095-1107.

Rosa-Putra S., Nalin R., Domenach A.-M. and Rohmer M. (2001) Novel hopanoids from *Frankia spp.* and related soil bacteria. *European J. Biochem.* **268**, 4300-4306.

Sáenz J. P., Wakeham S. G., Eglinton T. I. and Summons R. E. (2011) New constraints on the provenance of hopanoids in the marine geologic record: Bacteriohopanepolyols in marine suboxic and anoxic environments. *Org. Geochem.* **42**, 1351-1362.

Schaeffer P., Schmitt G., Adam P. and Rohmer M. (2010) Abiotic formation of 32,35-anhydrobacteriohopanetetrol: A geomimetic approach. *Org. Geochem.* **41**, 1005-1008.

Schirrmeister L., Grosse G., Schnelle M., Fuchs M., Krbetschek M., Ulrich M., Kunitsky V., Grigoriev M., Andreev A., Kienast F., Meyer H., Babiy O., Klimova I., Bobrov A., Wetterich S. and Schwamborn G. (2011) Late Quaternary paleoenvironmental records from the western Lena Delta, Arctic Siberia. *Palaeogeography, Palaeoclimatology, Palaeoecology* **299**, 175-196.

Seemann M., Bisseret P., Tritz J.-P., Hooper A. B. and Rohmer M. (1999) Novel bacterial triterpenoids of the hopane series from *Nitrosomonas europaea* and their significance for the formation of the C35 bacteriohopane skeleton. *Tetrahedron Letters* **40**, 1681-1684.

Soil Survey Staff (2010) *Keys to soil taxonomy*, 11 ed. US. Dept. of Agriculture & Natural Resources Conservation Service, Washington, D.C.

Steven B., Pollard W. H., Greer C. W. and Whyte L. G. (2008) Microbial diversity and activity through a permafrost/ground ice core profile from the Canadian high Arctic. *Environ. Microbiol.* **10**, 3388-3403.

Summons R. E., Jahnke L. L., Hope J. M. and Logan G. A. (1999) 2-Methylhopanoids as biomarkers for cyanobacterial oxygenic photosynthesis. *Nature* **400**, 554-557.

Talbot H. M., Watson D. F., Murrell J. C., Carter J. F. and Farrimond P. (2001) Analysis of intact bacteriohopanepolyols from methanotrophic bacteria by reversed-phase high-performance liquid chromatography–atmospheric pressure chemical ionisation mass spectrometry. *J. of Chromatography A* **921**, 175-185.

Talbot H. M., Summons R., Jahnke L. and Farrimond P. (2003) Characteristic fragmentation of bacteriohopanepolyols during atmospheric pressure chemical ionisation liquid chromatography/ion trap mass spectrometry. *Rapid Communications in mass spectrometry* **17**, 2788-2796.

Talbot H. M. and Farrimond P. (2007) Bacterial populations recorded in diverse sedimentary biohopanoid distributions. *Organic Geochemistry* **38**, 1212-1225.

Talbot H. M., Rohmer M. and Farrimond P. (2007a) Structural characterisation of unsaturated bacterial hopanoids by atmospheric pressure chemical ionisation liquid chromatography/ion trap mass spectrometry. *Rapid Communications in Mass Spectrometry* **21**, 1613-1622.

Talbot H. M., Rohmer M. and Farrimond P. (2007b) Rapid structural elucidation of composite bacterial hopanoids by atmospheric pressure chemical ionisation liquid chromatography/ion trap mass spectrometry. *Rapid Communications in Mass Spectrometry* **21**, 880-892.

Talbot H. M., Summons R. E., Jahnke L. L., Cockell C. S., Rohmer M. and Farrimond P. (2008) Cyanobacterial bacteriohopanepolyol signatures from cultures and natural environmental settings. *Org. Geochem.* **39**, 232-263.

Talbot H. M., Handley L., Spencer-Jones C. L., Dinga B. J., Schefuß E., Mann P. J., Poulsen J. R., Spencer R. G. M., Wabakanghanzi J. N. and Wagner T. (2014) Variability in aerobic methane oxidation over the past 1.2 Myrs recorded in microbial biomarker signatures from Congo fan sediments. *Geochim. Cosmochim. Acta* **133**, 387-401.

Taylor K. A. and Harvey H. R. (2011) Bacterial hopanoids as tracers of organic carbon sources and processing across the western Arctic continental shelf. *Org. Geochem.* **42**, 487-497.

van Bergen P. F., Nott C. J., Bull I. D., Poulton P. R. and Evershed R. P. (1998) Organic geochemical studies of soils from the Rothamsted Classical Experiments—IV. Preliminary results from a study of the effect of soil pH on organic matter decay. *Org. Geochem.* **29**, 1779-1795.

van Dongen B. E., Semiletov I., Weijers J. W. H. and Gustafsson Ö. (2008) Contrasting lipid biomarker composition of terrestrial organic matter exported from across the Eurasian Arctic by the five great Russian Arctic rivers. *Global Biogeochem. Cycles* **22**, GB1011.

van Winden J. F., Talbot H. M., Kip N., Reichart G.-J., Pol A., McNamara N. P., Jetten M. S. M., Op den Camp H. J. M. and Sinninghe Damsté J. S. (2012) Bacteriohopanepolyol signatures as markers for methanotrophic bacteria in peat moss. *Geochim. Cosmochim. Acta* **77**, 52-61.

Vilcheze C., Llopiz P., Neunlist S., Poralla K. and Rohmer M. (1994) Prokaryotic triterpenoids: new hopanoids from the nitrogen-fixing bacteria *Azotobacter vinelandii*, *Beijerinckia indica* and *Beijerinckia mobilis*. *Microbiol.* **140**, 2749-2753.

Wagner D., Lipski A., Embacher A. and Gattinger A. (2005) Methane fluxes in permafrost habitats of the Lena Delta: effects of microbial community structure and organic matter quality. *Environ. Microbiol.* **7**, 1582–1592.

Wagner D., Kobabe S. and Liebner S. (2009) Bacterial community structure and carbon turnover in permafrost-affected soils of the Lena Delta, northeastern Siberia. *Canadian J. Microbiol.* **55**, 73-83.

Wagner T., Kallweit W., Talbot H. M., Mollenhauer G., Boom A. and Zabel M. (2014) Microbial biomarkers support organic carbon transport from methane-rich Amazon wetlands to the shelf and deep sea fan during recent and glacial climate conditions. *Org. Geochem.* **67**, 85-98.

Welander P. V., Hunter R. C., Zhang L., Sessions A. L., Summons R. E. and Newman D. K. (2009) Hopanoids play a role in membrane integrity and pH homeostasis in *Rhodopseudomonas palustris TIE-1*. *J. Bacteriology* **191**, 6145-6156.

Welander P. V., Coleman M. L., Sessions A. L., Summons R. E. and Newman D. K. (2010) Identification of a methylase required for 2-methylhopanoid production and implications for the interpretation of sedimentary hopanes. *Proc. Natl. Acad. Sci. USA* **107**, 8537-8542.

Xu Y., Cooke M. P., Talbot H. M. and Simpson M. J. (2009) Bacteriohopanepolyol signatures of bacterial populations in Western Canadian soils. *Org. Geochem.* **40**, 79-86.

Yergeau E., Hogues H., Whyte L. G. and Greer C. W. (2010) The functional potential of high Arctic permafrost revealed by metagenomic sequencing, qPCR and microarray analyses. *ISME J.* **4**, 1206-1214.

Zhang C. L., Huang Z., Li Y.-L., Romanek C. S., Mills G. L., Gibson R. A., Talbot H. M., Wiegel J., Noakes J., Culp R. and White D. C. (2007) Lipid Biomarkers, Carbon Isotopes, and

Phylogenetic Characterization of Bacteria in California and Nevada Hot Springs. *Geomicrobiol. J.* **24**, 519-534.

Zhu C., Talbot H. M., Wagner T., Pan J. M. and Pancost R. D. (2010) Intense aerobic methane oxidation in the Yangtze Estuary: A record from 35-aminobacteriohopanepolyols in surface sediments. *Org. Geochem.* **41**, 1056-1059.

Zhu C., Talbot H. M., Wagner T., Pan J.-M. and Pancost R. D. (2011) Distribution of hopanoids along a land to sea transect: Implications for microbial ecology and the use of hopanoids in environmental studies. *Limnology and Oceanography* **56**, 1850-1865.

Zubrzycki S., Kutzbach L., Pfeiffer E.-M. and Vakhrameeva P. (2012) Variability of soil organic carbon stocks of different permafrost-affected soils: Initial results from a North-South transect in Siberia, in: H. K.M. (Ed.), Tenth International Conference on Permafrost (TICOP). The Northern Publisher, Salekhard, Salekhard, Yamal-Nenets Autonomous District, Russia, pp. 485-490.

Zubrzycki S. (2013) Organic Carbon Pools in Permafrost-Affected Soils of Siberian Arctic Regions. PhD Thesis, Universität Hamburg, www.geowiss.uni-hamburg.de/i-boden/hba/HBA71%20Zubrzycki%202013%20Dissertation%20Overview.pdf.

# 6. Manuscript IV: Microbial degradation of organic matter – $^{14}C$ *contents of microbial phospholipids fatty acids reveal preferential metabolism of labile organic matter in Arctic permafrost soils*

by
**Höfle S.**, Roobroeck D., Boeckx P., Rethemeyer J.

in preparation

# $^{14}$C contents of microbial phospholipid fatty acids reveal preferential metabolism of labile organic matter in Arctic permafrost soils

Silke Höfle[1*], Dries Roobroeck[2], Pascal Boeckx[2], Janet Rethemeyer[1]

[1] *Institute for Geology and Mineralogy, University of Cologne, Zuelpicher Str. 49a, 50674 Cologne, Germany*

[2] *Faculty of Bioscience Engineering, Ghent University, Coupure 653, 9000 Gent, Belgium*

**Abstract**

Arctic permafrost regions will be affected most strongly by the global warming probably turning the permafrost soils from carbon sinks into carbon sources for the atmosphere as previous frozen-looked carbon pools are thawed. Microbial metabolic activity is a key factor in the mineralization of soil organic matter and the active layer thawing during summer is the main place for soil organic matter decomposition within the permafrost. So far little is known about which organic carbon sources microorganisms metabolise in permafrost soils. This study investigated the organic matter composition and its microbial utilization in two active layer profiles of the polygonal tundra in the Siberian Lena Delta, Russia by using lipid biomarker analysis and compound-specific radiocarbon analysis of individual lipids. The organic matter was in each of the investigated polygon rim and centre mainly composed of labile plant-derived material as indicated by the dominance of long-chain lipid biomarker (*n*-alkanes and *n*-fatty acids) and their higher $^{14}$C contents compared to the bulk soil from which they were isolated. The increasing $^{14}$C ages of microbial PLFAs with increasing soil depth suggested that the microorganisms utilize older carbon sources in greater depth but these sources are still the most labile carbon pools available as free plant-derived particular organic matter has similar $^{14}$C ages as the PLFAs. Thus, it is possible that 'old', presumably more stable carbon pools are either not in favour for microbial decomposition or are not bioavailable or are metabolised by other microorganisms than the (aerobic) soil bacteria we investigated.

## 1. Introduction

Global warming, which is affecting northern high latitudes most strongly (Kirtman et al., 2013) may lead to the degradation of up to 60% of the present permafrost area by 2200 as model simulations suggest (Saito et al., 2007; Schaefer et al., 2011). Thereby deeper soil organic carbon (OC) formed during the Pleistocene and early Holocene might become available for decomposition whereby this large OC reservoir may be turned into a considerable source of carbon emissions as suggested by a recent modelling study of Koven et al. (2011). However, the response of the microbial metabolic activity, a key factor in the soil OC mineralization, and the resulting carbon emissions into the atmosphere due to global warming are not well understood. Therefore, the permafrost carbon feedback to warming is still under debate (Davidson and Janssens, 2006; Ciais et al., 2013) including uncertainties about the size and the bioavailability of the carbon that is released from the thawing permafrost (e.g., Shaver et al., 2006; Schuur et al., 2008; Nowinski et al., 2010; Harden et al., 2012; Schuur et al., 2013). A recent published synthesis study by Schädel et al. (2014) of long-term (>1 year) incubations of permafrost effected soils across the Arctic showed that using a three-pool decomposition model at 5°C less than 5% of all carbon was labile and quickly decomposed within one year. However, the organic carbon loss was projected to be between 20% and 90% within 50 incubation years (Schädel et al., 2014). Nevertheless, incubations studies base only on respiration lab experiments not including the in-situ environmental conditions. In-situ studies at permafrost thawing sites and sites with increasing thickness of the seasonal upper thawing soil layer (active layer) due to snow fence experiments in Alaska showed greater amounts of old carbon emissions with increasing thawing of the permafrost (Schuur et al., 2009; Nowinski et al., 2010). These results of incubation and in-situ studies could indicate that the OC in permafrost soils is highly bioavailable but so far little is known about which carbon pools (‘young’ and presumably more labile or ‘old’ and presumably more stable) microorganism prefer to metabolise.

One method to study the microbial community and their activity in soils is the analysis of the membrane phospholipid fatty acids (PLFAs). PLFAs have been widely used to characterize the living soil microbial biomass because of their fast degradation within days after cell death (Zelles, 1999; Frostegård et al., 2011). Microbes in permafrost regions are able to utilize different carbon sources including ancient carbon as PLFA studies in combination with incubations and stable isotopic carbon measurements have showed (Biasi et al., 2005; Bardgett et al., 2007). PLFAs contain only low specific taxonomy information and cannot compete e.g. with RNA/DNA methods in the phylogenetic resolution in which a microbial community can be characterised (Frostegard et al., 2011; Blagodatskaya and Kuzyakov, 2013). However, they are a useful biomarker for compound specific radiocarbon analysis as individual PLFAs can by extracted and isolated in large enough amounts (ca. 20 – 100 µgC) for $^{14}$C-AMS measurements. By the radiocarbon analysis of single PLFAs from soil samples different OC pools ($^{14}$C ‘young’/presumably labile or $^{14}$C ‘old’/presumably more stable) can be identified which are metabolised by different microorganism groups (e.g. Rethemeyer et al., 2004; Rethemeyer et al., 2005;

Kramer et al., 2010; Ziolkowski et al., 2013). Nevertheless, it remains difficult to understand the processes of soil OC decomposition in detail as OC is a heterogenic composition of materials from various sources (e.g. plants, microorganisms) in various stages of decomposition (e.g. Six et al., 2002) which differ in age, turnover rates and stabilization mechanisms (von Lützow et al., 2007). Therefore, a comparison between the $^{14}C$ ages of the microbial PLFAs and the $^{14}C$ ages of various soil OC pools which differ in decomposition rates may identify potential carbon sources of the microbial degradation.

The aim of this paper is to gain information on the decomposability of OC in the active layer of a polygon rim and a centre in the Siberian Lena Delta. The OC composition is characterised by lipid biomarker (*n*-alkanes and *n*-fatty acids) distribution and compound-specific radiocarbon analysis of individual mostly plant-derived lipids. As we are specifically interested in which OC pools are metabolised by microorganisms compound-specific radiocarbon analysis of microbial membrane lipids (PLFAs) was done. By comparing our $^{14}C$ contents of the lipids with other carbon pools which differ in degradation rates, as free (fPOM) or in soil aggregated occluded particular organic matter (oPOM), potential carbon sources of the microbes could be further identified.

## 2. Material and methods

### 2.1 Study area

The study was performed in the polygonal tundra on Samoylov Island (N 72.37°, E 126.48°) which belongs to the recent active part of the Siberian Lena-Delta, Russia (Fig. 1). The delta is located in the zone of continuous permafrost. The climate is Arctic continental with low annual mean precipitation (125 mm), low annual mean temperatures (-12.5°C), and a great seasonal temperature amplitude between winter (February -33.1°C) and summer (July 10.1°C; Boike et al., 2013). Ice-wedge based polygonal tundra dominates the landscape (Mueller, 1997) and forms due to ground freezing-thawing cycles which can further displace and mix soil material (cryoturbation; Fiedler et al., 2004).

On Samoylov Island depressed polygon centres cover 17%, the by several decimetres elevated polygon rims 58% and water surfaces 25% of the landscape (Muster et al., 2012). The polygons have a diameter of about 9-15 m. According to the US Soil Taxonomy the soils on Samoylov belong to the soil type Gelisols (Soil Survey Staff, 2010). The dominant soils are Glacic Aquiturbels on polygon rims and Typic or Ruptic Historthel in polygon centres (Zubrzycki et al., 2012). The vegetation on Samoylov Island is dominated by mosses and sedges in the wet polygon centres and by mosses, herbs, lichens and some small shrubs like *Salix spp.* or *Betula spp.* on the dry polygon rims (Mueller, 1997; Boike et al., 2013).

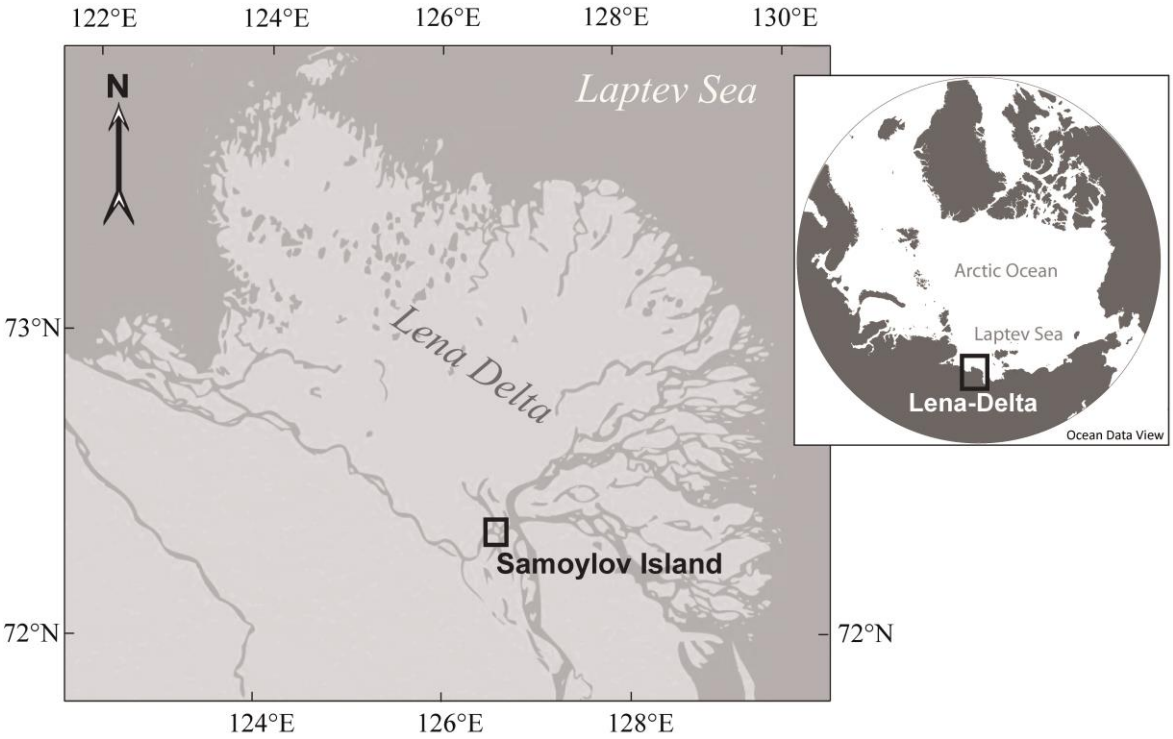


Fig. 1: Location of Samoylov Island in the Siberian Lena-Delta, Russia

## 2.2 Sampling and bulk parameters

Samples were taken from two soil pits of about 1x1 m in the depressed polygon centre and on the polygon rim. The different soil horizons of the active layer were sampled, when the active layer depth is greatest, in August 2010. Furthermore, material of the still frozen permafrost top layer of the polygon rim was sampled. Immediately after sampling the material was frozen and kept at -20°C until analysis. All samples were freeze-dried and manually ground using liquid nitrogen to be able to grind the undecomposed plants of the upper organic rich O horizons for further analysis. Total carbon and nitrogen values were determined of 5 mg soil with 20 mg oxidant (Vario MICRO cube, Elementar, Germany). The samples contained no inorganic carbon therefore total carbon contents (TOC) were equal to total OC contents. Soil pH values were measured in $H_20$ (1:2.5 by weight) one hour after water addition (IUSS Working Group WRB, 2006).

## 2.3 Lipid analysis

### 2.3.1 *n*-alkanes and *n*-fatty acids

Total extractable lipids were recovered by accelerated solvent extraction (ASE 200, Dionex, USA; 75 bar, 120°C, 20 min) with dichloromethane:methanol (9:1, v:v) from 5 g dry soil. After saponification of the lipid extract with methanolic potassium hydroxide (0.5 M potassium hydroxide in methanol:water, 9:1, v:v) to free bounded fatty acids, neutral lipids were gained by liquid-liquid phase separation and fatty acids after acidification with

10% hydrochloric acid. The neutral lipid fraction was separated on a $SiO_2$ (deactivated, mesh size 60) column into *aliphatic*, aromatic and hetero-compounds with hexane, dichloromethane:hexane (2:1, v:v) and methanol, respectively. The fatty acid fraction was transesterified with methanolic hydrochloric acid (methanol: hydrochloric $acid_{concentrated}$ 95:5, v:v) to fatty acid methyl esters (FAMEs) and purified on a $SiO_2$-$Na_2SO_4$ column eluted with dichloromethane:hexane (2:1, v:v). Both, *n*-alkanes and FAMEs were measured on a gas chromatography with a flame ionisation detector (GC-FID; 5890 series II plus, HP, Germany) equipped with a DB-5MS column (50 m, 0.2 mm ID, 0.33 µm df). Measurements were done in split mode (He constant flow: 30 $ml.min^{-1}$) and the following temperature program: injection at 40°C with a 2 min hold followed by a ramp of 10°$C.min^{-1}$ up to 140°C, and a second ramp of 3°$C.min^{-1}$ up to 320°C with a 28 min hold. *n*-Alkanes and *n*-fatty acids were identified and quantified using external standard mixtures.

2.3.2. Phospholipid fatty acids

The extraction of the PLFAs was adapted from Bossio and Scow (1998) based on the method from Bligh and Dyer (1959). Briefly, 10 g of soil were extracted by shaking with phosphate-buffer/chloroform/methanol (0.9:1:2, v:v:v). The total lipid fraction, which was gained in the chloroform phase, was separated on a SiO column into glycol-, neutral- and phospholipids with chloroform, acetone, and methanol, respectively. The phospholipids were methylated with methanolic potassium hydroxide and measured on a GC-mass spectrometry (GC-MS; DeltaPLUS XP, Thermo Scientific, USA) equipped with a Varian Factor Four VF-23ms column (60 m, 0.32 mm ID, 0.15 µm df). Measurements were done in splitless mode with a constant flow (1$ml.min^{-1}$) and the following temperature program: injection at 50°C with a 2 min hold, followed by a ramp of 15°$C.min^{-1}$ up to 100°C, followed by a second ramp of 2°$C.min^{-1}$up to 220°C, and a final ramp of 15°$C.min^{-1}$ up to 240°C with a 5 min hold. Identification of PLFAs was done using internal standards (FAMEs 12:0 and 21:0). Every sample was measured twice (standard deviation 0 – 3.4%).

The nomenclature of the PLFAs is of the following principal: A:BωC, where A stands for the number of carbon atoms, B for the number of double bounds and C indicates the position of the double bounds determined from the aliphatic (ω) molecule end. Cis and trans configurations are indicated by c or t after the C. Anteiso- and isobranching are specified by the prefix a or i. Methylation on the $10^{th}$ carbon atom from the carboxyl molecule end is noted by the prefix 10Me.

The identified PLFAs included 13 biomarkers characteristic for several microbial groups; iso- and anteiso-branched PLFAs (i14:0, i15:0, a15:0, i16:0, i17:0, and a17:0) for Gram-positive bacteria, monounsaturated PLFAs with a ω7cis unsaturation (16:1ω7c and 18:1ω7c) for Gram-negative bacteria, methylated PLFAs on the $10^{th}$ C atom (10Me17:0 and 10Me18:0) for actinomycetes, the PLFAs 18:1ω9c and 18:2ω6,9c for fungi, and the PLFA 16:1ω5c for arbuscular mycorrhizal fungi (Vestal and White, 1989; Olsson et al., 1995; Zelles, 1997, 1999). PLFA biomarkers characteristic for methanotrophic bacteria (16:1ω8c and 18:1ω8c) were not determined.

Bacterial cell content was calculated using the sum of the bacterial PLFA biomarkers (Gram-positive and Gram-negative) and the conversion factor of $1.40*10^{-17}$ mol bacterial PLFA.cell$^{-1}$ (Frostegard and Bååth, 1996). For the fungal to bacterial PLFA ratio the concentrations of the fungal PLFA 18:2ω6,9c are related to sum of the bacterial PLFA content. Only the PLFA 18:2ω6,9c was used for this ratios as it has been shown to be positively correlated with the fungal specific ergosterol therefore suggested as an indicator for the fungal biomass (Frostegard and Bååth, 1996; Joergensen and Wichern, 2008).

### 2.4 Radiocarbon analysis of bulk soil material

Bulk soil samples were pre-treated with 1% hydrochloric acid (ca. 10 h) to remove possible inorganic carbon and humic substances. Afterwards the acid was removed by washing repeatedly with Milli-Q water (Millipore, USA) and the samples were dried (60°C). The samples were then graphitized with an automatic graphitization system at CologneAMS, Germany (Wacker et al., 2010; Rethemeyer et al., 2013). Radiocarbon analysis of bulk soil material of each horizon was done with the MICADS at ETH in Zurich, Switzerland, except for one sample (polygon rim Oi horizon) which was measured at the CologneAMS. All $^{14}C$ results of the bulk soil material (bulk OC) are reported as percent modern carbon (pMC, related to 1950; Stuiver and Polach, 1977) with one-sigma uncertainties. $^{14}C$ contents above 100 pMC show an influence of bomb-$^{14}C$ which was introduced to the atmosphere due to the above-ground nuclear bomb tests of the late 1950s and early 1960s (Levin et al., 1985). The $^{14}C$ content ($\Delta^{14}C$) of the atmosphere of the northern hemisphere was at the times of sampling 2010) 42.5‰ (Levin et al., 2013) translated into 105.0 pMC.

### 2.5 Compound-specific radiocarbon analyses

PLFAs, *n*-fatty acids, and *n*-alkanes were isolated from two horizons of the active layer in the polygon rim (Ajj and Bjjf horizon) and the polygon centre (Oi and B horizon). PLFAs were extracted from 200-250 g freeze-dried soil following the same protocol as describe above (section 2.3.2). *n*-Fatty acids and *n*-alkanes were extracted in a Soxhlet aperture (24 h) with dichloromethan:methanol (9:1, v:v) from 35-300 g freeze-dried soil, depending on the TOC content and the amount of material available. Further analytical steps for *n*-alkanes and *n*-fatty acids analysis are identical to the description above (section 2.3.1).

Due to size requirements of the $^{14}C$ AMS measurements the aim was to retrieve 30-100 µg of carbon. Therefore, individual *n*-fatty acids ($C_{16}$, $C_{24}$, $C_{26}$, and $C_{28}$), *n*-alkanes ($C_{23}$ and $C_{27}$), and PLFAs ($C_{16:0}$) or groups of PLFAs ($C_{i15:0}$ plus $C_{a15:0}$, $C_{16:1er}$, and $C_{18:1er}$), which were present in high concentrations, were isolated using a preparative GC device (Eglinton et al., 1996). PLFAs had to be grouped together because of lower concentrations of individual compounds.

The preparative GC (7890A GC Agilent, USA; Restek Rxi-XLB column 30 m, 0.53 mm ID, 0.50 µm df;) was equipped with a cooled injector (KAS 4, Gerstel, Germany) and a programmable fraction collector (PFC; Gerstel, Germany). Only glass traps pre-combusted in the night before the isolation started were used. Trap heating was only used for the PLFA isolation of one sample (rim Ajj horizon) because higher recoveries were expected to gain. However, a trap heating test with *n*-fatty acid standards of different chain-length showed that higher recoveries could be obtained for short-chain compounds ($C_{16}$-$C_{18}$) without heating (Rethemeyer et al., 2013). Therefore, further isolations were done without trap heating. Isolated compounds were rinsed out of the glass traps with 1 ml dichloromethane into pre-combusted glass vials. The isolated compounds were checked for purity and quantified on a GC-FID (5890 series II, HP, Germany; 50 m DB-5MS column, 0.2 mm ID, 0.33 µm df) prior to the $^{14}C$ analysis. Only lipid biomarkers with a high purity (>96%) were selected for $^{14}C$ analysis, except a few compounds which had only a purity of 94% (highlighted in Table 5) but were still $^{14}C$ measured to complete the set of analysed lipids.

The isolated lipid was transferred with dichloromethane into a pre-combusted small quartz tube (950°C, 4h). The solvent was removed using a rotary evaporator (quartz tube placed into pre-combusted glass round bottom flask) and pre-combusted copper oxide (150 µg) and silver wool (50-60 µg) were added. The small tube was placed into a big pre-combusted quartz tube (950°C, 4h). The samples were evacuated while cooled in dry ice for at least 60 min until a stable pressure ($1*10^{-4}$ - $8*10^{-4}$ mbar) was reached. Then the dry ice was replaced by liquid nitrogen and tubes were flame-sealed and combusted (950°C, 4 h). The $CO_2$ evolved was purified and quantified (23-286 µgC) under vacuum and then flame-sealed in small pre-combusted glass tubes (450°C, 4h). These glass tubes were sent to ETH Zurich, Switzerland and directly connected to the ion gas source of the MICADAS.

The $^{14}C$ content of the derivatized compounds (PLFAs and *n*-fatty acids) was corrected for the methanol group added (0 pMC; COL1011 and COL1020 CologneAMS). Furthermore, a correction for exogenous carbon introduced during the chromatographic isolation and subsequent sample handling (process blank) was done for all compounds using an isotopic mass balance calculation (equation 1).

$$^{14}C_{Lipid} = (m_L * ^{14}C_L - m_F * ^{14}C_F - m_M * ^{14}C_M) / (m_L - m_F - m_M) \quad (1)$$

where $^{14}C_{Lipid}$ is the $^{14}C$ value of the target lipid without contamination. $^{14}C_L$ is the $^{14}C$ content and $m_L$ the mass of the measured lipid. $^{14}C_M$ is the 14C content and $m_M$ the mass of the modern contamination and $^{14}C_F$ is the $^{14}C$ content and $m_F$ the mass of $^{14}C$-free contamination. Rethemeyer et al. (2013) determined the process blank ($^{14}C_M$, $^{14}C_F$, $m_M$, and $m_F$) for the prepGC isolation and further sample handling for compound-specific radiocarbon analysis at the CologneAMS. The masses of modern ($m_M$) and $^{14}C$-free ($m_F$)

contaminations are shown in table 1. The evaluated process blank was verified on a regularly basis during the compound-specific radiocarbon analyses of this study. The $^{14}C$ values are reported in pMC (related to 1950) with process blank correction and one sigma measurement uncertainty.

Table 1: Process blank due to exogenous carbon introduced during chromatogramic isolation with the preparative GC and subsequent sampling handling from Rethemeyer et al. (2013)

| Compound class | Standard type | Carbon number | Sample ID[a] | Calculated mass of exogenous carbon (µg C)[b] |
|---|---|---|---|---|
| *n*-alkane | $^{14}C$-free | C18 | 43362 | $m_F$ = 1.10 |
| | modern | C30 | 43363 | $m_M$ = 3.80 |
| *n*-fatty acid | modern | C18 | 43390 | $m_M$ = 3.90 |
| | $^{14}C$-free | C30 | 43391 | $m_F$ = 2.10 |

[a] ETH Zurich laboratory number
[b] using an isotopic mass balance calculation, for details on calculation see Rethemeyer et al., 2013

## 3. Results

### 3.1 Basic soil characteristics

The bulk soil properties of the two different landscape structures – rim and centre – investigated are summarized in Table 2 (Höfle et al., 2013; Höfle et al., submitted, and this study). The polygon rim soil is a Glacic Aquiturbels with a thin upper organic rich soil horizon (Oi: 7 cm) and the water saturated centre soil is a Typic Historthels with thick organic rich horizons (Oi and Oe: 40 cm) on top. The TOC contents, which decrease in both soils with depth, are higher in the polygon centre (4-23%) than in the rim (2-11%). C/N ratios are significantly higher in the polygon centre soils (35-51) than in the polygon rim (around 18). The pH values are slightly higher in the polygon rim soils (5.0-6.7) than in the centre soils (4.8-5.9). The two profiles differ in active layer thickness with 32 cm in the polygon rim and 43 cm in the water saturated centre. However, the most prominent difference is the apparent $^{14}C$ age of the organic matter. The bulk OC of the polygon rim shows a strong and constant decrease in $^{14}C$ content with depth (from 115 pMC to 68 pMC; Table 2) indicating that cryoturbation is negligible. In contrast the centre bulk OC decreases only little from 113 pMC to 96 pMC with soil depth being in general significantly younger than the rim bulk OC.

Table 2: Bulk soil parameters of the polygon rim and centre soils on Samoylov Island

| Polygonal structure | Depth (cm) | Horizon | pH | TOC (%) | Total N (%) | C/N | $^{14}$C content (pMC) | $^{14}$C age (yrs BP) | Sample ID[a] |
|---|---|---|---|---|---|---|---|---|---|
| Rim[b] | 0-7 | Oi | 5.0 | 10.3 | na | na | 115 ± 0.4 | modern | COL1152 |
| | 7-13 | Ajj | 6.1 | 3.0 | 0.16 | 19 | 90 ± 0.2 | 866 ± 26 | COL1025 |
| | 13-18 | Bjjg | 6.4 | 1.5 | 0.08 | 18 | 83 ± 0.2 | 1538± 27 | COL1026 |
| | 18-32 | Bjjg2 | 6.3 | 3.0 | 0.17 | 18 | 78 ± 0.3 | 1964± 28 | COL1027 |
| | 32-37 | Bjjf | 6.7 | 2.5 | 0.15 | 16 | 68 ± 0.3 | 3052± 29 | COL1028 |
| Centre | 0-14 | Oi | na | 23.0[c] | 0.52[c] | 45[c] | 113 ± 0.2 | modern | COL1050 |
| | 14-40 | Oe | 4.8[c] | 8.7[c] | 0.17[c] | 51[c] | 97 ± 0.3 | 228± 23 | COL1051 |
| | 40-43 | B | 5.9[c] | 4.2[c] | 0.12[c] | 35[c] | 96 ± 0.2 | 301± 23 | COL1052 |

[a] Cologne AMS laboratory number
[b] data from Höfle et al. (2013) (depth of Ajj set to zero in the paper)
[c] data from Höfle et al. (in review)
TOC – total organic carbon
na – not analysed

### 3.2 Distribution and $^{14}$C content of *n*-alkanes and *n*-fatty acids

#### 3.2.1 Distribution of *n*-alkanes and *n*-fatty acids

In both soil profiles, the *n*-alkane distribution ($C_{19}$ to $C_{33}$) shows a clear odd-over-even predominance with $C_{21}$ to $C_{33}$ being the dominant compounds (Table 3 and Höfle et al. 2013). In the polygon rim the highest total concentrations (17-20 µg.g$^{-1}$ DW) are found in the Ajj and Bjjg2 horizons (7-13 cm and 18-32 cm), while the uppermost organic horizon Oi (0-7 cm) contains minor amounts (5 µg.g$^{-1}$ DW). In contrast, the Oi and Oe horizons of the centre contain each relatively similar *n*-alkane concentrations (14-17 µg.g$^{-1}$ DW) which are significantly higher than the concentration in the B horizon (7 µg.g$^{-1}$ DW).

Besides different *n*-alkane concentrations, the rim and centre differ also in the dominated *n*-alkane compounds. In the rim soils the *n*-alkanes $C_{27}$ and $C_{29}$ dominate whereas in the centre $C_{27}$ clearly dominates alone. Noticeable are the highest concentration of the $C_{23}$ *n*-alkane in Oi and Oe horizons of the centre compared to all other soil horizons.

*n*-Fatty acid concentrations ($C_{14}$ to $C_{30}$) in the active layer of the polygon rim and centre are an order of magnitude higher than *n*-alkane concentrations and show an even-over-odd predominance (Table 4 and Höfle et al. 2013). In both soil profiles concentrations are highest in the Oi horizons (rim: 313 µg.g$^{-1}$ DW; centre: 361 µg.g$^{-1}$ DW). The concentrations in the polygon centre decrease with depth from 361 µg.g$^{-1}$ DW down to 106 µg.g$^{-1}$ DW. On the contrary, in the polygon rim no trend over depth is seen and total concentrations vary between 52 µg.g$^{-1}$ DW (Bjjg horizon) and 313 µg.g$^{-1}$ DW (Oi horizon). In both soil profiles the short chain *n*-fatty acids ($C_{14}$-$C_{19}$) are present in lower concentrations (17-135 µg.g$^{-1}$ DW) than the long-chain compounds ($C_{20}$-$C_{30}$; 35-220 µg.g$^{-1}$ DW) representing 19-41% of the total concentration. Nevertheless, in the upper rim horizons Oi, Ajj and Bjjg and in the centre Oi horizon the *n*-fatty acid $C_{16}$ dominates whereas the deeper horizons (rim: Bjjg2 and Bjjf; centre: Oe and B) have $C_{24}$ as the main compound.

Table 3: *n*-Alkane concentrations (µg.g$^{-1}$ DW) in the polygon rim and centre soil horizons on Samoylov Island

| Polygonal structure | Horizon | Depth (cm) | 19 | 20 | 21 | 22 | 23 | 24 | 25 | 26 | 27 | 28 | 29 | 30 | 31 | 32 | 33 | Total[b] | Σ $C_{19}$-$C_{20}$ | Σ $C_{21}$-$C_{33}$ | Σ $C_{27,29,31}$ |
|---|---|---|---|---|---|---|---|---|---|---|---|---|---|---|---|---|---|---|---|---|---|
| Rim[a] | Oi | 0-7 | bdl | 0.01 | 0.1 | 0.04 | 0.2 | 0.06 | 0.3 | 0.07 | 1.4 | 0.14 | 1.6 | 0.05 | 0.4 | 0.02 | 0.1 | 4.5 | 0.01 | 4.5 | 3.4 |
| | Ajj | 7-13 | 0.2 | 0.3 | 0.6 | 0.4 | 1.0 | 0.4 | 1.1 | 0.5 | 4.5 | 0.7 | 5.0 | 0.3 | 1.3 | 0.2 | 0.5 | 16.9 | 0.4 | 16.5 | 10.8 |
| | Bjjg | 13-18 | 0.1 | 0.2 | 0.5 | 0.3 | 0.9 | 0.4 | 1.0 | 0.5 | 3.6 | 0.6 | 4.2 | 0.3 | 1.2 | 0.2 | 0.4 | 14.2 | 0.3 | 14.0 | 9.1 |
| | Bjjg2 | 18-32 | 0.1 | 0.2 | 0.7 | 0.5 | 1.3 | 0.6 | 1.6 | 0.8 | 4.1 | 0.9 | 5.0 | 0.7 | 2.2 | 0.5 | 0.9 | 20.1 | 0.4 | 19.8 | 11.3 |
| | Bjjf | 32-37 | 0.1 | 0.2 | 0.5 | 0.4 | 0.9 | 0.4 | 1.1 | 0.5 | 2.1 | 0.5 | 2.2 | 0.3 | 1.5 | 0.2 | 0.5 | 11.5 | 0.3 | 11.2 | 5.9 |
| Centre | Oi | 0-14 | 0.1 | 0.1 | 1.1 | 0.3 | 2.5 | 0.2 | 1.5 | 0.3 | 7.3 | 0.2 | 2.3 | 0.1 | 0.7 | 0.1 | 0.3 | 17.3 | 0.1 | 17.2 | 10.5 |
| | Oe | 14-40 | 0.1 | 0.1 | 1.0 | 0.3 | 2.3 | 0.3 | 1.4 | 0.3 | 3.6 | 0.3 | 1.8 | 0.2 | 1.3 | 0.2 | 0.3 | 13.6 | 0.3 | 13.3 | 6.7 |
| | B | 40-43 | 0.1 | 0.1 | 0.4 | 0.2 | 0.9 | 0.2 | 0.8 | 0.2 | 1.7 | 0.2 | 1.0 | 0.1 | 0.9 | 0.1 | 0.2 | 7.1 | 0.2 | 6.9 | 3.6 |

[a] Data from Höfle et al., 2013 (depth of Ajj was set to zero)
[b] Differences to sum of individual concentrations due to rounding of individual concentrations
bdl – below detection limit

Table 4: *n*-Fatty acid concentrations (µg.g$^{-1}$ DW) in the polygon rim and centre soil horizons on Samoylov Island

| Polygonal structure | Horizon | Depth (cm) | 14 | 15 | 16:1 | 16:0 | 17 | 18 | 19 | 20 | 21 | 22 | 23 | 24 | 25 | 26 | 27 | 28 | 29 | 30 | Total[b] | Σ $C_{14}$-$C_{19}$ | Σ $C_{20}$-$C_{30}$ | Σ $C_{24,26,28}$ |
|---|---|---|---|---|---|---|---|---|---|---|---|---|---|---|---|---|---|---|---|---|---|---|---|---|
| Rim[a] | Oi | 0-7 | 6 | 5 | 10 | 85 | 3 | 17 | 1 | 23 | 4 | 39 | 9 | 40 | 6 | 24 | 4 | 22 | 5 | 7 | 312 | 128 | 184 | 87 |
| | Ajj | 7-13 | 3 | 2 | 3 | 18 | 1 | 6 | 1 | 9 | 2 | 14 | 5 | 14 | 2 | 6 | 1 | 4 | 0.3 | 1 | 90 | 33 | 57 | 24 |
| | Bjjg | 13-18 | 1 | 1 | 1 | 10 | 1 | 3 | 0.3 | 5 | 1 | 8 | 3 | 9 | 1 | 4 | 1 | 2 | bdl | 1 | 52 | 17 | 35 | 15 |
| | Bjjg2 | 18-32 | 4 | 2 | 2 | 28 | 2 | 10 | 1 | 15 | 4 | 34 | 12 | 61 | 10 | 35 | 5 | 24 | 2 | 5 | 255 | 48 | 207 | 120 |
| | Bjjf | 32-37 | 3 | 2 | 2 | 19 | 1 | 6 | 1 | 10 | 3 | 23 | 10 | 42 | 7 | 24 | 3 | 16 | 1 | 4 | 178 | 34 | 144 | 82 |
| Centre | Oi | 0-14 | 11 | 12 | 12 | 78 | 6 | 14 | 2 | 30 | 4 | 40 | 10 | 56 | 6 | 29 | 3 | 41 | 1 | 1 | 361 | 135 | 220 | 126 |
| | Oe | 14-40 | 3 | 3 | 2 | 28 | 2 | 8 | 1 | 18 | 3 | 26 | 7 | 37 | 3 | 16 | 1 | 15 | bdl | 2 | 179 | 48 | 128 | 68 |
| | B | 40-43 | 3 | 2 | 2 | 20 | 1 | 6 | 1 | bdl | 2 | 14 | 4 | 22 | 2 | 11 | 1 | 10 | 0.2 | 1 | 106 | 36 | 68 | 44 |

[a] Data from Höfle et al., 2013 (depth of Ajj was set to zero)
[b] Differences to sum of individual concentrations due to rounding of individual concentrations
bdl – below detection limit

### 3.2.2 $^{14}C$ contents of individual *n*-alkanes and *n*-fatty acids

The $^{14}C$-AMS measurements require a minimum of carbon amount (>20 µg C). Therefore, only *n*-alkanes and *n*-fatty acids present in high concentrations in our samples were used for the compound-specific radiocarbon analysis. We used the *n*-alkanes $C_{23}$ and $C_{27}$ and the *n*-fatty acids $C_{16}$, $C_{24}$, $C_{26}$, and $C_{28}$. The $^{14}C$ contents of the isolated *n*-alkanes and *n*-fatty acids are, with the exception of the $C_{27}$ *n*-alkane from the rim Bjjf horizon, higher or similar than the bulk OC from which they were isolated (Table 5). In each of the two centre soil horizons the investigated $^{14}C$ concentrations of the individual *n*-alkanes and *n*-fatty acids are within the process blank and one sigma measurement uncertainties of each other. The bigger errors of the $^{14}C$ values of the two *n*-fatty acids $C_{26}$ and $C_{28}$ in the B horizon of the polygon centre are correlated with the smallest amounts of the isolated, single lipids (23-33 µgC) compared to the other $^{14}C$ measured lipids (Table 5).

In the polygon rim the *n*-fatty acid $C_{16}$ has the highest $^{14}C$ concentrations in both horizons (Ajj and Bjjf) compared to the other *n*-alkane and *n*-fatty acid lipids. Furthermore, the *n*-fatty acids $C_{24}$, $C_{26}$ and $C_{28}$ and the *n*-alkane $C_{27}$ of the rim Ajj horizon are similar to each other. In the rim Bjjf horizon only the *n*-fatty acids $C_{24}$ and $C_{26}$ are similar to each other whereas the *n*-alkane $C_{27}$ has a significantly lower $^{14}C$ content (Table 5).

Further *n*-alkanes ($C_{23}$ of the rim Bjjg and Bjjf horizons; $C_{23}$ and $C_{27}$ of the centre B horizon) or *n*-fatty acids ($C_{28}$ of the rim Bjjg horizon; $C_{26}$ and $C_{28}$ of the centre Oi horizon; $C_{16}$ of the centre B horizon) could not be compound-specific $^{14}C$ analysed. This was due to too small amounts of the compounds (<23 µgC) or because they could not be separated chromatographic well enough on the preparative GC so that the isolated compounds had high contaminations.

Table 5: Compound-specific $^{14}C$ contents (pMC) of isolated lipids with process blank and measurement (one sigma) uncertainty. $^{14}C$ contents of particular organic matter (POM) fractions only with one sigma uncertainty.

| Structure | Horizon | Compound class | Carbon number | Carbon amount isolated (µg C) | Carbon amount used (µg C)[a] | $^{14}C$ content (pMC) | Sample ID[b] |
|---|---|---|---|---|---|---|---|
| Rim | Ajj | *n*-alkane | C23 | | | na | |
| | | | C27 | 86 | 33 | 95.2 ± 3.6c[c] | 55860 |
| | | *n*-fatty acid | C16 | 101 | 44 | 103.8 ± 2.6 | 57256 |
| | | | C24 | 262 | 18 | 94.2 ± 1.7 | 57257 |
| | | | C26 | 235 | 47 | 93.3 ± 1.3 | 57258 |
| | | | C28 | 177 | 14 | 95.5 ± 1.7 | 57270 |
| | | PLFA | Ci+a15:0 | 147 | 42 | 111.2 ± 4.3 | 43370 |
| | | | C16:1 | 205 | 43 | 110.7 ± 2.1 | 43371 |
| | | | C16:0 | 183 | | 107.3 ± 2.2 | 43372 |
| | | | C18:1 | | | na | |
| | | fPOM | | | | 102 + 0.4[d] | COL1352 |
| | | $oPOM_{>20µm}$ | | | | 99 + 0.4[d] | COL1356 |
| | | $oPOM_{<20µm}$ | | | | 95 + 0.4[d] | COL1360 |
| | Bjjf | *n*-alkane | C23 | | | na | |
| | | | C27 | 54 | 37 | 63.2 ± 3.2 | 55859 |
| | | *n*-fatty acid | C16 | 69 | 60 | 79.3 ± 2.1 | 57265 |
| | | | C24 | 286 | 21 | 75.1 ± 1.2 | 57263 |
| | | | C26 | 206 | 25 | 73.2 ± 1.2 | 57269 |
| | | | C28 | | | na | |
| | | PLFA | Ci+a15:0 | 172 | 42 | 85.7 ± 1.6 | 43364 |
| | | | C16:1 | 160 | 39 | 92.5 ± 1.9 | 43365 |
| | | | C16:0 | 178 | 44 | 89.0 ± 1.7 | 43368 |
| | | | C18:1 | 71 | 39 | 94.6 ± 3.2 | 43369 |
| | | fPOM | | | | 86 + 0.3 [d] | COL1355 |
| | | $oPOM_{>20µm}$ | | | | 68 + 0.3[d] | COL1359 |
| | | $oPOM_{<20µm}$ | | | | 70 + 0.3 [d] | COL1363 |
| Centre | Oi | *n*-alkane | C23 | 131 | 31 | 118.4 ± 3.4 | 55857 |
| | | | C27 | 51 | 36 | 121.3 ± 8.0 | 55858 |
| | | *n*-fatty acid | C16 | 116 | 44 | 119.0 ± 2.8 | 57259 |
| | | | C24 | 107 | 36 | 122.6 ± 3.1 | 57266 |
| | | | C26 | | | na | |
| | | | C28 | | | na | |
| | | PLFA | Ci+a15:0 | | | na | |
| | | | C16:1 | 81 | 32 | 120.7 ± 4.0[c] | 55863 |
| | | | C16:0 | 128 | 32 | 116.1 ± 2.7 | 55861 |
| | | | C18:1 | 284 | 12 | 114.7 ± 2.3[c] | 55866 |
| | B | *n*-alkane | C23 | | | na | |
| | | | C27 | | | na | |
| | | *n*-fatty acid | C16 | | | na | |
| | | | C24 | 121 | 39 | 100.4 ± 2.2 | 57264 |
| | | | C26 | 23 | 23 | 112.7 ± 14.3 | 57262 |
| | | | C28 | 33 | 33 | 108.0 ± 8.1 | 57560 |
| | | PLFA | Ci+a15:0 | | | na | |
| | | | C16:1 | 77 | 34 | 104.3 ± 3.3[c] | 55865 |
| | | | C16:0 | 91 | 30 | 104.1 ± 3.0[c] | 55862 |
| | | | C18:1 | 117 | 23 | 106.4 ± 2.7[c] | 55864 |

[a] amount C (µg) sent to ETH Zurich, Switzerland, and used for AMS $^{14}C$ measurement
[b] ETH Zurich laboratory number or Cologne AMS laboratory number (COL)
[c] purity of isolated compound only 94-95 %
[d] data from Höfle et al., 2013 (depth of Ajj set to zero in the paper)
na – not analysed
fPOM – free particular organic matter
oPOM – occluded particular organic matter

## 3.3 Microbial PLFAs

### 3.3.1 PLFA concentrations, calculated bacterial cell contents and fungal:bacterial ratio

The total concentrations of PLFAs range between 158 nmol.g$^{-1}$ DW and 862 nmol.g$^{-1}$ DW in the active layers of the polygon rim and centre and the still frozen permafrost top layer of the polygon rim (Table 6). Concentrations increase with depth in the soil horizons Ajj, Bjjg, and Bjjg2 of the active layer of the polygon rim (from 158 to 654 nmol.g$^{-1}$ DW) and decrease slightly in the permafrost top layer (Bjjf horizon: 549 nmol.g$^{-1}$ DW). In contrast, in the centre PLFA concentrations are highest in the Oi horizon (862 nmol.g$^{-1}$ DW) and decrease significantly to similar contents in the deeper Oe and B horizons (160 nmol.g$^{-1}$ DW and 167 nmol.g$^{-1}$ DW, respectively). The PLFA $C_{16:0}$ dominates the soil horizons Ajj, Bjjg2 and Bjjf and PLFA $C_{24:0}$ dominates the Bjjg horizon of the polygon rim. The polygon centre horizons show a greater variance in the dominate PLFAs: $C_{18:1\omega7c}$ in the horizon Oi; $C_{16:0}$, $C_{a15:0}$, and $C_{16:1\omega7c}$ in the Oe horizon; and $C_{22:2\omega6,9c\ in}$ the B horizon. However, our results need to be verified and then methanotrophic bacterial PLFAs will also be identified and qualified.

The higher PLFA concentrations in the polygon rim occur in the soil horizons with slightly higher pH values. Unfortunately, due to material limitation it was not possible to determine the pH values of the Oi horizon of the polygon centre which has the highest measured PLFA concentration of all investigated horizons. Other bulk soil parameters as C/N ratio or TOC show no clear trends with the PLFA concentration, except the highest measured PLFA concentration of 864 nmol.g$^{-1}$ DW in the centre Oi horizon is associated with the highest TOC value of 23.0% of all horizons.

Bacterial PLFA biomarker concentrations vary between 59 nmol.g$^{-1}$ DW and 485 nmol.g$^{-1}$ DW in the polygon rim and centre soil horizons comprising 35-56% of the total PLFA content (Table 6). The concentration trends of the bacterial biomarkers over soil depth are identical to the trends of the total PLFA concentrations; except in the sandy horizon Bjjg which has similar bacterial PLFA concentrations than the upper Ajj horizon. In the polygon rim Gram-negative PLFA biomarkers $C_{18:1\omega7c}$ and $C_{16:1\omega7c}$ dominate the soil horizons Ajj and Bjjg, respectively whereas the Gram-positive biomarker $C_{a15:0}$ dominates the deeper horizons Bjjg2 and Bjjf. The Gram-negative biomarker $C_{18:1\omega7c}$ dominates the upper Oi horizon of the polygon centre,–however in the deeper horizons Oe and B the Gram-positive and Gram-negative biomarkers $C_{a15:0}$ and $C_{16:1\omega7c,}$ respectively dominate.

Table 6: Phospholipid fatty acids (PLFA in nmol.g$^{-1}$ DW) concentrations in the active layer of the polygon rim and centre on Samoylov Island and their biomarker function with supporting references and calculated bacterial cell contents (cell.g$^{-1}$ DW) and fungal:bacterial ratios

| PLFAs | Polygon rim | | | | | Polygon centre | | | Biomarker | Reference |
|---|---|---|---|---|---|---|---|---|---|---|
| | Oi | Ajj | Bjjg | Bjjg2 | Bjjf | Oi | Oe | B | | |
| 13:0 | na | bdl | bdl | bdl | bdl | 2 | bdl | bdl | | |
| i14:0 | na | 2 | 1 | 6 | 6 | 1 | 0.3 | 0.1 | Gram+ | Zelles, 1997 |
| 14:00 | na | 2 | 6 | 16 | 16 | 26 | 6 | 5 | | |
| i15:0 | na | 12 | 17 | 64 | 55 | 77 | 16 | 11 | Gram+ | Zelles, 1997 |
| a15:0 | na | 14 | | 73 | 65 | 111 | 23 | 15 | Gram+ | Zelles, 1997 |
| 15:00 | na | 1 | 3 | 9 | 7 | 16 | 3 | 3 | | |
| i16:0 | na | 2 | 3 | 9 | 8 | 21 | 4 | 3 | Gram+ | Zelles, 1997 |
| a16:0 | na | 1 | 1 | 2 | 1 | 1 | bdl | bdl | Gram+ | Zelles, 1997 |
| 2OH 12:0 | na | bdl | bdl | 1 | 1 | 3 | 1 | 0.3 | | |
| 16:00 | na | 24 | 38 | 118 | 97 | 118 | 23 | 20 | | |
| 16:1ω9t | na | 3 | 1 | 3 | 1 | 3 | bdl | bdl | | |
| 16:1ω7t | na | 3 | 12 | 12 | 15 | 34 | 14 | 18 | | |
| 10Me-16:0 | na | bdl | 5 | 15 | 24 | 16 | 4 | 4 | | |
| 16:1ω7c | na | 19 | 19 | 68 | 54 | 121 | 23 | 18 | Gram- | Zelles, 1999 |
| 16:1ω5c | na | bdl | bdl | bdl | 4 | 11 | bdl | bdl | AM fungi | Olsson et al., 1995 |
| i17:0 | na | 10 | 7 | 12 | 16 | 13 | 3 | 2 | Gram+ | Zelles, 1997 |
| a17:0 | na | 2 | 2 | 7 | 6 | 11 | 2 | 2 | Gram+ | Zelles, 1997 |
| 17:00 | na | 1 | 1 | 4 | 2 | 3 | 0.2 | 0.2 | | |
| 10Me-17:0 | na | 1 | bdl | bdl | bdl | 6 | bdl | bdl | AC | Zelles, 1999 |
| 17:1ω7c | na | 4 | 5 | 17 | 22 | 14 | 2 | 2 | | |
| 2OH-14:0 | na | 0.5 | bdl | bdl | bdl | bdl | bdl | bdl | | |
| 18:00 | na | bdl | 5 | 13 | 9 | 16 | 2 | 3 | | |
| 18:1ω9t | na | 1 | bdl | bdl | bdl | bdl | bdl | 0.3 | | |
| 10Me-18:0 | na | 16 | bdl | 4 | 3 | 4 | 1 | 1 | AC | Vestal and White, 1989 |
| 18:1ω9c | na | bdl | 5 | 11 | 8 | 26 | 4 | 4 | fungi | Vestal and White, 1989 |
| 18:1ω7c | na | 23 | 18 | 34 | 13 | 127 | 8 | 7 | Gram- | Zelles, 1999 |
| 18:2ω6,9c | na | 5 | 2 | 3 | 2 | 2 | 1 | 0.4 | fungi | Vestal and White, 1989 |
| 18:3ω6,9,12c | na | 1 | 2 | 4 | 3 | bdl | bdl | 0.3 | | |
| 18:3ω3,6,9c | na | 2 | bdl | bdl | bdl | 4 | bdl | bdl | | |
| 20:00 | na | bdl | 2 | 8 | bdl | bdl | bdl | bdl | | |
| 22:00 | na | bdl | 3 | bdl | 6 | bdl | bdl | bdl | | |
| 22:2ω6,9c | na | 8 | 21 | 36 | 27 | 76 | 22 | 46 | | |
| 24:00:00 | na | bdl | 58 | 107 | 78 | bdl | bdl | bdl | | |
| Total | na | 158 | 253 | 654 | 549 | 862 | 160 | 167 | | |
| Sum bacterial biomarker | na | 87 | 86 | 273 | 225 | 485 | 79 | 59 | | |
| Bacterial cell content[a] ($10^9$ cell.g$^{-1}$ DW) | na | 6.0 | 6.1 | 20 | 16 | 35 | 5.6 | 4.2 | | |
| Fungal:bacterial ratio[b] | na | 0.06 | 0.02 | 0.01 | 0.01 | 0.005 | 0.01 | 0.01 | | |

na – not analysed
bdl – below detection limit
Gram+ – Gram positive bacteria
Gram- – Gram negative bacteria
AM fungi – arbuscular mycorrhizal fungi
AC – actinomycetes
[a] – Calculations based on the sum of bacterial biomarker PLFAs and the conversion factor $1.40*10^{-17}$ mol bacterial PLFA.cell$^{-1}$ (Frostegard and Bååth, 1996)
[b] – Fungal PLFA 18:2ω6,9c relative to the sum of bacterial biomarker PLFAs (based on Frostegard and Bååth, 1996)

The calculated bacterial cell content based on the bacterial PLFA biomarker concentrations vary between $4.2*10^9$ cell.g DW$^{-1}$ and $35*10^9$ cell.g DW$^{-1}$ and show

identical trend with depth as the total PLFA concentration and the bacterial PLFA biomarker content (Table 6).

The two fungal PLFAs $C_{18:1\omega9c}$ and $C_{18:2\omega6,9c}$ decrease with soil depth in the polygon centre from 26 nmol.g$^{-1}$ DW to 4 nmol.g$^{-1}$ DW and 2 nmol.g$^{-1}$ DW to 0.4 nmol.g$^{-1}$ DW, respectively. In the polygon rim the two PLFAs show different trends over depth. PLFA 18:1ω9c shows a bimodal pattern of increasing and decreasing concentrations with depth (between 5 and 11 nmol.g$^{-1}$ DW) whereas 18:2ω6,9c maximises in the upper Ajj horizon (5 nmol.g$^{-1}$ DW) and decreases with soil depth to an almost constant concentration of 2-3 nmol.g$^{-1}$ DW in the deeper horizons Bjjg, Bjjg2 and Bjjf (Table 6). The fungal to bacterial PLFA ratio decreases from 0.06 to 0.01 with soil depth in the polygon rim whereas the ratio varies little (0.005-0.01) with depth in the different soil horizons of the polygon centre (Table 6).

### 3.3.2 $^{14}$C contents of microbial PLFAs

Because of size-requirements of the $^{14}$C AMS measurements only PLFAs present in high concentrations in our soil samples were used for compound-specific $^{14}$C-analysis. Four single or group of PLFAs were isolated: $C_{i15:0}$ plus $C_{i15:0}$ characteristic for Gram-positive bacteria, $C_{16:0}$ universal PLFA as it occurs in membranes of all organisms, the group of $C_{16:1}$ a mixture of Gram-negative bacterial, AM fungal and unknown source, and the group of $C_{18:1}$ a mixture of Gram-negative bacterial, fungal, and unknown source. $C_{i15:0}$ plus $C_{i15:0}$ had to be pooled for $^{14}$C analysed due to low concentrations of the single compounds. $C_{16:1}$, and $C_{18:1}$ were also pooled for $^{14}$C measurements due to low concentrations of individual compounds and because of no possible further chromatographic separation on the preparative GC.

In each of the four soil horizons the PLFAs have $^{14}$C contents similar to each other and are within the process and measurement uncertainties of each other (Table 5). In the rim Ajj horizon and the centre Oi horizon the PLFA have higher $^{14}$C contents than the northern atmosphere at the time of sampling (2010: 105.0 pMC, Levin et al., 2013). However, the PLFA $^{14}$C contents in the Ajj horizon (107-111 pMC) are much higher that the corresponding bulk $^{14}$C content (90 pMC) whereas in the Oi horizon the bulk $^{14}$C content (113 pMC) is also higher than the atmosphere value and similar to the PLFA $^{14}$C contents (114-120 pMC). In the deeper soil horizons of the polygon rim (Bjjf) and the centre (B) the PLFA $^{14}$C contents are lower (86-95 pMC and 104-109 pMC, respectively) compared to those of the corresponding upper horizons. The $^{14}$C concentrations of the PLFAs are in each horizon higher than the bulk OC from which they originate. However, the difference between the $^{14}$C content of the bulk OC and the PLFAs is much higher in the rim Bjjf horizon than in the centre B horizon.

Several preparative GC isolated PLFAs ($C_{18:1}$ of the rim Bjjg horizon; $C_{i+a15:0}$ of the centre horizons Oi and B) could not be $^{14}$C measured due too high contaminations.

## 4. Discussion

Organic matter composition is characterised by the distribution and the $^{14}C$ ages of the lipid biomarkers *n*-alkanes and *n*-fatty acids (section 4.1). Possible carbon sources of the microbial communities and the bioavailability of the soil OC (section 4.2.2) can be identified by the $^{14}C$ content of microbial PLFA biomarkers in comparison with the $^{14}C$ contents of the atmosphere, bulk OC, *n*-alkane and *n*-fatty acid biomarkers, and particular organic matter (POM). $^{14}C$ data of the POM fraction is only exemplary for the polygon rim available as the centre consists mainly of undecomposed plant material which was not possible to fractioned. Prior the selection of the PLFAs for $^{14}C$ analysis an analysis of the PLFA composition in the soils is necessary (4.2.1).

### 4.1 Organic matter composition

The soil organic matter of the two cryogenic structures investigated - the polygon rim and centre - is composed of little-decomposed plant-derived material as the higher C/N ratios and the dominance of long-chain *n*-alkanes (>$C_{20}$) and *n*-fatty acids (>$C_{20}$), characteristic for higher terrestrial plant waxes (Kögel-Knabner and Amelung, 2014), indicate (Table 2, Table 3, Table 4, and Höfle et al., 2013). However, higher TOC contents and TOC/N ratios in the polygon centre compared to the rim suggest that the organic matter in the water saturated centre is even less decomposed compared to the rim organic matter.

#### 4.1.1 The polygon centre

The organic matter composition in the active layer is reflecting predominantly plant-derived input. The *n*-alkane composition of the polygon centre is dominated by the compounds $C_{23}$, $C_{27}$, and $C_{29}$ (Table 3) indicating a plant origin as plant-wax lipid biomarker studies of modern Siberian plants (Zech et al., 2010) and European and Russian peats have shown (e.g. Ficken et al., 1998; Pancost et al., 2002; Andersson et al., 2011). Thereafter and taken the recent vegetation into account (Boike et al., 2013), $C_{27}$ could have derived from sedges (Ficken et al., 1998) whereas $C_{29}$ could derive also from sedges (Zech et al., 2010) but also from mosses (Ficken et al., 1998). Additionally, the compound $C_{23}$, the second most abundance *n*-alkane in the upper horizons Oi and Oe, could have derived from submerging and floating plant species of the water saturated polygon centre which can maximise in $C_{23}$ and/or $C_{25}$ (Matsumoto et al., 1995; Ficken et al., 2000).

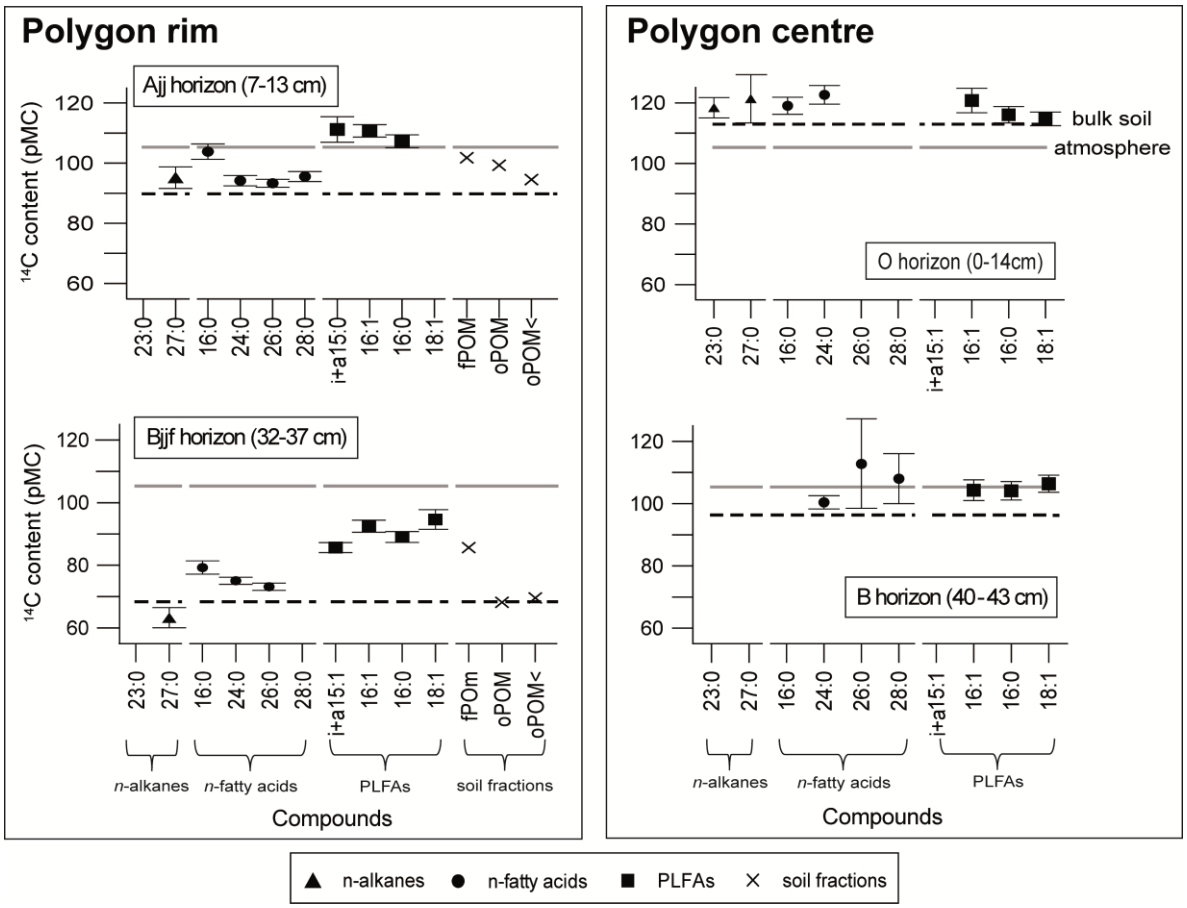


Fig. 2: $^{14}C$ contents of isolated lipid biomarkers (*n*-alkanes, *n*-fatty acids, and phospholipid fatty acids - PLFAs) and selected soil fractions (free particular organic matter – fPOM, occluded particular organic matter > 20µm – oPOM, occluded particular organic matter < 20µm – oPOM<). Error bars represent process blank and AMS measurement (one sigma) uncertainties. Data of the soil fractions are from Höfle et al., 2013.

*n*-Fatty acid compositions are less frequently used for source assessment as $C_{16}$ and $C_{18}$ compounds occur in plants as well as in bacteria and fungi (Amelung et al., 2008). In our polygon centre the universal *n*-fatty acid $C_{16}$ dominates in the upper Oi horizon and the plant-derived $C_{24}$ dominates in the deeper soil horizons Oe and B. This suggests that the soil organic matter derives mainly from plants, as the *n*-alkane compositions also show, plus a small contribution of the soil microbial community. Furthermore, the total *n*-fatty acid concentrations ($C_{14}$-$C_{30}$) and total *n*-alkane concentrations ($C_{19}$-$C_{33}$) decrease both strongly with depth in the polygon centre (Table 3 and 4) indicating degradation of the organic material with increasing soil depth.

The $^{14}C$ age of the bulk OC in the polygon centre increases only little with soil depth (from modern to 300 yrs BP at 40-43 cm depth) which could indicate plant introduced modern atmospheric carbon released by the plant roots. The little-decomposed organic matter of the polygon centre seems labile as in each soil horizon the plant-derived long-chain lipids (*n*-alkanes and *n*-fatty acids) contain more $^{14}C$ than the bulk OC from which they were isolated (Fig. 2). Furthermore, the organic matter of the upper Oi horizon is most likely composed of plant material grown in the last 50 years indicated by the bomb-$^{14}C$ elevated

concentrations of the bulk OC and the plant-derived *n*-alkanes ($C_{23}$ and $C_{27}$) and *n*-fatty acid ($C_{24}$). The plant-derived organic matter of the deeper B horizon is less enriched in bomb-$^{14}C$ indicated by the lower $^{14}C$ contents of the *n*-fatty acids ($C_{24}$, $C_{26}$, and $C_{28}$) compared to the plant-derived biomarkers of the upper Oi horizon. Summarized, the organic matter of the polygon centre is composed of plant-derived labile material as the dominance of $^{14}C$ young long-chain lipid biomarkers *n*-alkanes and *n*-fatty acids show.

### 4.1.2 The polygon rim

The organic matter of the polygon rim is also composed by plant-derived material which could have originated from various plant groups indicated by the dominance of $C_{27}$ and $C_{29}$ *n*-alkanes (Table 3 and Höfle et al., 2013). The recent vegetation differs between the dry polygon rim and the water saturated polygon centre (Boike et al., 2013) suggesting different plant sources for the lipid biomarkers of the polygon rim. $C_{27}$ could have derived from lichens (Zygadlo et al., 1993), segdes (Ficken et al., 1998), or small shrubs as *Betula spp.*, *Salix spp.*, and *Larix sibirica* (Zech et al., 2010). $C_{29}$ could have derived from mosses (Ficken et al., 1998), lichens (Zygadlo et al., 1993; Ficken et al., 1998) or sedges (Zech et al., 2010). In the rim soil horizon Bjjg2 the concentration of the *n*-alkane $C_{31}$ maximises indicating that additionally plant roots could have contributed to the *n*-alkane composition as observed in an European Russian peat site in the zone of discontinuous permafrost (Andersson et al., 2011). The universal *n*-fatty acid $C_{16}$ dominates in the upper rim horizons Oi, Ajj, and Bjjg whereas the plant-derived $C_{24}$ dominates in the deeper horizons Bjjg2 and Bjjf (Table 4). These results suggest, as discussed above for the polygon centre, that organic matter of the polygon rim is mainly composed from plant-derived material with a small contribution of microbial derived material.

Similarly to the high C/N ratios (around 18), the strong and nearly linear increasing apparent $^{14}C$ ages of the bulk OC with depth in the polygon rim (from modern to 3052 yrs BP at 32-37 cm depth) suggest slow decomposition rates in this cold environment, accumulation of ‘old’ carbon and little mixing by cryoturbation (Table 2 and Höfle et al., 2013). The high apparent $^{14}C$ age of 3052 yrs BP at 32-37 cm depth (Bjjf horizon) of the polygon rim is relative old compared to a previous study of a drilled core of a polygon centre on Samoylov (2306 yrs BP at 289 cm depth; Wagner et al., 2007). However, another study on a cliff of Samoylov Island showed similar $^{14}C$ ages (3130-3650 yrs BP between 0.8 and 5.6 m depth; Zimmermann, 2007). These different $^{14}C$ ages reveal the heterogeneity of these cryogenic influenced soils.

The total concentrations of *n*-alkanes and *n*-fatty acids show no increasing or decreasing trend with soil depth and its distribution has been discussed earlier by Höfle et al. (2013).

The dominating plant-derived lipid biomarkers (*n*-alkane $C_{27}$ and *n*-fatty acids $C_{24}$, $C_{26}$, and $C_{28}$) in the upper rim Ajj horizon have higher $^{14}C$ contents than the bulk OC suggesting organic matter composition of plant-derived labile material (Table 5 and Fig. 2). The lipids have lower $^{14}C$ contents than the free, mostly undecomposed (Golchin et al., 1994) particular organic matter (fPOM) but similar than the particular organic matter occluded in

soil aggregate (oPOM) which reflects more degraded plant tissue (Golchin et al., 1994). In the deeper Bjjf horizon the plant-derived *n*-fatty acids $C_{24}$ and $C_{26}$ compounds are older than those in the Ajj horizon but contain also more $^{14}C$ than the corresponding bulk OC and the oPOM. Furthermore, the $^{14}C$ content of the plant-derived *n*-alkane $C_{27}$ is lower than the $^{14}C$ content of the bulk OC, fPOM, and oPOM. These results indicate that *n*-alkanes may also be in permafrost soils a more stable component of the soil organic matter as a study of British peaty soils with higher $^{14}C$ ages of *n*-alkanes than the bulk OC suggested (Bol et al., 1996). These results indicate that the organic matter in the polygon rim is composed of various plant-derived pools in different stages of degradation as common seen in soils (reviewed in Kögel-Knabner and Amelung, 2014).

In summary, the soil OC of the polygon rim and centre is labile and mainly plant derived but contains also contributions of microbial origin. The *n*-fatty acid $C_{16}$ can derive from both microbial and plant sources (Kögel-Knabner and Amelung, 2014) and has in each of both rim horizons Ajj and Bjjf the highest $^{14}C$ content of all measured *n*-alkanes and *n*-fatty acids (Fig. 2). However, the difference to the $^{14}C$ content of the long-chain, only plant-derived *n*-fatty acids ($C_{24}$, $C_{26}$, $C_{28}$) is less in the deeper Bjjf horizon, where also the microbial input seems less as $C_{16}$ is not the dominate *n*-fatty acid anymore. For the centre such a comparison is not possible as the $C_{16}$ of the B horizon was not $^{14}C$ analysed due to contamination problems during the isolation process. These results of the polygon rim could indicate that the microbial input, which is less in the Bjjf horizon, is $^{14}C$ young as the $^{14}C$ concentration of the $C_{16}$ *n*-fatty acid of the Bjjf horizon is more similar to the plant-derived *n*-fatty acids $C_{24}$ and $C_{26}$. Nevertheless, PLFAs are better microbial biomarkers which have also been $^{14}C$ analysed and are discussed in the following section.

## 4.2 Substrate utilization and bioavailability of the organic matter

### 4.2.1 Microbial soil community

The living microbial communities of both cryogenic structures polygon rim and polygon centre are dominated by Gram-positive and Gram-negative bacteria as indicated by the dominance of their PLFA biomarkers. These results are consisted with an earlier PLFA-based study of the bacterial dominated microbial communities of the active layer on a similar polygon (rim and centre) on Samoylov Island (Wagner et al., 2005). However, as methanotrophic PLFAs were not determined we need to verify our results and then also identify and qualify methanotrophic biomarkers.

In the water saturated polygon centre the living microbial community is large in the upper Oi horizon indicated by the highest measured total PLFA concentrations (862 $nmol.g^{-1}$ DW). The PLFA concentration decreases with soil depth maybe indicating oxygen limitation with depth as Gram-negative biomarkers, representing more aerobic conditions (Bossio and Scow, 1998), decrease slightly more than Gram-positive biomarkers (Table 6). Wagner et al. (2005) determined also increasing PLFA concentrations with soil depth of a polygon centre on Samoylov. Furthermore, Liebner and Wagner (2007) and Liebner et al. (2008) found decreasing sizes of bacterial communities

with depth in polygon centres on Samoylov by bacterial cell counting. This is consistent with our PLFA-based calculated bacterial cell contents which also decrease with soil depth. However, our cell contents are in general slightly higher ($10^9$ cell.$g^{-1}$ DW) than the manual counted cell contents ($10^7$ – $10^8$ cell.$g^{-1}$ DW) from Liebner and Wagner (2007) and Liebner et al. (2008). It seems as our calculation overestimates the bacterial community which could be due to the use of a common conversion factor, which was developed without any permafrost or active layer soil sample (Frostegard and Bååth, 1996).

In the rim soil horizons Ajj, Bjjg, and Bjjg2 of the active layer the microbial biomarkers increase with depth suggesting a greater microbial community in deeper horizons. Liebner and Wagner (2007) and Liebner et al. (2008) found decreasing bacterial communities with soil depth in similar polygon rims on Samoylov by using bacterial cell counts. Nevertheless our results are similar to an earlier PLFA study on Samoylov by Wagner et al. (2005). Accordingly to the polygon centre, our calculated PLFA-based bacterial cell contents for the polygon rim are also higher compared to the direct cell counts for polygon rim soils of Liebner and Wagner (2007) and Liebner et al. (2008) probably due to an overestimation as discussed above.

The active layer is characterised in its thawed state by a great temperature gradient from the surface down to the permafrost interface ranging from 10°C to 0°C (Boike et al., 2013). One way for microorganisms to adapt to cold environmental temperatures is the regulation of their cell membrane fluidity by modifications of its lipid composition (Jansson and Tas, 2014). Two common mechanisms for this are the increasing proportion of anteiso-branched compared to iso-branched PLFAs (anteiso/iso ratio) and the increase of unsaturated to saturated PLFAs (unsaturated/saturated ratio) as anteiso and unsaturated

fatty acids have lower melting points than their iso and saturated analogues (Kaneda, 1991). Earlier studies on Samoylov have showed that the microbial communities have adapted to lower temperatures in permafrost-near soils (Liebner and Wagner, 2007; Mangelsdorf et al., 2009). In our active layer soil horizons Ajj, Bjjg, and Bjjg2 of the polygon rim the anteiso/iso ratio increases with depth (from 0.6 to 0.9 in 32 cm depth) and remains on a similar level in the still frozen permafrost top Bjjf horizon (0.8). In the polygon centre the anteiso/iso ratio, constant over soil depth (1.1), is greater than in the polygon rim and is almost identical to the mean ratio of 1.2 for a similar polygon (rim and centre) on Samoylov determined by Wagner et al. (2005). The unsaturated/saturated ratio decreases with soil depth in the polygon rim (from 0.6 to 0.2 in 37 cm depth) but increases with depth in the polygon centre (0.7 to 1.0 in 43 cm depth). Wagner et al. (2005) calculated higher unsaturated/saturated ratios (1.4-1.6) for a polygon (rim and centre) on Samoylov. These results indicate that the bacterial communities are heterogeneous on Samoylov but seem in general well adapted to the low temperatures.

The fungal to bacterial PLFA ratio decreases from 0.06 to 0.01 with soil depth in the polygon rim whereas the ratio varies little (0.005-0.01) with depth in the different soil horizons of the polygon centre (Table 6) indicating a higher fungal presence in the upper rim horizon Oi compared to the deeper rim and all three centre horizons.

### 4.2.2 Bioavailability of organic matter

Permafrost soils seem to emit carbon metabolised from a mixture of carbon pools with modern, atmospheric $^{14}C$ ages and older ages as shown by $^{14}C$ measurements of $CO_2$ emissions at Alaskan, Russian and Greenland sites (Schuur et al., 2009; Czimczik and Welker, 2010; Biasi et al., 2013; Hicks Pries et al., 2013). Additionally, Schuur et al. (2009) calculated that between 7% and 23% of the respired $CO_2$ was old carbon which increased in amount with increasing permafrost thaw. Incubation studies with permafrost soils also showed that with rising temperature a greater amount of carbon is decomposed (Neff and Hooper, 2002; Shaver et al., 2006; Biasi et al., 2008) including most likely older carbon (Biasi et al., 2005; Lavoie et al., 2011). However, it remains unclear how old the older carbon is and from which sources the carbon derives. The $^{14}C$ age of microbial membrane lipids (PLFAs) identifies which carbon sources are metabolised by the living microorganisms. One first study, to our knowledge, has determined the $^{14}C$ content of PLFAs from Arctic Alaskan organic rich soils and Canadian mineral soils. Ziolkowski et al. (2013) found smaller differences in the $^{14}C$ contents of the microbial PLFAs and the bulk OC in the organic rich soils compared to the mineral soils. The authors suggested that the microbes in the organic rich soils were interacting with the bulk OC whereas the microbes in the mineral soils were disconnected from the bulk OC. Our results also show a much smaller difference in the $^{14}C$ content of the microbial PLFAs and the bulk OC in both organic rich polygon centre horizons (Oi and B) compared to the two rim mineral horizons (Ajj and Bjjf; Fig. 2). This could also indicate that the microbes in the centre horizons are interacting with the bulk OC whereas the microbes in the rim horizons are disconnected from the bulk OC. Comparison of the $^{14}C$ contents of the microbial PLFA biomarkers with those of plant-derived soil fractions and biomarkers can be used to gain further information about the carbon sources microorganism metabolise.

In the upper Oi horizon of the polygon centre microorganisms seem to metabolise the freshest and presumably most labile material available indicated by the high $^{14}C$ contents of the microbial PLFAs ($C_{16:1}$, $C_{16:0}$, and $C_{18:1}$) which are similar or even slightly higher than the bulk soil OC (Fig. 2). It seems that the microorganisms utilize plant-derived material produced in the last 50 years as the $^{14}C$ contents of the microbial PLFA biomarkers are in the same range as the plant lipid biomarkers (*n*-alkanes $C_{23}$ and $C_{27}$; *n*-fatty acids $C_{24}$) containing elevated levels of bomb-$^{14}C$. In the deeper centre B horizon microorganism seem also to metabolise labile plant-derived organic material as the microbial PLFAs ($C_{16:1}$, $C_{16:0}$, and $C_{18:1}$) and the plant-derived *n*-fatty acids ($C_{24}$, $C_{26}$, and $C_{28}$) have $^{14}C$ contents similar to each other and higher than the bulk OC.

In the upper Ajj horizon of the polygon rim the microbial biomarker have only slightly higher $^{14}C$ contents (107-111 pMC) than the microbial PLFAs of the deeper centre B horizon (104-106 pMC) even though the bulk OC of the rim Ajj horizon has a significant higher $^{14}C$ age than the bulk OC of the centre B horizon (Fig. 2). Nevertheless, microorganisms in the rim Ajj horizon seem to metabolise also the freshest material available as the microbial PLFAs ($C_{i+a15:0}$, $C_{16:1}$, $C_{16:0}$, and $C_{18:1}$) have significantly higher $^{14}C$ contents than the corresponding bulk OC. However, the microbial PLFAs have even

higher $^{14}C$ values than the free particular organic matter (fPOM) fraction representing undecomposed and partly decomposed plant and root material (Golchin et al., 1994), the plant-derived lipid biomarkers (*n*-alkanes $C_{27}$ and *n*-fatty acids $C_{24}$, $C_{26}$, and $C_{28}$), and the atmospheric value. This suggests that microorganisms metabolise maybe plant-derived material but an additional carbon pool needs to be available for the microorganisms. This additional carbon pool needs to have a bomb-$^{14}C$ signature so that the microorganisms can have their high $^{14}C$ content (>107 pMC). It could be possible that the microorganisms utilize dissolved organic carbon (DOC) draining from the upper Oi horizon which has a bulk OC $^{14}C$ content of 115 pMC. An earlier study of permafrost soils from North-eastern Siberia showed that DOC contributed significantly to the $^{14}C$ content of the respired $CO_2$ (Dutta et al., 2006) meaning that DOC in active layer and permafrost soils can be bioavailable for microbial degradation making the microbial uptake of DOC-derived carbon in our soils very likely. However, to verify this suggestion $^{14}C$ analyses of soil DOC are necessary.

In the deeper, still frozen permafrost top part (Bjjf horizon) of the polygon rim bulk OC and microbial PLFA biomarkers ($C_{i+a15:0}$, $C_{16:1}$, $C_{16:0}$, and $C_{18:1}$) have the lowest $^{14}C$ contents of all four investigated horizons (Fig. 2). Again the microbial biomarkers show higher $^{14}C$ contents than the bulk OC and the plant-derived lipid biomarkers indicating a metabolism of 'younger', presumably more labile plant-derived OC by the microorganisms. It is most likely that the microorganisms utilize free, little degraded dead plant tissues as the labile fPOM fraction has a similar $^{14}C$ content than the PLFA biomarkers. Furthermore, an additional OC source for microbial metabolism could also be mobile DOC introducing carbon with higher $^{14}C$ contents into the deeper soil horizons as discussed above for the Ajj horizon. Additionally, the lower $^{14}C$ contents of the long-chain *n*-fatty acids ($C_{24}$ and $C_{26}$) compared to the microbial PLFAs suggest that *n*-fatty acids may represent a more degradation resistant plant-derived pool than the fPOM fraction and the carbon sources which microorganisms prefer to metabolise.

In summary, in each of the soil horizons the microbial PLFAs have higher $^{14}C$ concentrations compared to the corresponding bulk OC and higher or similar $^{14}C$ contents than the plant-derived *n*-alkanes and *n*-fatty acids biomarkers. These results suggest that mainly the freshest, presumably labile plant-derived material available is metabolised, while older carbon is not in favour of decomposition for these microorganisms. In contrast, ecosystem respiration measurements of permafrost soils determined increasing contributions of old carbon to the emitted $CO_2$ with increasing permafrost thaw (Schuur et al., 2009). Nevertheless, the old carbon contribution can be a mix signal of various carbon pools with different ages from different soil depths below the measured emissions as $^{14}C$ contents of heterotrophic respiration from incubated Alaskan soil samples of different depths suggest (Hicks Pries et al., 2013). Our results show that the potential plant-derived carbon sources for microbial decomposition are increasing in $^{14}C$ age with soil depth (Fig. 2) which could result in an old $^{14}C$ age of the surface $CO_2$ emission being a mixed signal of the different $^{14}C$ aged carbon emissions of all underlying soil horizons.

## 5. Conclusions

The organic matter of the polygon rim and centre consist mainly of labile plant-derived and little-decomposed material with small contributions of microbial origin indicated by the dominance of $^{14}C$ young long-chain *n*-alkanes and *n*-fatty acids and high C/N ratios. The rim organic matter seems more decomposed than the organic matter of the centre as indicated by lower C/N ratios of rim soils.

The microbial communities of the polygon rim and centre seem to metabolise the freshest, presumably most labile plant-derived organic material independent of the soil depth as indicated in each soil horizon by the higher $^{14}C$ contents of the microbial biomarkers compared to the bulk OC. Nevertheless, potential OC sources (plant-derived biomarkers and POM fractions) increase in age with soil depth similar to the corresponding bulk OC age of each horizon and also microbial PLFAs increase in age with soil depth. Therefore, microorganisms metabolise older carbon sources in greater soil depth but these sources are still the most labile OC pools available. Our results suggest that either more stable ('old') carbon pools are not in favour for the microbial decomposition or are not bioavailable or are degraded by microorganism other than (aerobic) soil bacteria which we mainly investigated. There are first evidences from an incubation study with permafrost soils that the microbial community will change with increasing temperature towards microorganisms which favour 'older', presumably more stable OC pools (Biasi et al., 2005). Further investigations are planned to identifying the carbon sources of changing microbial communities with warming in permafrost soils.

## Acknowledgements

The European Science Foundation (ESF) is acknowledged for providing a grant (MOLTER Research Networking Programme) to SH. This study was also funded by the German Ministry of Education and Research (BMBF) within the German-Russian joint project CarboPerm (grant 03G0836 to JR). S. Zubrzycki is thanked for his help with soil sampling and the Alfred-Wegener-Institute for Polar and Marine Research, Unit Potsdam for logistic support during the expedition "Lena-2010". We thank A. Cording, S. John, Sv. John, and B. Stapper for helping with sample preparation and J. Vermeulen for assistance with GC-MS measuring. For AMS measurements we thank S. Fahrni, S. Heinze, and L. Wacker.

# 7. Synthesis and overall discussion

The studies comprising this thesis aimed at gaining a better understanding of the OM composition and dynamics including stabilization mechanisms and bioavailability for microbial decomposition in active layer soils in the polygonal tundra of the Siberian Lena Delta. Arctic permafrost is most likely to be influenced by the ongoing global warming leading to longer thawing periods in summer resulting also in greater an active layer thickness. It is still under debate if and how much old OM, previously frozen and looked up, will be microbial decomposed (e.g. Davidson and Janssens, 2006; Schuur et al., 2013; Schädel et al., 2014). Therefore, a detailed knowledge of the today's processes within the OM dynamics is crucial in understanding and predicting how the soil OM will respond to the warming.

To ensure high precision and accuracy of compound-specific radiocarbon dating, one of the methods used in this thesis, intense pre-tests of dated GC standards (*n*-alkanes and *n*-fatty acids) isolated with the preparative GC were done. The tests revealed small contaminations of both, fossil and modern exogenous carbon introduced into the isolated compound during the GC isolation plus further sampling handling and combustion procedure prior to the $^{14}C$ measurement (process blank; manuscript I). Therefore, compound-specific radiocarbon analysis of individual lipid biomarkers as part of this thesis (manuscript IV) was possible.

## 7.1 Organic matter composition and its distribution in polygonal tundra soils

On Samoylov Island in the Lena Delta the OM composition in the active layer is reflecting the plant-derived input. Substantial differences between the soil OM composition of the two cryogenic structures polygon rim and centre were observed (manuscript II and IV). The OM $^{14}C$ age is very young throughout the whole active layer of the water-saturated polygon centre (0-43 cm depth: modern to 300 yrs BP) indicating that plant roots introduced modern carbon into deeper soil horizons. The TOC values (between 4-23%) of these active layer soils are typical for OM developed in wet, depressed polygon centres of this area (Liebner and Wagner, 2007; Zubrzycki et al., 2013). The OM is dominated by undecomposed material as high C/N ratios (35-51) indicate. OM originates mainly from higher plants as indicated by the dominance of long-chain lipid biomarkers ($C_{27}$ *n*-alkanes and $C_{24}$ *n*-fatty acids) which are major compounds of epicuticular waxes (Eglinton and Hamilton, 1967) and are frequently used as biomarkers for higher plant input to soils and aquatic sediments (e.g. Jambu et al., 1991; Huang et al., 2000). The plant-derived OM is composed of mainly young material as indicated by the higher $^{14}C$ contents of individual plant-derived lipid biomarkers from the Oi and B horizons compared to their corresponding bulk soil. The uppermost Oi horizon is dominated by the $C_{16}$ *n*-fatty acid, an universal lipid found in plants, bacteria, and fungi (Amelung et al., 2008) suggesting a higher microbial contribution to the OM here than in the deeper horizons Oe and B.

In contrast to the polygon centre, the $^{14}C$ age of the bulk OM of the polygon rim revealed significantly higher ages in the active layer (0-32 cm depth: modern to 1960 yrs BP) which

decrease further in the still frozen permafrost top layer (32-37cm depth: 3050 yrs BP). This suggests slow OM transformation in this cold environment and accumulation of 'old' material. The nearly linear age increase with depth suggests no significant mixing by cryoturbation, a common feature in permafrost soils (Jones et al., 2010). The rim OM is also dominated by little-decomposed, plant-derived material with high C/N ratios around 18 and a dominance of long-chain lipid biomarkers ($C_{27}$ and $C_{29}$ *n*-alkanes and $C_{24}$ *n*-fatty acids) with a minor contribution of microbial origin indicated by the dominance of $C_{16}$ *n*-fatty acid in the uppermost soil horizons Oi, Ajj and Bjjg. Furthermore, the plant material is also younger than the corresponding bulk soils shown by the higher $^{14}C$ contents of the plant-derived single lipid biomarkers of the soil horizons Ajj and Bjjf compared to the corresponding bulk soil. Generally, the high $^{14}C$ ages of the bulk soil and plant-derived lipids in the deeper rim soil horizons are considered to result from the accumulation of highly processed OM (Rumpel and Kögel-Knabner, 2011). Therefore, it is possible that the little-degraded and plant-derived OM in these horizons may be protected against biodegradation by stabilization mechanisms like the interactions with clay particles (organo-mineral associations) which increase in abundance in these deeper horizons or physical protection within soil aggregates.

Furthermore, the OM composition of two polygons (rim and centre) on Kurungnakh Island was studied, however only by TOC analyses and C/N ratios (manuscript III). Generally, the centre OM contains mostly little-decomposed material as indicated by the high TOC values (4-28%) and high C/N ratios (18-35) whereas the rim OM has slightly less TOC (4-23%) but is also composed of highly undecomposed material suggested by the high C/N ratios (16-69).

### 7.2 Stabilization mechanisms of the organic matter in polygonal tundra soils

In temperate soils physical stabilization as formation of soil aggregates and organo-mineral associations (reviewed in Sollins et al., 1996; Kögel-Knabner et al., 2008) seem of more importance for OM preservation than the chemical recalcitrance of the organic compounds (Marschner et al., 2008). On Samoylov Island soil aggregation seems to be of relevance only at greater depth in polygon rim soils (manuscript II). At greater depth plant-derived particular organic matter occluded in soil aggregates (oPOM) contains more TOC and has higher $^{14}C$ contents than the plant-derived free particular organic matter (fPOM) suggesting a preservation of the OM within soil aggregates. Nevertheless, soil aggregation seems less important in permafrost soils compared to temperate soils where the oPOM fractions made up 5% of the total soil mass but contained over 30% of the TOC (Mueller and Koegel-Knabner, 2009). In the soil horizons of the Samoylov polygon rim oPOM comprises only 1% of the total soil mass and contains only 8-16% of the TOC.

Organo-mineral associations seem to be of little importance in the active layer of permafrost soils on Samoylov. In temperate soils clay and fine silt fractions contain minerals with great surfaces which preserve OM over a long time by binding the OM strongly (Kögel-Knabner et al., 2008) resulting in a very old $^{14}C$ age compared to the more coarse sand fractions (von Lützow et al., 2007). In the active layer profile of the Samoylov

polygon rim most soil organic carbon is stored in the clay and fine silt fractions which is composed mainly of little-decomposed plant material indicated by the dominance of long-chain *n*-alkanes and *n*-fatty acids and low alkyl/O-alkyl C ratios. Regardless of the high TOC contents, the clay and fine silt fractions have younger or similar $^{14}C$ ages (higher $^{14}C$ contents) than the bulk soil suggesting little to non OM preservation via organo-mineral associations.

### 7.3 Microbial communities in polygonal tundra soils

The living microbial communities of a polygon rim and a polygon centre on Samoylov Island are dominated by Gram-positive and Gram-negative bacteria based on the analysis of the membrane phospholipid fatty acids (PLFAs; manuscript IV). A more detailed view of the bacterial community composition can be achieved by analysing bacteriohopanepolyols (BHPs) which are almost exclusively produced by bacteria (Ourisson and Albrecht, 1992). The investigations of one polygon (rim and centre) on Samoylov Island and two polygons (rim and centre) on Kurungnakh Island show that soil horizons differ in their BHP composition (manuscript III). The upper Oi horizons consist mainly of undecomposed plant material (manuscript II, III and IV) as discussed above (chapter 7.1) and have the highest structural diversity of BHPs including several highly functionalised composite BHPs almost exclusively present here. This suggests greater bacterial diversity in the Oi horizons compared to the deeper soil horizons. These results could indicate further that the highly functionalised BHPs are produced by yet unknown specialised bacteria species which are responsible for the decomposition of plant-derived organic matter. Furthermore, soil pH and temperature seem to have also an influence on the structural diversity which is higher at lower soil pH and at higher mean soil temperatures.

BHP biomarkers characteristic for different bacterial groups, such as methanotrophs, cyanobacteria, and soil-marker bacteria, are present in the investigated soil horizons. Type I methanotrophs seem to be the dominate amino-BHP source as the BHPs aminotetrol and aminopentol both occur in similar quantities in the soil, even though aminpentol is only produced by type I methanotrophs (Neunlist and Rohmer, 1985; Talbot et al., 2001; van Winden et al., 2012). Methanotrophic BHP biomarkers are almost exclusively present in the centre soils of the polygons. This is in contrast to Wagner et al. (2005) and Liebner and Wagner (2007) who found methanotrophs in rim and centre soil profiles suggesting that either the concentrations of the two BHPs were below the detection limit or these BHPS are rapidly oxidised under the more oxygenic conditions in the rims. Adenosylhopane and its related structures are considered as soil-marker BHPs because they occur in high abundances in soils (Cooke et al., 2008) and have been found in several $N_2$-fixing and purple non-sulphur bacteria (e.g. Bravo et al., 2001; Talbot et al., 2007). Soil-marker BHPs occur in significantly higher relative abundances in mineral soil horizons of the polygon rims compared to the rim organic horizons and all centre soil horizons. This suggests that soil-marker BHP producing bacteria prefer maybe soil horizons with lower carbon contents. Cyanobacterial BHP biomarkers are present at almost all depth of the soil profiles and not only in the top soils as Liebner et al (2008) and

Liebner (2007) determined for a similar polygon on Samoylov with 16S rRNA analysis. This could indicate that either the 16S rRNA analysis could not identify all cyanobacteria or that these BHPs are preserved at greater soil depth. Overall, the BHP data agree well with the 16S rRNA data of a polygon on Samoylov (Liebner, 2007; Liebner et al., 2008) suggesting that BHPs are promising biomarkers to represent bacterial communities in permafrost soils.

### 7.4 Microbial utilization of organic matter

The microorganisms seem to metabolise the freshest, presumably most labile material available independent of the soil horizon or polygon structure as the microbial membrane PLFA biomarkers have in each of the four soil horizons higher $^{14}C$ contents (lower $^{14}C$ ages) then the corresponding bulk OM (manuscript IV). Nevertheless, there are variations between the two polygon structures (rim and centre) and the soil horizons. In the Oi and B horizons of the polygon centre the differences between the $^{14}C$ contents of the microbial PLFAs and the bulk OM are small suggesting that the microbes seem to interact with the bulk material. In contrast, the differences between the $^{14}C$ contents of the PLFAs and the bulk soil are significant in the Ajj and Bjjf horizons of the polygon rim. This suggests that microbes are disconnected from the bulk OM as Ziolkowski et al. (2013) concluded from a study with Alaskan and Canadian permafrost soils also using compound-specific radiocarbon analysis of PLFAs.

In the polygon centre microorganisms seem to metabolise plant-derived material build up during the last 50 years as the $^{14}C$ contents of the microbial PLFAs are in the same range as the plant wax lipid biomarkers (*n*-alkanes $C_{23}$ and $C_{27}$ and *n*-fatty acid $C_{24}$) containing elevated levels of bomb-$^{14}C$. In the deeper B horizon microorganisms seem to utilize also labile plant-derived material as the PLFAs and the plant biomarker *n*-fatty acids ($C_{24}$, $C_{26}$, and $C_{28}$) have $^{14}C$ concentrations similar to each other and higher than the bulk OM.

In the upper Ajj horizon of the polygon rim an additional carbon source besides plant-derived material seems to be metabolised by the microorganisms as the $^{14}C$ contents of the microbial PLFAs are higher than the plant-derived fPOM fraction and lipids (*n*-alkane $C_{27}$; *n*-fatty acids $C_{24}$, $C_{26}$, and $C_{28}$). The additional carbon source needs to have a bomb-$^{14}C$ signature (> 100 pMC) so that the microbial PLFAs can have bomb-$^{14}C$ elevated contents (>107 pMC). It seems likely that downwards moving dissolved organic carbon (DOC) constitutes this additional source as the bulk OM of the uppermost Oi horizon has a $^{14}C$ content of 115 pMC. It was demonstrated by an earlier study of permafrost soils from North-Eastern Siberia that DOC contributes significantly to the $^{14}C$ content of the respired $CO_2$ (Dutta et al., 2006) meaning that DOC was bioavailable for microbial degradation. Therefore, microbial utilization of carbon from the DOC-fraction is also possible in the here investigated soils. Nevertheless, to verify this suggestion detailed analyses of the soil DOC are necessary.

In the deeper, still frozen rim permafrost top part (Bjjf horizon) microorganisms seem to metabolise the $^{14}C$ youngest, presumably most labile plant material as microbial PLFAs

have similar $^{14}C$ contents than the plant-derived fPOM fraction but significantly higher than the bulk soil. It can further be concluded that the fractions fPOM and long-chain *n*-fatty acids represent different plant remains as the $^{14}C$ content of the fPOM is significantly higher than the $^{14}C$ contents of the *n*-fatty acids ($C_{24}$ and $C_{26}$).

In summary, microorganisms in each of the investigated soil horizons seem to metabolise mainly the freshest, presumably most labile plant-derived material available as the microbial PLFAs have lower $^{14}C$ ages than the corresponding bulk OM. This suggests that 'old' carbon is not in favour for the microbial degradation. In contrast, ecosystem respiration measurements of permafrost soils have observed increasing contributions of old carbon to the emitted $CO_2$ with increasing permafrost thaw (Schuur et al., 2009; Nowinski et al., 2010). However, the emitted $CO_2$ is a mixed signal of all utilized carbon sources in the whole soil profile and $^{14}C$ measurements of heterotrophic respiration from incubated Alaskan soil samples showed that different soil depth emit different $^{14}C$ ages with the highest $^{14}C$ contents near the soil surface and decreasing contents with depth (Hicks Pries et al., 2013). The $^{14}C$ signatures of the microbially decomposed carbon sources (plant-derived fPOM and *n*-alkane and *n*-fatty acid lipids) increasing in $^{14}C$ age with depth whereby the emitted $CO_2$ is probably also a mixed signal containing younger $^{14}C$ from near soil surface horizons and significantly older $^{14}C$ from near or below permafrost table.

These results give insights into the today's conditions and processes with today's microbial community. However, there is first evidence from an incubation study that the microbial communities will change with increasing temperature towards microorganisms that favour 'older', presumably more stable carbon pools (Biasi et al., 2005). Therefore, it is likely that the on-going global warming introduces changes in the microbial communities in permafrost soils which will make also more stable carbon pools of the active layers bioavailable, in addition to the deeper buried labile (and stable) carbon released by permafrost thawing.

# 8. Summary, conclusions and future perspectives

## 8.1 Summary and conclusions

Permafrost soils contain about twice the amount of the current atmospheric carbon content and northern permafrost regions are predicted to be most strongly affected by the on-going global warming turning probably permafrost soils from carbon sinks into carbon sources for the atmosphere. Therefore, a detailed understanding of the carbon dynamics in permafrost soils including the bioavailability of organic carbon is crucial to generate reliable models for predicting future carbon fluxes. In this thesis bulk, molecular, and radiocarbon analyses of bulk OM and soil fractions and compound-specific radiocarbon analysis of individual plant-derived and microbial lipids have been used to characterise the OM composition, determine possible stabilization mechanisms and identify which carbon pools microorganisms metabolise in polygonal tundra soils of the Siberian Lena Delta. This study can serve as baseline to detect future changes in these permafrost soils.

The active layers of the two cryogenic structures, polygon rim and polygon centre, differ in their OM composition. Bulk OM of the polygon rims consist mainly of little-decomposed plant material with a relative high $^{14}C$ age whereas the polygon centre has younger, mostly undecomposed plant-derived bulk OM. Organo-mineral associations, which are suggested to be a key mechanisms in OM stabilization in temperate soils, seem of little importance in the active layer of the polygon rim indicated by the younger, mainly plant-derived clay and fine silt fractions compared to the bulk OM. Formation of soil aggregates, another important stabilization mechanisms in temperate soils, seems to be important only at greater soil depth in the polygon rim where particular organic matter (POM) occluded in aggregates is older than free POM which consist mainly of undecomposed plant debris. Therefore, it can be concluded that OM stabilization is mainly driven by the frozen-look up of the soils leading to little or none microbial activity, a key factor of OM degradation, and minor contributions of soil aggregation.

The Bjjf horizon of the polygon rim which was still frozen at the time of sampling is probably part of the transition layer between the annually thawing active layer and the deeper continuously frozen permafrost. The OM of this Bjjf horizon also consists of mainly young plant-derived material with little stabilization through soil aggregates. Therefore, it is most likely that with increase warming and active layer thickening the deeper buried labile OM will be included in the active carbon dynamics of permafrost soils. Furthermore, microorganisms seem to metabolise the most labile plant-derived OM available as indicated by the young $^{14}C$ ages of microbial lipids which are similar to the free POM but lower than the bulk OM regardless the age increase of all compounds (bulk soil, plant-derived material and microbial lipids) with soil depth. This pilot study shows that little OM stabilization by soil aggregates and almost non by organo-mineral associations is occurring in the active layer soils resulting in high bioavailablability of most OM once thawing has included the carbon today still frozen-looked up “back” into the active carbon cycle.

## 8.2 Future perspectives

Overall, it was demonstrated that compound-specific radiocarbon analyses and the radiocarbon analyses of soil fractions are powerful tools to investigate depth related OM dynamics for northern permafrost regions. However, further investigations on different Arctic sites are needed to broaden the conclusions of this thesis. Possible further locations should also include the southern continuous permafrost zone which will have even longer summers and greater active layer thicknesses than the Siberian Lena Delta and also within the zone of discontinuous permafrost which has sites where permafrost will most likely disappear completely with increased warming. Furthermore, the top part (several decimetres) of the still frozen permafrost should also be investigated as this part will be included in the annual thawing active layer as warming continues. By combining incubation studies and respiration measurements of the permafrost top part with bulk and compound-specific radiocarbon analysis it is most likely to identify which carbon pools are favoured by the (changed) microbial community and evaluate the size of these carbon pools.

Additionally, microorganisms seem to have another (minor) carbon source than plant-derived material in the active layer of permafrost soils. Soil pore water could transport young, presumably labile dissolved organic carbon (DOC) downwards within a soil profile resulting in an additional young carbon source for microbial metabolism (manuscript IV). Radiocarbon analysis of permafrost soil DOC could verify this hypothesis; microbial utilization of the DOC is most likely if the soil DOC has similar $^{14}C$ contents than the microbial lipids (PLFAs).

# 9. References of the chapters 1, 2, 6, and 7


Amelung, W., Brodowski, S., Sandhage-Hofmann, A., Bol, R., 2008. Chapter 6 Combining Biomarker with Stable Isotope Analyses for Assessing the Transformation and Turnover of Soil Organic Matter, In: Donald, L.S. (Ed.), Advances in Agronomy. Academic Press, pp. 155-250.

Andersson, R.A., Kuhry, P., Meyers, P., Zebühr, Y., Crill, P., Mörth, M., 2011. Impacts of paleohydrological changes on n-alkanes biomarker compositions of a Holocene peat sequence in the eastern European Russian Artic. Organic Geochemistry 42, 1065-1075.

Are, F., Reimnitz, E., 2000. An overview of the Lena River Delta setting: Geology, tectonics, geomorphology, and hydrology. Journal of Coastal Research 16, 1083-1093.

Bardgett, R.D., Richter, A., Bol, R., Garnett, M.H., Bäumler, R., Xu, X., Lopez-Capel, E., Manning, D.A.C., Hobbs, P.J., Hartley, I.R., Wanek, W., 2007. Heterotrophic microbial communities use ancient carbon following glacial retreat. Biology Letters 3, 487-490.

Biasi, C., Jokinen, S., Marushchak, M.E., Hämäläinen, K., Trubnikova, T., Oinonen, M., Martikainen, P.J., 2013. Microbial respiration in Arctic upland and peat soils as a source of atmospheric carbon dioxide. Ecosystems 17, 112-126.

Biasi, C., Meyer, H., Rusalimova, O., Hämmerle, R., Kaiser, C., Baranyi, C., Daims, H., Lashchinsky, N., Barsukov, P., Richter, A., 2008. Initial effects of experimental warming on carbon exchange rates, plant growth and microbial dynamics of a lichen-rich dwarf shrub tundra in Siberia. Plant and Soil 307, 191-205.

Biasi, C., Rusalimova, O., Meyer, H., Kaiser, C., Wanek, W., Barsukov, P., Junger, H., Richter, A., 2005. Temperature-dependent shift from labile to recalcitrant carbon sources of arctic heterotrophs. Rapid communications in mass spectrometry 19, 1401–1408.

Blagodatskaya, E., Kuzyakov, Y., 2013. Active microorganisms in soil: Critical review of estimation criteria and approaches. Soil Biology and Biochemistry 67, 192-211.

Bligh, E.G., Dyer, W.J., 1959. A rapid method of total lipid extraction and purification. Canadian Journal of Biochemistry and Physiology 37, 911-917.

Boike, J., Kattenstroth, B., Abramova, K., Bornemann, N., Chetverova, A., Fedorova, I., Fröb, K., Grigoriev, M., Grüber, M., Kutzbach, L., Langer, M., Minke, M., Muster, S., Piel, K., Pfeiffer, E.M., Stoof, G., Westermann, S., Wischnewski, K., Wille, C., Hubberten, H.W., 2013. Baseline characteristics of climate, permafrost and land cover from a new permafrost observatory in the Lena River Delta, Siberia (1998-2011). Biogeosciences 10, 2105-2128.

Bol, R., Huang, Y., Meridith, J.A., Eglinton, G., Harkness, D.D., Ineson, P., 1996. The 14C age and residence time of organic matter and its lipid constituents in a stagnohumic gley soil. European Journal of Soil Science 47, 215-222.

Bossio, D.A., Scow, K.M., 1998. Impacts of Carbon and Flooding on Soil Microbial Communities: Phospholipid Fatty Acid Profiles and Substrate Utilization Patterns. Microbial Ecology 35, 265-278.

Bravo, J.-M., Perzl, M., Härtner, T., Kannenberg, E.L., Rohmer, M., 2001. Novel methylated triterpenoids of the gammacerane series from the nitrogen-fixing bacterium *Bradyrhizobium japonicum* USDA 110. European Journal of Biochemistry 268, 1323-1331.

Ciais, P., Sabine, C., Bala, G., Bopp, L., Brovkin, V., Canadell, J., Chhabra, A., DeFries, R., Galloway, J., Heimann, M., Jones, C., Quéré, C.L., Myneni, R.B., Piao, S., Thornton, P., 2013. Carbon and Other Biogeochemical Cycles, In: Stocker, T.F., Qin, D., Plattner, G.-K., Tignor, M., Allen, S.K., Boschung, J., Nauels, A., Xia, Y., Bex, V., Midgley, P.M. (Eds.), Climate change 2013: The physical science basis. Contribution of working group I to the fifth assessment report of the intergovernmental panel on climate change. Cambridge University Press, Cambridge, United Kingdom and New York, NY, USA.

Collins, M., Knutti, R., Arblaster, J., Dufresne, J.-L., Fichefet, T., Friedlingstein, P., Gao, X., Gutowski, W.J., T. Johns, Krinner, G., Shongwe, M., Tebaldi, C., Weaver, A.J., Wehner, M., 2013. Long-term climate change: Projections, commitments and irreversibility, In: Stocker, T.F., Qin, D., Plattner, G.-K., Tignor, M., Allen, S.K., Boschung, J., Nauels, A., Xia, Y., Bex, V., Midgley, P.M. (Eds.), Climate change 2013: The physical science basis. Contribution of working group I to the fifth assessment report of the Intergovernmental Panel on Climate Change (IPCC). Cambridge University Press, Cambridge, United Kingdom and New York, NY, USA.

Cooke, M.P., Talbot, H.M., Farrimond, P., 2008. Bacterial populations recorded in bacteriohopanepolyol distributions in soils from Northern England. Organic Geochemistry 39, 1347-1358.

Czimczik, C.I., Welker, J.M., 2010. Radiocarbon Content of CO2 Respired from High Arctic Tundra in Northwest Greenland. Arctic Antarctic and Alpine Research 42, 342-350.

Davidson, E.A., Janssens, I.A., 2006. Temperature sensitivity of soil carbon decomposition and feedbacks to climate change. Nature 440, 165-173.

Dorrepaal, E., Toet, S., Logtestijn, R.S.P.v., Swart, E., Weg, M.J.v.d., Callaghan, T.V., Aerts, R., 2009. Carbon respiration from subsurface peat accelerated by climate warming in the subarctic. Nature 460, 616-619.

Dutta, K., Schuur, E.A.G., Neff, J.C., Zimov, S.A., 2006. Potential carbon release from permafrot soils of Northerstern Siberia. Global Change Biology 12, 2336-2351.

Eglinton, G., Hamilton, R.J., 1967. Leaf epicuticular waxes. Science 156, 1322-1335.

Eglinton, T.I., Aluwihare, L.I., Bauer, J.E., Druffel, E.R.M., McNichol, A.P., 1996. Gas Chromatographic Isolation of Individual Compounds from Complex Matrices for Radiocarbon Dating. Anal. Chem. 68, 904-912.

Euskirchen, E.S., McGuire, A.D., Kicklighter, D.W., Zhuang, Q., Clein, J.S., Dargaville, R.J., Dye, D.G., Kimball, J.S., McDonald, K.C., Melillo, J.M., Romanovsky, V.E., Smith, N.V., 2006. Importance of recent shifts in soil thermal dynamics on growing season length, productivity, and carbon sequestration in terrestrial high-latitude ecosystems. Global Change Biology 12, 731-750.

Ficken, K.J., Barber, K.E., Eglinton, G., 1998. Lipid biomarker, δ13C and plant macrofossil stratigraphy of a Scottish montane peat bog over the last two millennia. Organic Geochemistry 28, 217-237.

Ficken, K.J., Li, B., Swain, D.L., Eglinton, G., 2000. An n-alkane proxy for the sedimentary input of submerged/foating freshwater aquatic macrophytes. Organic Geochemistry 31, 745-749.

Fiedler, S., Wagner, D., Kutzbach, L., Pfeiffer, E.-M., 2004. Element redistribution along hydraulic and redox gradients of low-centered polygons, Lena Delta, Northern Siberia. Soil Sci. Soc. Am. J. 68, 1002-1011.

Frostegard, A., Bååth, E., 1996. The use of phospholipid fatty acid analysis to estimate bacterial and fungal biomass in soil. Biol Fertil Soils 22, 59-65.

Frostegard, A., Tunlid, A., Bååth, E., 2011. Use and misuse of PLFA measurements in soils. Soil Biology and Biochemistry 43, 1621-1625.

Golchin, A., Oades, J., Skjemstad, J., Clarke, P., 1994. Study of free and occluded particulate organic matter in soils by solid state $^{13}C$ CP/MAS NMR spectroscopy and scanning electron microscopy. Soil Research 32, 285-309.

Grigoriev, M.N., 1993. Criomorphogenesis in the Lena Delta. Permafrost Institute Press, Yakutsk.

Harden, J.W., Koven, C.D., Ping, C.-L., Hugelius, G., David McGuire, A., Camill, P., Jorgenson, T., Kuhry, P., Michaelson, G.J., O'Donnell, J.A., Schuur, E.A.G., Tarnocai, C., Johnson, K., Grosse, G., 2012. Field information links permafrost carbon to physical vulnerabilities of thawing. Geophysical Research Letters 39, L15704.

Harden, J.W., Mark, R.K., Sundquist, E.T., Stallard, R.F., 1992. Dynamics of Soil Carbon During Deglaciation of the Laurentide Ice Sheet. Science 258, 1921-1924.

Hartley, I.P., Garnett, M.H., Sommerkorn, M., Hopkins, D.W., Fletcher, B.J., Sloan, V.L., Phoenix, G.K., Wookey, P.A., 2012. A potential loss of carbon associated with greater plant growth in the European Arctic. Nature Clim. Change 2, 875-879.

Hicks Pries, C.E., Schuur, E.A.G., Crummer, K.G., 2013. Thawing permafrost increases old soil and autotrophic respiration in tundra: Partitioning ecosystem respiration using δ13C and ∆14C. Global Change Biology 19, 649-661.

Höfle, S., Kusch, S., Talbot, H.M., Mollenhauer, G., Zubrzycki, S., Burghardt, S., Rethemeyer, J., in review. Characterization of bacterial populations in Arctic permafrost soils using bacteriohopanepolyols. Org. Geochem.

Höfle, S., Rethemeyer, J., Mueller, C.W., John, S., 2013. Organic matter composition and stabilization in a polygonal tundra soil of the Lena Delta. Biogeosciences 10, 3145-3158.

Huang, Y.S., Dupont, L., Sarnthein, M., Hayes, J.M., Eglinton, G., 2000. Mapping of C4 plant input from North West Africa into North East Atlantic sediments. Geochemica et Cosmochimica Acta 64, 3505-3513.

Hugelius, G., Strauss, J., Zubrzycki, S., Harden, J.W., Schuur, E.A.G., Ping, C.L., Schirrmeister, L., Grosse, G., Michaelson, G.J., Koven, C.D., O'Donnell, J.A., Elberling, B., Mishra, U., Camill, P., Yu, Z., Palmtag, J., Kuhry, P., 2014. Estimated stocks of circumpolar permafrost carbon with quantified uncertainty ranges and identified data gaps. Biogeosciences 11, 6573-6593.

Hugelius, G., Tarnocai, C., Broll, G., Canadell, J.G., Kuhry, P., Swanson, D.K., 2013. The Northern Circumpolar Soil Carbon Database: spatially distributed datasets of soil coverage and soil carbon storage in the northern permafrost regions. Earth Syst. Sci. Data 5, 3-13.

IUSS Working Group WRB, 2006. World Reference Base for Soil Resources 2006. Erstes Update 2007. Deutsche Ausgabe. – Übersetzt von Peter Schad. Bundesanstalt für Geowissenschaften und Rohstoffe, Hannover.

Jambu, P., Amblès, A., Dinel, H., Secouet, B., 1991. Incorporation of natural hydrocarbons from plant residues into an hydromorphic humic podzol following afforestation and fertilization. Journal of Soil Science 42, 629-636.

Jansson, J.K., Tas, N., 2014. The microbial ecology of permafrost. Nat Rev Micro 12, 414-425.

Joergensen, R.G., Wichern, F., 2008. Quantitative assessment of the fungal contribution to microbial tissue in soil. Soil Biology and Biochemistry 40, 2977-2991.

Jones, A., Stolbovoy, V., Tarnocai, C., Broll, G., Spaargaren, O., Montanarella, L., 2010. Soil Atlas of the northern circumpolar region. European Commission, Publications Office of the European Union, Luxembourg.

Kaneda, T., 1991. Iso- and Anteiso-Fatty Acids in Bacteria: Biosynthesis, Function, and Taxonomic Significancet. Microbiological reviews 55, 288-302.

Khvorostyanov, D.V., Ciais, P., Krinner, G., Zimov, S.A., Corradi, C., Guggenberger, G., 2008. Vulnerability of permafrost carbon to global warming. Part II: sensitivity of permafrost carbon stock to global warming. Tellus 60B, 265–275.

Kirtman, B., Power, S.B., Adedoyin, J.A., Boer, G.J., Bojariu, R., Camilloni, I., Doblas-Reyes, F.J., Fiore, A.M., Kimoto, M., Meehl, G.A., Prather, M., Sarr, A., Schär, C., Sutton, R., Oldenborgh, G.J.v., Vecchi, G., H.J. Wang, 2013. Near-term Climate Change: Projections and Predictability, In: Stocker, T.F., Qin, D., Plattner, G.-K., Tignor, M., Allen, S.K., Boschung, J., Nauels, A., Xia, Y., Bex, V., Midgley, P.M. (Eds.), Climate Change 2013: The Physical Science Basis. Contribution of Working Group I to the Fifth Assessment Report of the Intergovernmental Panel on Climate Change. Cambridge University Press, Cambridge, United Kingdom and New York, NY, USA.

Kögel-Knabner, I., Amelung, W., 2014. Dynamics, Chemistry, and Preservation of Organic Matter in Soils, In: Holland, H.D., Turekian, K.K. (Eds.), Treatise on Geochemistry (Second Edition). Elsevier, Oxford, pp. 157-215.

Kögel-Knabner, I., Guggenberger, G., Kleber, M., Kandeler, E., Kalbitz, K., Scheu, S., Eusterhues, K., Leinweber, P., 2008. Organo-mineral associations in temperate soils: Integrating biology, mineralogy, and organic matter chemistry. Journal of Plant Nutrition and Soil Science 171, 61-82.

Kramer, C., Trumbore, S., Fröberg, M., Cisneros Dozal, L.M., Zhang, D., Xu, X., Santos, G.M., Hanson, P.J., 2010. Recent (<4 year old) leaf litter is not a major source of microbial carbon in a temperate forest mineral soil. Soil Biology and Biochemistry 42, 1028-1037.

Kwok, R., Rothrock, D.A., 2009. Decline in Arctic sea ice thickness from submarine and ICESat records: 1958–2008. Geophysical Research Letters 36, L15501.

Lavoie, M., Mack, M.C., Schuur, E.A.G., 2011. Effects of elevated nitrogen and temperature on carbon and nitrogen dynamics in Alaskan arctic and boreal soils. Journal of Geophysical Research: Biogeosciences 116, G03013.

Levin, I., Kromer, B., Hammer, S., 2013. Atmospheric $D^{14}CO_2$ trend in Western European background air from 2000 to 2012. Tellus B 65.

Levin, I., Kromer, B., Schoch-Fischer, H., Bruns, M., Münnich, M., Dietrich Berdau, Vogel, J.C., Münnich, K.O., 1985. 25 years of tropospheric $^{14}C$ observations on central Europe. Radiocarbon 27, 1-19.

Liebner, S., 2007. Adaptation, spatial variability, and phylogenetic characterization of methanotrophic communities in permafrost soils of the Lena Delta, Siberia, Fachbereich Biologie/Chemie. Universität Bremen, p. 108.

Liebner, S., Harder, J., Wagner, D., 2008. Bacterial diversity and community structure in polygonal tundra soils from Samoylov Island, Lena Delta, Siberia. International Microbiology 11, 195-202.

Liebner, S., Wagner, D., 2007. Abundance, distribution and potential activity of methane oxidizing bacteria in permafrost soils from the Lena Delta, Siberia. Environmental Microbiology 9, 107-117.

Mangelsdorf, K., Finsel, E., Liebner, S., Wagner, D., 2009. Temperature adaptation of microbial communities in different horizons of Siberian permafrost-affected soils from the Lena Delta. Chemie der Erde - Geochemistry 69, 169-182.

Marschner, B., Brodowski, S., Dreves, A., Gleixner, G., Gude, A., Grootes, P.M., Hamer, U., Heim, A., Jandl, G., Ji, R., Kaiser, K., Kalbitz, K., Kramer, C., Leinweber, P., Rethemeyer, J., Schäffer, A., Schmidt, M.W.I., Schwark, L., Wiesenberg, G.L.B., 2008. How relevant is recalcitrance for the stabilization of organic matter in soils? Journal of Plant Nutrition and Soil Science 171, 91-110.

Matsumoto, G.I., Friedmann, E.I., Gilichinsky, D.A., 1995. Geochemical characteristics of organic compounds in a permafrost sediment core sample from northeast Siberia, Russia. Proc. NIPR Symp. Antarct. Geosci. 8, 258-267.

McGuire, A.D., Anderson, L.G., Christensen, T.R., Dallimore, S., Guo, L., Hayes, D.J., Heimann, M., Lorenson, T.D., Macdonald, R.W., Roulet, N., 2009. Sensitivity of the carbon cycle in the Arctic to climate change. Ecological Monographs 79, 523-555.

Minke, M., Donner, N., Karpov, N.S., Klerk, P.d., Joosten, H., 2007. Distribution, diversity, development and dynamics of polygon mires: examples from Northeast Yakutia (Siberia). Peatlands International 1, 36-40.

Morgenstern, A., Grosse, G., Günther, F., Fedorova, I., Schirrmeister, L., 2011. Spatial analyses of thermokarst lakes and basins in Yedoma landscapes of the Lena Delta. The Cryosphere 5, 849-867.

Mueller, C., Koegel-Knabner, I., 2009. Soil organic carbon stocks, distribution, and composition affected by historic land use changes on adjacent sites. Biology and Fertility of Soils 45, 347-359.

Mueller, K., 1997. Oberflächenstrukturen und Eigenschaften von Permafrostböden im nordsibirischen Lena-Delta. Zeitschrift für Pflanzenernährung und Bodenkunde 160, 497-503.

Muster, S., Langer, M., Heim, B., Westermann, S., Boike, J., 2012. Subpixel heterogeneity of ice-wedge polygonal tundra: a multi-scale analysis of land cover and evapotranspiration in the Lena River Delta, Siberia. 2012 64.

Neff, J.C., Hooper, D.U., 2002. Vegetation and climate controls on potential CO2, DOC and DON production in northern latitude soils. Global Change Biology 8, 872-884.

Neunlist, S., Rohmer, M., 1985. The Hopanoids of '*Methylosinus trichosporium*': aminobacteriohopanetriol and aminobacteriohopanetetrol. Journal of General Microbiology 131, 1363-1367.

Nowinski, N.S., Taneva, L., Trumbore, S.E., Welker, J.M., 2010. Decomposition of old organic matter as a result of deeper active layers in a snow depth manipulation experiment. Oecologia 163, 785–792.

Olsson, P.A., Bååth, E., Jakobsen, I., Söderström, B., 1995. The use of phospholipid and neutral lipid fatty acids to estimate biomass of arbuscular mycorrhizal fungi in soil. Mycological Research 99, 623-629.

Ourisson, G., Albrecht, P., 1992. Hopanoids. 1. Geohopanoids: The most abundant natural products on earth? Acc. Chem. Res 25, 398-402.

Overland, J.E., Wang, M., Salo, S., 2008. The recent Arctic warm period. Tellus A 60, 589-597.

Pancost, R.D., Baas, M., van Geel, B., Sinninghe Damsté, J.S., 2002. Biomarkers as proxies for plant inputs to peats: an example from a sub-boreal ombrotrophic bog. Organic Geochemistry 33, 675-690.

Rethemeyer, J., Fülöp, R.H., Höfle, S., Wacker, L., Heinze, S., Hajdas, I., Patt, U., König, S., Stapper, B., Dewald, A., 2013. Status report on sample preparation facilities for 14C analysis at the new CologneAMS center. Nuclear Instruments and Methods in Physics Research Section B: Beam Interactions with Materials and Atoms 294, 168-172.

Rethemeyer, J., Kramer, C., Gleixner, G., John, B., Yamashita, T., Flessa, H., Andersen, N., Nadeau, M.-J., Grootes, P.M., 2005. Transformation of organic matter in agricultural soils: radiocarbon concentration versus soil depth. Geoderma 128, 94– 105.

Rethemeyer, J., Kramer, C., Gleixner, G., Wiesenberg, G.L.B., Schwark, L., Andersen, N., Nadeau, M.-J., Grootes, P.M., 2004. Complexity of soil organic matter: AMS $^{14}$C analysis of soil lipid fractions and individual Compounds. Radiocarbon 46, 465–473.

Romanovskii, N.N., Hubberten, H.-W., 2001. Results of permafrost modelling of the lowlands and shelf of the Laptev Sea Region, Russia. Permafrost and periglacial processes 12, 191-202.

Romanovsky, V.E., Smith, S.L., Christiansen, H.H., Shiklomanov, N.I., Streletskiy, D.A., Drozdov, D.S., Oberman, N.G., Kholodov, A.L., Marchenko, S.S., 2013. Permafrost. In: Arctic Report Card 2013, http://www.arctic.noaa.gov/reportcard.

Rumpel, C., Kögel-Knabner, I., 2011. Deep soil organic matter—a key but poorly understood component of terrestrial C cycle. Plant and Soil 338, 143-158.

Saito, K., Kimoto, M., Zhang, T., Takata, K., Emori, S., 2007. Evaluating a high-resolution climate model: Simulated hydrothermal regimes in frozen ground regions and their change under the global warming scenario. Journal of Geophysical Research: Earth Surface 112, F02S11.

Schädel, C., Schuur, E.A.G., Bracho, R., Elberling, B., Knoblauch, C., Lee, H., Luo, Y., Shaver, G.R., Turetsky, M.R., 2014. Circumpolar assessment of permafrost C quality and its vulnerability over time using long-term incubation data. Global Change Biology 20, 641-652.

Schaefer, K., Zhang, T., Bruhwiler, L., Barrett, A.P., 2011. Amount and timing of permafrost carbon release in response to climate warming. Tellus B 63, 165-180.

Schirrmeister, L., Grosse, G., Schnelle, M., Fuchs, M., Krbetschek, M., Ulrich, M., Kunitsky, V., Grigoriev, M., Andreev, A., Kienast, F., Meyer, H., Babiy, O., Klimova, I., Bobrov, A., Wetterich,

S., Schwamborn, G., 2011. Late Quaternary paleoenvironmental records from the western Lena Delta, Arctic Siberia. Palaeogeography, Palaeoclimatology, Palaeoecology 299, 175-196.

Schirrmeister, L., Grosse, G., Schwamborn, G., Andreev, A.A., Meyer, H., Kunitsky, V.V., Kuznetsova, T.V., Dorozhkina, M.V., Pavlova, E.Y., Bobrov, A.A., Oezen, D., 2003. Late Quaternary History of the Accumulation Plain North of the Chekanovsky Ridge (Lena Delta, Russia): A Multidisciplinary Approach. Polar Geography 27, 277-319.

Schuur, E.A.G., Abbott, B.W., Bowden, W.B., Brovkin, V., Camill, P., Canadell, J.G., Chanton, J.P., Chapin III, F.S., Christensen, T.R., Ciais, P., Crosby, B.T., Czimczik, C.I., Grosse, G., Harden, J., Hayes, D.J., Hugelius, G., Jastrow, J.D., Jones, J.B., Kleinen, T., Koven, C.D., Krinner, G., Kuhry, P., Lawrence, D.M., McGuire, A.D., Natali, S.M., O'Donnell, J.A., Ping, C.L., Riley, W.J., Rinke, A., Romanovsky, V.E., Sannel, A.B.K., Schädel, C., Schaefer, K., Sky, J., Subin, Z.M., Tarnocai, C., Turetsky, M.R., Waldrop, M.P., Anthony, K.M.W., Wickland, K.P., Wilson, C.J., Zimov, S.A., 2013. Expert assessment of vulnerability of permafrost carbon to climate change. Climatic Change 119, 359-374.

Schuur, E.A.G., Bockheim, J., Canadell, J.G., Euskirchen, E., Field, C.B., Goryachkin, S.V., Hagemann, S., Kuhry, P., Lafleur, P.M., Lee, H., Mazhitova, G., Nelson, F.E., Rinke, A., Romanovsky, V.E., Shiklomanov, N., Tarnocai, C., Venevsky, S., Vogel, J.G., Zimov, S.A., 2008. Vulnerability of permafrost carbon to climate change: implications for the global carbon cycle. BioScience 58, 701-714.

Schuur, E.A.G., Vogel, J.G., Crummer, K.G., Lee, H., Sickman, J.O., Osterkamp, T.E., 2009. The effect of permafrost thaw on old carbon release and net carbon exchange from tundra. Nature 459, 556-559.

Schwamborn, G., Rachold, V., Grigoriev, M.N., 2002. Late Quaternary sedimentation history of the Lena Delta. Quaternary International 89, 119-134.

Shaver, G.R., Giblin, A.E., Nadelhoffer, K.J., Thieler, K.K., Downs, M.R., Laundre, J.A., Rastetter, E.B., 2006. Carbon turnover in Alaskan tundra soils: effects of organic matter quality, temperature, moisture and fertilizer. Journal of Ecology 94, 740-753.

Sistla, S.A., Moore, J.C., Simpson, R.T., Gough, L., Shaver, G.R., Schimel, J.P., 2013. Long-term warming restructures Arctic tundra without changing net soil carbon storage. Nature 497, 615-618.

Six, J., Conant, R.T., Paul, E.A., Paustian, K., 2002. Stabilization mechanisms of soil organic matter: Implications for C-saturation of soils. Plant and Soil 241, 155-176.

Soil Survey Staff, 2010. Keys to soil taxonomy, 11 ed. US. Dept. of Agriculture & Natural Resources Conservation Service, Washington, D.C.

Sollins, P., Homann, P., Caldwell, B.A., 1996. Stabilization and destabilization of soil organic matter: mechanisms and controls. Geoderma 74, 65-105.

Steven, B., Pollard, W.H., Greer, C.W., Whyte, L.G., 2008. Microbial diversity and activity through a permafrost/ground ice core profile from the Canadian high Arctic. Environmental Microbiology 10, 3388-3403.

Stuiver, M., Polach, H.A., 1977. Discussion reporting of $^{14}C$ data. Radiocarbon 19, 355-363.

Talbot, H.M., Rohmer, M., Farrimond, P., 2007. Rapid structural elucidation of composite bacterial hopanoids by atmospheric pressure chemical ionisation liquid chromatography/ion trap mass spectrometry. Rapid communications in mass spectrometry 21, 880-892.

Talbot, H.M., Watson, D.F., Murrell, J.C., Carter, J.F., Farrimond, P., 2001. Analysis of intact bacteriohopanepolyols from methanotrophic bacteria by reversed-phase high-performance liquid chromatography–atmospheric pressure chemical ionisation mass spectrometry. Journal of Chromatography A 921, 175-185.

Tarnocai, C., Canadell, J.G., Schuur, E.A.G., Kuhry, P., Mazhitova, G., Zimov, S., 2009. Soil organic carbon pools in the northern circumpolar permafrost region. Global Biogeochem. Cycles 23, GB2023.

van Winden, J.F., Talbot, H.M., Kip, N., Reichart, G.-J., Pol, A., McNamara, N.P., Jetten, M.S.M., Op den Camp, H.J.M., Sinninghe Damsté, J.S., 2012. Bacteriohopanepolyol signatures as markers for methanotrophic bacteria in peat moss. Geochimica et Cosmochimica Acta 77, 52-61.

Vaughan, D.G., Comiso, J.C., Allison, I., Carrasco, J., Kaser, G., Kwok, R., Mote, P., Murray, T., Paul, F., Ren, J., Rignot, E., Solomina, O., Steffen, K., Zhang, T., 2013. Observations: Cryosphere, In: Stocker, T.F., Qin, D., Plattner, G.-K., Tignor, M., Allen, S.K., Boschung, J., Nauels, A., Xia, Y., Bex, V., Midgley, P.M. (Eds.), Climate change 2013: The physical science basis. contribution of working group I to the fifth assessment report of the intergovernmental panel on climate change. Cambridge University Press, Cambridge, United Kingdom and New York, NY, USA, pp. 317-382.

Vestal, J.R., White, D.C., 1989. Lipid Analysis in Microbial Ecology. BioScience 39, 535-541.

von Lützow, M., Kögel-Knabner, I., Ekschmitt, K., Flessa, H., Guggenberger, G., Matzner, E., Marschner, B., 2007. SOM fractionation methods: Relevance to functional pools and to stabilization mechanisms. Soil Biology & Biochemistry 39, 2183–2207.

Wacker, L., Němec, M., Bourquin, J., 2010. A revolutionary graphitisation system: Fully automated, compact and simple. Nuclear Instruments and Methods in Physics Research Section B: Beam Interactions with Materials and Atoms 268, 931-934.

Wagner, D., Gattinger, A., Embacher, A., Pfeiffer, E.-M., Schloter, M., Lipski, A., 2007. Methanogenic activity and biomass in Holocene permafrost deposits of the Lena Delta, Siberian Arctic and its implication for the global methane budget. Global Change Biology 13, 1089–1099.

Wagner, D., Lipski, A., Embacher, A., Gattinger, A., 2005. Methane fluxes in permafrost habitats of the Lena Delta: effects of microbial community structure and organic matter quality. Environmental Microbiology 7, 1582–1592.

Washburn, A.L., 1973. Periglacial processes and environments. Edward Arnold, London.

Yergeau, E., Hogues, H., Whyte, L.G., Greer, C.W., 2010. The functional potential of high Arctic permafrost revealed by metagenomic sequencing, qPCR and microarray analyses. ISME J 4, 1206-1214.

Zech, M., Andreev, A., Zech, R., Müller, S., Hambach, U., Frechen, M., Zech, W., 2010. Quaternary vegetation changes derived from a loess-like permafrost palaeosol sequence in northeast Siberia using alkane biomarker and pollen analyses. Boreas 39, 540-550.

Zelles, L., 1997. Phospholipid fatty acid profiles in selected members of soil microbial communities. Chemosphere 35, 275-294.

Zelles, L., 1999. Fatty acid patterns of phospholipids and lipopolysaccharides in the characterisation of microbial communities in soil: a review. Biol Fertil Soils 29, 111-129.

Zimmermann, U., 2007. Methanoxidierende Bakteriengemeinschaften in Böden und Sedimenten des sibirischen Permafrostes, Geowissenschaften. Universität Hamburg, Hamburg, p. 123.

Zimov, S.A., Schuur, E.A.G., Chapin III, F.S., 2006. Permafrost and the Global Carbon Budget. Science 312, 1612-1613.

Ziolkowski, L.A., Slater, G.F., Onstott, T.C., Whyte, L., Townsend-Small, A., 2013. Microbes residing in young organic rich Alaskan soils contain older carbon than those residing in old mineral high Arctic soils, American Geophysical Union Fall Meeting, San Francisco.

Zubrzycki, S., 2013. Organic Carbon Pools in Permafrost-Affected Soils of Siberian Arctic Regions, Fachbereich Geowissenschaften. Universität Hamburg, Hamburg, p. 166.

Zubrzycki, S., Kutzbach, L., Grosse, G., Desyatkin, A., Pfeiffer, E.M., 2013. Organic carbon and total nitrogen stocks in soils of the Lena River Delta. Biogeosciences 10, 3507-3524.

Zubrzycki, S., Kutzbach, L., Pfeiffer, E.-M., Vakhrameeva, P., 2012. Variability of soil organic carbon stocks of different permafrost-affected soils: Initial results from a North-South transect in Siberia, in: K.M., H. (Ed.), Tenth International Conference on Permafrost (TICOP). The Northern Publisher, Salekhard, Salekhard, Yamal-Nenets Autonomous District, Russia, pp. 485-490.

Zygadlo, J.A., Pignata, M.L., Gonzalez, C.M., Levin, A., 1993. Alkanes in lichens. Phytochemistry 32, 1453-1456.

# 10. Acknowledgements

The time of my PhD thesis was a great adventure with all the ups and downs that belong to a PhD project. And I met so many people on the way in training courses, on conferences, on meetings, in seminars, on expeditions and during my daily work who all contributed in one way or the other to help me finish my thesis. Thank you.

A great thank you goes to Prof. Dr. Janet Rethemeyer who gave me the chance to work in the field of organic biogeochemistry and radiocarbon analysis something I had not done before. You supported me over the last years in so many ways and you had always time for me – thank you. And I will never forget all the sandwiches you made me during our expedition! But most of all I am thankful for your guidance and advice which went beyond science and work.

I am also grateful that Prof. Dr. Lars Kutzbach accepted to be my second supervisor and that Prof. Dr. Tim Mansfeldt took the chair of my examination committee. Furthermore, I thank Dr. Sonja Berg for being the assessor at my defence.

My work at the institute was and still is great und fun because of all the support from our working group (Ulrike Patt, Bianca Stapper, Lana John, Matthias Thienemann, Stephan John, Anja Cording, Stephie Kusch, Daniela Warok, Sandra Jivcov, Sonja Berg, Reka Fülöp, Anna Distelrath, Jan Feder, Marvin Kellner, Elisabeth Krewer, Sina Lehning, Jannik Martens, Vera Schmitt, Andrea Lauss, Daria Friesen, Sven Gelking, Tobias Hagemann, and Sophia Burghardt) and from many more people (Hannah, Jasmjen, Janna, Thomas, Andreas, Silke, Nicole, Doro, and more – I guess ☺ ). And I say especially thank you to Barbara Bock, Reka Fülöp, and Stephan John for great times in our office. You all motivated me to keep going – thanks!

I really enjoy my two stays in the Siberian Lena Delta, Russia and I am most thankful to the Alfred-Wegener Institute (AWI), Research Unit Potsdam for organization and logistic. The weeks on Samoylov Island had been full of work and intense life on the station. For these great times I thank everyone who had been there with me on the station, especially I thank Waldemar, Molo, Sacha Makarov, Sveta, Inken, Seba, Luba, Anna, Pete, Manu, Kathrin, Hanno, Thomas, Betti, and Iulia.

I thank Prof. Dr. Pascal Boeckx for receiving me in Gent, Belgium and Dries Roobroeck for his dedicated lab training he gave me. And thanks to everyone in the lab for showing me your work and the city Gent.

A big thank you goes to Mats Björkman, Joachim Franz-Höfle, Manfred Höfle, Alistair Taylor and Sonja Taylor for proof reading.

This thesis would not have been possible without funding. I therefore thank the European Science Foundation (Molter – Program), the University of Cologne (Jennifer Gusky-Preis and “Wiedereinstiegsprogramm” as part of the Exzellenzinitiative), the Permafrost Young Researchers Network (travel grant for PYRN- 4$^{th}$ EUCOP 2014), and the German Ministry of Education and Research (BMBF, German-Russian project CarboPerm).

Of course there were many people outside the science world who supported me over the last years. I thank my parents Ute und Alex. Höfle for their encouragement and interest in my work (I hope you finally understood what I am doing). My parents-in-law Hedwig and Wolfgang Franz I thank for their understanding and for letting me work during our visits. I acknowledge especially the engagement of my parents and my parents-in-law in the last weeks – without your help and support I would not have able to finish this thesis properly. Thank you so much! My brother Felix and his wife Marina I thank for great dinners at their home which often brought the whole family at one table. And I am very grateful for my friends Sonja, Kathi, Jule, and Elske. Thanks for always listening to my excitement, doubts, and worries about my work.

This thesis would have never been finished without the never-ending support of my dear husband Joachim Franz-Höfle who always believed in me even if I had no confidence in myself anymore. Thank you so much for lonely summers in Germany while I was in Siberia, for spending Sunday mornings in the park with Jannik so I could work, for endless discussions on my work and just for being there whenever I needed you. And I am grateful for all the love and joy I receive from Jannik. You added a new perspective to my life.

## Vielen Dank - Thank you.

# 11. Author contributions

1. Rethemeyer J., Fülöp R.H., **Höfle S.**, Wacker L., Heinze S., Hajdas I., Patt U., König S., Stapper B., Dewald A. (2013): Status report on sample preparation facilities for $^{14}C$ analysis at the new CologneAMS center. *Nuclear Instruments and Methods in Physics Research Section B: Beam Interactions with Materials and Atoms* **294**, 168-172. doi:10.1016/j.nimb.2012.02.012

   S. Höfle contucted a detailed evaluation of sample contamination with exogenous carbon during the multiple steps of compound-specific radiocarbon analysis. The methodical section as well as the interpretation of the results was written by S. Höfle. The contribution of S. Höfle was ca. 50% to the paper.

2. **Höfle S.**, Rethemeyer J., Mueller C.W., John S. (2013): Organic matter composition and stabilization in a polygonal tundra soil of the Lena Delta. *Biogeosciences* **10**, 3145-3158. doi:10.5194/bg-10-3145-2013

   S. Höfle cooridnated and - together with J. Rethemeyer - carried out the fieldwork. The organic geochemical and radiocarbon analyses were conducted by S. Höfle together with S. John and C.W. Mueller (TU Munich). The text was written by S. Höfle with contributions from all co-authors. Overall, S. Höfle contributed 80% to the paper.

3. **Höfle S.**, Kusch S., Talbot H. M., Mollenhauer G., Zubrzycki S., Burghardt S., Rethemeyer J. (under review): Characterization of bacterial populations in Arctic permafrost soils using bacteriohopanepolyols. submitted to *Organic Geochemistry* (07.01.2015)

   The fieldwork was coordinated and carried out by S. Höfle with assistance by J. Rethemeyer and S. Zubrzycki (Univ. Hamburg). S. Höfle conducted the organic geochemial analysis with assistance of Diploma student S. Burghardt and H. M. Talbot (Newcastle University). The text was written by S. Höfle with contributions from all co-authors. Overall, S. Höfle contributed 80% to the paper.

4. **Höfle S.,** Roobroeck D., Boeckx P., Rethemeyer J. (in preperation): $^{14}C$ contents of microbial phospholipid fatty acids reveal preferential metabolism of labile organic matter in Arctic permafrost soils (in preperation)

   S. Höfle performed the analysis of microbial membrane lipid biomarker at the University of Ghent (Belgium) under the guidance of P. Boeckx and D. Roobroeck (financial support from the European Science Foundation, MOLTER program) and the gas-chromatographic isolation of single lipids at the University of Cologne. The text was written by S. Höfle with contributions from all co-authors. Overall, S. Höfle contributed 85% to the paper.

# 12. Erklärung (Explanation in German)

Ich versichere, dass ich die von mir vorgelegte Dissertation selbständig angefertigt, die benutzten Quellen und Hilfsmittel vollständig angegeben und die Stellen der Arbeit – einschließlich Tabellen, Karten, und Abbildungen -, die anderen Werken im Wortlaut oder dem Sinn nach entnommen sind, in jedem Einzelfall als Entlehnung kenntlich gemacht habe; dass diese Dissertation noch keiner anderen Fakultät oder Universität zur Prüfung vorgelegen hat; dass sie – abgesehen von unten angegebenen Teilpublikationen – noch nicht veröffentlicht worden ist, sowie, dass ich eine solche Veröffentlichung vor Abschluss des Promotionsverfahrens nicht vornehmen werde.

Die Bestimmungen der Promotionsordnung sind mir bekannt. Die von mir vorgelegte Dissertation ist von Prof. Dr. Janet Rethemeyer betreut worden.

Nachfolgend genannte Teilpublikationen liegen vor:

1. Rethemeyer J., Fülöp R.-H., Höfle S., Wacker L., Heinze S., Hajdas I., Patt U., Konig S., Stapper B., Dewald A. (2013) Status report on sample preparation facilities for 14C analysis at the new CologneAMS center. *Nuclear Instruments and Methods in Physics Research B* **294**, 168–172.

2. Höfle S., Rethemeyer J., Mueller C. W. and John S. (2013) Organic matter composition and stabilization in a polygonal tundra soil of the Lena Delta. *Biogeosciences* **10**, 3145-3158.

3. Höfle S., Kusch S., Talbot H. M., Mollenhauer G., Zubrzycki S., Burghardt S., Rethemeyer J. (under review) Characterization of bacterial populations in Arctic permafrost soils using bacteriohopanepolyols. submitted to *Organic Geochemistry* (07.01.2015)

Köln, 09.02.2015

Silke Höfle